Ph.D. Thesis

Implications of lysyl oxidase and lysyl oxidase-like 2 enzyme expression for epithelial and neuroepithelial tumor progression

Hollósi Péter

Semmelweis University
Pathological Sciences Doctoral School
1st Department for Pathology and Experimental Cancer Research

Budapest, Hungary
2009

Supervisors and consultants:
Kovalszky Ilona, D.Sc. M.D. Ph.D.
Csiszár Katalin, Ph.D.
Sheri Fumiko Tsuda Fong, M.D. Ph.D.
Dissertation committee:
Sasvári Mária, D.Sc. M.D. Ph.D. Chairperson
Döme Balázs, M.D. Ph.D.
Firneisz Gábor, M.D. Ph.D.
Official reviewers:
Deák Ferenc, D.Sc. Ph.D.
Lotz Gábor, M.D. Ph.D.

Table of contents

List of abbreviations 5
1. Introduction 10
1.1. Malignant transformation and tumor progression 10
1.1.1. Heritable alterations in cancer 11
1.1.2. Astrocytic tumors 13
1.1.3. Colon tumors 15
1.1.4. Esophageal tumors 17
1.1.5. Breast tumors 18
1.2. The context of tumor microenvironment 18
1.2.1. Collagens 19
1.2.2. Elastin 20
1.2.3. Focal adhesion 20
1.2.3.1. FAK 21
1.2.3.2. Src 22
1.2.3.3. Paxillin 23
1.3. Mammalian amine oxidases 24
1.3.1. Lysyl oxidases 25
1.3.1.1. LOX 28
1.3.1.2. LOXL2 30
1.3.1.3. Lysyl oxidases in tumor suppression 31
1.3.1.4. Lysyl oxidases in tumor promotion 32
2. Objectives 34
3. Materials and methods 37
3.1. Cell lines and cell culture conditions 37
3.2. Chemicals 38
3.3. Lentiviral vector construction and viral transduction of cells 39
3.4. Southern blot analysis 40
3.5. Microsatellite analysis 40
3.6. Promoter analysis 41
3.7. Northern blot analysis 41
3.8. Real time qPCR analysis 42

3.9. Western blot analysis 42
3.10. Immunocytochemical and immunohistochemical analyses 44
3.11. Lysyl oxidase activity assay 47
3.12. Cell migration assay 48
3.13. Patient population 48
4. Results 50
4.1. LOX antibody characterization 50
4.2. LOX is expressed by normal and malignant astrocytes *in vivo* 50
4.3. LOX is expressed in normal and malignant astrocytes *in vitro* 52
4.4. LOX enzymatic activity positively correlates with astrocytic tumor grade 54
4.5. Active LOX contributes to astrocytic migration 56
4.6. Active LOX promotes astrocytic cell migration by facilitating FAK(Tyr576) and paxillin(Tyr118) phosphorylation 58
4.7. LOXL2 antibody characterization 59
4.8. Increased LOXL2 expression is associated with less differentiated colon tumors 61
4.9. Increased expression of LOXL2 in esophageal tumors 63
4.10. LOH analysis of the *loxl2* gene in colon and esophageal tumors 64
4.11. Characterization of the *loxl2* CpG island and promoter 65
4.12. Activation of *loxl2* gene expression by 5-aza-dC treatment 67
4.13. Characterization of LOXL2 expression in stably transduced cell lines 69
4.14. Overexpression of LOXL2 induces a mesenchymal-like phenotype in MCF-7 and MCF-10A clones 72
4.15. LOXL2 overexpression promotes migratory ability in MCF-7 but not in MCF-10A cells 73
4.16. LOXL2 is catalytically active in both MCF-7 and MCF-10A cells 75
4.17. Altered localization of LOXL2 in breast tumor tissue 77
4.18. Altered localization and size of LOXL2 in breast cell lines 79
4.19. Activation of *loxl2* gene expression by 5-aza-dC and TSA treatment 81
5. Discussion 83
6. Conclusions 92
Abstract 94
Összefoglaló 95
References 96
Publications 118

Acknowledgements 120

List of abbreviations

5-aza-dC	5-aza-2'-deoxycytidine
AI	allelic imbalance
AJCC	American Joint Committee on Cancer
anti-VIII factor	anti-hemophilic factor
APC	adenomatous polyposis coli
APSCL	acetone precipitated soluble cell lysate
APUD	amine precursor uptake and decarboxylation
ATCC	American Type Culture Collection
BAPN	beta-aminopropionitrile
bFGF	basic fibroblast growth factor
Blk	B lymphoid tyrosine kinase
BMP-1	bone morphogenic protein-1
Brk	protein tyrosine kinase 6
BSA	bovine serum albumin
CCM	conditioned cell medium
CD31	platelet endothelial cell adhesion molecule
CD34	hematopoietic progenitor cell antigen
CD45	receptor protein tyrosine phosphatase C
cDNA	complementary DNA
c-ErbB1	cellular erythroblastic leukemia viral oncogene homolog 1
c-ErbB2	cellular erythroblastic leukemia viral oncogene homolog 2
Chk	megakaryocyte-associated tyrosine kinase
CL	cell lysate
CNS	central nervous system
CpG	cytosine-guanine dinucleotide
Crk	v-crk sarcoma virus CT10 oncogene homolog
CRL	cytokine receptor-like
Csk	c-src tyrosine kinase
c-Src	cellular Rous sarcoma oncogen
DAO	diamine oxidase

DAPI	4',6-diamidino-2-phenylindole
DCC	deleted in colorectal cancer
DMEM	Dulbecco's Modified Eagle's Medium
DNA	deoxyribonucleic acid
DNMT	DNA cytosine methyltransferase
DTT	dithiothreitol
ECM	extracellular matrix
EDTA	ethylenediaminetetraacetic acid
EGF	epidermal growth factor
EGFR	epidermal growth factor receptor
EMT	epithelial-mesenchymal transition
FAD	flavin-adenine dinucleotide
FAK	focal adhesion kinase
FBS	fetal bovine serum
Fgr	Gardner-Rasheed feline sarcoma oncogene
Frk	Fyn related kinase
Fyn	oncogene related to Src, Fgr, Yes
GAPDH	glyceraldehyde 3-phosphate dehydrogenase
GFAP	glial fibrillary acidic protein
HAT	histone acetyltransferase
Hck	hemopoietic cell kinase
HER1	human epidermal growth factor receptor 1
HER2	human epidermal growth factor receptor 2
HGF	hepatocyte growth factor
HIV-1	human immunodeficiency virus-1
H-Ras	Harvey rat sarcoma viral oncogene homolog
IgG	immunoglobulin G
IRF-1	interferon regulatory element-1
ISCL	insoluble cell lysate
K_i	inhibitory constant
Ki-67	antigen identified by monoclonal antibody Ki-67
K-Ras	Kirsten rat sarcoma viral oncogene homolog

Lck	lymphocyte-specific protein tyrosine kinase
LO	lysyl oxidase
LOH	loss of heterozygosity
LOL	lysyl oxidase like
LOR-1	lysyl oxidase related 1
LOR-2	lysyl oxidase related 2
LOX	lysyl oxidase
LOXC	lysyl oxidase-like 4
LOXL	lysyl oxidase-like
LOXL2	lysyl oxidase-like 2
LOXL3	lysyl oxidase-like 3
LOXL4	lysyl oxidase-like 4
LTQ	lysyltyrosyl quinone
Lyn	v-yes-1 Yamaguchi sarcoma viral related oncogene homolog
MAO	monoamine oxidase
MEGM	Mammary Epithelial Growth Medium
MICS	Membrane Invasion Chamber System
MMP	matrix metalloproteinase
MOPS	3-(N-morpholino) propanesulfonic acid
mRNA	messenger RNA
mTLD	mammalian tolloid
mTLL-1	mammalian tolloid-like 1
mTLL-2	mammalian tolloid-like 2
Neu	neuro/glioblastoma derived oncogene homolog
NGS	normal goat serum
NHA	normal human astrocyte
NFκB	nuclear factor kappa B
NGS	normal goat serum
p53	tumor protein 53
PAC	P1 virus-derived artificial chromosome
PAGE	polyacrylamide gel electrophoresis
PAO	polyamine oxidase

PBS	phosphate buffered saline
PBST	phosphate buffered saline Tween-20
PCNA	proliferating cell nuclear antigen
PDGF	platelet-derived growth factor
PI	protease inhibitor
pp125FAK	focal adhesion kinase
pp60c-src	cellular Rous sarcoma oncogene
PTK2	protein tyrosine kinase 2
PVDF	polyvinylidene fluoride
PYK2	proline-rich tyrosine kinase-2
PVDF	polyvinylidene fluoride
RER	rough endoplasmic reticulum
RNA	ribonucleic acid
rpm	rotation per minute
RPMI	Royal Park Memorial Institute
RPTPα	receptor tyrosine phosphatase A
rrg	Ras recision gene
RSV	Rous sarcoma virus
RT-PCR	real time-polymerase chain reaction
SCC	squamous cell carcinoma
SDS	sodium dodecyl sulfate
SFKs	Src family of non-receptor protein tyrosine kinases
SH2	Src homology 2 domain
SH3	Src homology 3 domain
SHP-1	non-receptor protein tyrosine phosphatase type 6
SHP-2	non-receptor protein tyrosine phosphatase type 11
SNP	single nucleotide polymorphism
SOCS	suppressor of cytokine signaling
Src	Rous sarcoma oncogene
SRCR	scavenger receptor cysteine-rich
Srm	src-related kinase lacking C-terminal regulatory tyrosine and N-terminal myristylation sites

SSAO	semicarbizide-sensitive amine oxidase
TBS	Tris buffered saline
TBST	Tris buffered saline Tween-20
TGF-β1	transforming growth factor-beta 1
TNM	tumor-node-metastasis
TPQ	topaquinone
Tris	tris (hydroxymethyl) aminomethane
TSA	Trichostatin A
U	enzyme unit
uPA	urokinase-type plasminogen activator
uPAR	urokinase-type plasminogen activator receptor
VAP-1	vascular adhesion protein-1
VEGF	vascular endothelial growth factor
WHO	World Health Organization
WS9-14	lysyl oxidase-related protein WS9-14
Yes	Yamaguchi sarcoma viral oncogene homolog
Yrk	Yes related kinase

1. Introduction

Solid malignant neoplasms comprise a neoplastic clonal cell population and the tumor microenvironment or tumor stroma, both in a continuous state of evolution. The stroma provides mechanical support and sustenance, and is susceptible to facilitate the metastatic process of the malignant cell. Cellular composition of the stroma varies between and within tumor types, with primary participation of fibroblasts, endothelial cells, pericytes, and cells of the immune system. The final element of the tumor microenvironment is the extracellular matrix (ECM) with its scaffolding proteins, proteases, and numerous other important signaling molecules collectively referred to as primary messengers. The critical importance of stroma in tumorigenesis has been confirmed by a series of experiments that, by modulating the stromal cell and/or ECM composition, have demonstrated either an inhibitory or enhanced effect on cancer growth.

Among others, members of the lysyl oxidase enzyme family have come in focus of research investigating tumor-stromal interactions. Due to enzymatic activity of secreted lysyl oxidases, certain proteinaceous components of the ECM undergo oxidative deamination, and the newly formed aldehyde residues then interact spontaneously to form covalent cross-linkages [1; 2]. Extensive covalent cross-linking leads to a stiffer, more insoluble matrix, ultimately affecting cancer cell behavior [3; 4; 5; 6; 7; 8]. The expression pattern and essential function of lysyl oxidase activity in normal tissues is well described [9]. Recently, in addition to the basic cross-linking activity, a growing number of studies reported novel roles for lysyl oxidases in various types of tumors. However, data we gained show quite controversy, and address a massive quantity of problems remain to be elucidated.

The goal of this study was to clarify contradictory data, and identify potential novel roles of lysyl oxidase (LOX) and lysyl-oxidase like 2 (LOXL2) protein expression in cerebral, colon, esophageal and mammary neoplasms *in vitro* and *in vivo*.

1.1. Malignant transformation and tumor progression

It is not possible to define a tumor cell in absolute terms. According to our current view, cancer cells are dynamic entities where there is a gradual acquisition of new characteristics as the tumor develops. This process has been termed tumor progression.

1.1.1. Heritable alterations in cancer

The malignant milieu is characterized by the lack of fine balance between stimulatory and inhibitory stimuli, partially due to a variety of genetic changes within tumor cells, including point mutations, gene amplifications, deletions, chromosomal rearrangements, and an overall aneuploidy. Tumors of different origin and those with different dignity all bear different types of genetic alterations at different DNA sequences. Genetic changes unique to tumor types discussed in the thesis are summarized later in this chapter.

Besides the genetic alterations mentioned above, epigenetic control of gene expression is also recognized as an important factor in cancer formation and progression. Altered epigenetic information represents another trait of the malignant neoplasm, differing from genetic changes in that they occur at defined regions in a gene, at a higher frequency, and are reversible by treatment with pharmaceutical agents [10; 11]. In mammals, several types of epigenetic inheritance systems play a role in what becomes the actual phenotype of a cell. Among those, DNA methylation and chromatin remodeling are most understood. Shutting down gene expression is most often associated with hypermethylation of the promoter region and/or formation of a tight chromatin structure achieved by histone deacetylation [12; 13; 14; 15]; two epigenetic processes, which have been found to be dynamically and directly linked [16; 17; 18; 19]. Beyond question, partial or complete loss of certain genes' expression can significantly influence the process of tumor progression.

The majority of 5-methylcytosine in mammalian DNA is present in the context of the cytosine-guanine dinucleotide (CpG) [20], although some non-CpG sequences may also exhibit methylation, but generally at a much lower frequency [21]. The distribution of 5-methylcytosine and the CpG dinucleotide itself are neither uniform nor

random. Approximately 70% of the CpGs that are present in the genome are methylated, whereas the majority of unmethylated CpGs occur in small clusters known as CpG islands, often found within or near promoters and first exons of genes [22]. CpG islands, which comprise 1–2% of the genome, are sequences of approximately 0.5–4 kb in length, with a CG content of over 55% [23; 24]. There are an estimated 45,000 CpG islands in the genome, and at least half of all genes contain a promoter-associated CpG island [25]. While most CpG islands are unmethylated and associated with transcriptionally active genes, such as 'housekeeping' genes, certain CpG islands are methylated, including those associated with imprinted genes and genes on the inactive X chromosome in females [26; 27]. The methylation process of the fifth carbon of a cytosine is catalyzed by three known DNA cytosine methyltransferase enzymes (DNMT1, 3a and 3b). Their activity is responsible for copying methylation patterns onto newly synthesized DNA strands based on the methylation status of the template strand, thus passing epigenetic information between cell generations [28; 29].

Certain cytidine nucleoside analogs e.g. 5-aza-2'-deoxycytidine (5-aza-dC), if present, interfere with the methylation reaction [30; 31]. 5-aza-dC incorporates into the DNA during replication, leading to cytotoxicity [32; 33]. Treatment of 5-aza-dC low levels enough to avoid triggering cell death, leads to the loss of DNMT activity, because the enzyme becomes irreversibly bound to the incorporated cytidine analog residues in the DNA strand. As a result of impaired DNA methylation, 5-aza-dC treatment triggers re-expression of the gene, restores lost gene function [31; 34; 35; 36]. 5-aza-dC was first synthesized in Czechoslovakia as potential chemotherapeutic agents for cancer [37], and 30 years later it was approved for clinical use for the treatment of myelodysplastic syndrome, a type of preneoplastic condition [38].

The link between DNA methylation and cancer was first implicated, when studies revealed that the amounts of 5-methylcytosine were lower in DNA form cancer cells as compared to normal cells [39; 40]. Later it was demonstrated, that the generic loss of DNA methylation occurs even at preneoplastic stages, so is an early event in the process of malignant transformation [41; 42; 43]. In line with the overall hypomethylation, the neoplastic genome exhibits hypermethylation at selected CpG sites. DNMTs are able to *de novo* methylate, which is responsible for the methylation of CpG sites that were previously unmethylated. Nevertheless, the mechanism by which

selective hypermethylation occurs in cancer cells undergoing an overall hypomethylation is not fully understood [44; 45; 46; 47; 48].

Transcription in mammalian cell does not occur on naked DNA, but instead occurs in the context of chromatin. Nucleosomes are the basic repeating unit of chromatin, made up of histone proteins wrapped by DNA. Histones in general consist of a globular domain and a 'tail' that protrudes out of the nucleosome. Acetylation and deacetylation of conserved lysine residues present in histone tails has long been linked to transcriptional activity and has been the most studied histone modification. Histone acetyltransferases (HATs) acetylate lysine residues to create an accessible and open chromatin configuration that facilitates transcriptional activity, whereas histone deacetylases (HDACs) can remove acetyl groups, leading to the assembly of a tightly packed chromatin, ultimately transcriptional repression [15].

Remodeling of the chromatin template by inhibition of HDAC activities represents a major goal for transcriptional therapy in neoplastic diseases. Deacetylation of nucleosomal core histone tails by the HDACs leads to a chromatin conformation that inhibits transcription, whereas histone acetylation results in transcriptional activation. Trichostatin A (TSA) is an antifungal antibiotic (*Streptomyces hygroscopicus*) that is a reversible, potent and specific inhibitor of mammalian HDACs both *in vivo* and *in vitro*. TSA treatment causes accumulation of highly acetylated histones *in vivo*, while inhibits the activity of partially purified histone deacetylases *in vitro*. Inhibition of HDAC activity causes chromatin relaxation and induces gene re-expression [49; 50; 51]. Moreover, a recent study suggested mechanism that TSA promotes the expression of apoptosis-related genes, leading to cancerous cells surviving at lower rates, thus slowing the progression of cancer [52].

Ultimately, this intricate interplay between various covalent modifications occurring in different sites on the histone tails and the DNA appears to ultimately impact gene expression, potentially leading to malignant transformation.

1.1.2. Astrocytic tumors

Astrocytes are found in all parts of the adult central nervous system (CNS) and contribute to 40% of the total cell population. Astrocytes originate from neuroepithelial cells, a subtype of stem cells of ectodermal origin. The broad scale of physiologic functions of astrocytes includes mechanical and metabolic support of neurons, formation of the blood-brain barrier, and repair of the CNS. After injury, astrocytes undergo morphological changes and increase synthesis of glial fibrillary acidic protein (GFAP). GFAP is an important intermediate filament protein that allows the astrocytes to begin synthesizing more cytoskeletal supportive structures and extend pseudopodia, and can be used to specifically identify astrocytes in the tissue of CNS [53]. GFAP is detected as a 51 kDa molecule by Western blot, but it was reported with a lower molecular mass of 48 kDa as well, which is probably a degradation product of the 51 kDa form [54]. Important, that the malignantly transformed astrocytes exhibit progressive loss of GFAP expression in a negative correlation with the tumor grade [55; 56].

In the CNS, astrocytes have the highest predisposition to malignant transformation of any CNS cell types. Although astrocytic tumors can develop at any age, they are the most frequent neoplasms among childhood brain tumors. In 2007, taken new pathological findings round, WHO classification of tumors of the central nervous system has changed. Accordingly, grading system of astrocytic tumors now include new entities. Subependymal giant cell astrocytomas and pilocytic astrocytomas are scored as grade I; pilomyxoid astrocytomas, diffuse astrocytomas, pleomorphic xanthoastrocytomas as grade II; anaplastic astrocytomas as grade III; and finally glioblastomas, giant cell glioblastomas, and gliosarcomas as grade IV. In general, grade I applies to lesions with low proliferative potential and the possibility of cure following surgical resection alone. Neoplasms designated grade II are generally infiltrative and, despite low-level proliferative activity, often recur. Some even progress to higher grades of malignancy, for example, low-grade diffuse astrocytomas that transform to anaplastic astrocytoma and glioblastoma. The designation WHO grade III is generally reserved for lesions with histological evidence of malignancy, including nuclear atypia and brisk mitotic activity. Patients with grade III tumors receive adjuvant radiation and/or chemotherapy. The designation WHO grade IV is assigned to cytologically malignant, mitotically active, necrosis-prone neoplasms with widespread infiltration of surrounding

tissue, typically associated with rapid pre- and postoperative disease evolution and a fatal outcome [57].

1.1.3. Colon tumors

Based on the information available from the American Cancer Society http://www.cancer.org), the most recent pathologic staging of colorectal cancer was developed by the American Joint Committee on Cancer (AJCC), known as the tumor-node-metastasis (TNM) system. The TNM system describes three key pieces of information: how far the primary tumor has grown into the wall of the intestine and whether it has grown into nearby areas (T categories); the extent of spread to regional lymph nodes (N categories); whether the cancer has metastasized to other organs of the body (M categories). While colorectal cancer can spread almost anywhere in the body, the most common sites of spread are the liver and lungs. After the TNM categories have been determined, this information is combined in a process called staging. The stage is indicated in Roman numerals from stage I (the least advanced) to stage IV (the most advanced). Actually, the least advanced stage is called stage 0, indicating that the cancer has not grown beyond the inner layer (mucosa) of the colon or rectum. Stage 0 colorectal cancer is also called carcinoma *in situ* or intramucosal carcinoma. Stage I colorectal cancer has grown through the mucosa layer and invaded the underlying muscular layers. Stage II cancer has grown into the outermost layers (subserosa, serosa) of the colon or rectum, or even grown into nearby tissues and organs. It has not yet spread to nearby lymph nodes or distant sites. Stage III tumors have grown past the mucosa layer, may even have grown through the wall of the colon or rectum, and they have spread to nearby lymph nodes but not to distant sites. Stage IV cancer may or may not have grown though the wall of the colon or rectum, and it may or may not have spread to nearby lymph nodes. It has spread to distant sites such as the liver, lung, peritoneum, or ovary. The actual staging system that was provided with the tissue slides used in our studies was an older system called Dukes staging system. Basically, Dukes stage A corresponds to AJCC/TNM stage I, stage B to stage II, stage C to stage III, and stage D to stage IV. Another factor that can affect the outlook for survival is the grade

of the cancer. Grade is a description of how closely the cancer resembles normal colorectal tissue when looked at under a microscope. The scale used for grading colorectal cancers goes from G1 (where the cancer looks much like normal colorectal tissue) to G4 (where the cancer looks very abnormal). The grade is often simplified as either "low-grade" (G1 or G2) or "high-grade" (G3 or G4).

Genetic predisposition contributes to approximately one third of all colon cancer cases [58]. Activating mutations of the K-Ras family of genes are the most common genetic events in the tumorigenesis of colorectal cancer [59]. The K-Ras oncoprotein controls transduction of signals required for cell proliferation, differentiation, and survival. Recently, specific target-directed therapies, including monoclonal antibodies against the epidermal growth factor receptor (EGFR, c-ErbB1, HER1) are novel approaches to the treatment of a number of human tumor types, offering a non-cytotoxic alternative to cancer treatment [60; 61]. It has been found, that patients with wild-type K-Ras have better clinical response to anti-EGFR therapy – in terms of prolonged median progression-free survival and overall response rates – when compared to mutant K-Ras [61]. Besides in colon cancer, enhanced EGFR expression has been documented in a variety of tumors, including gliomas [62; 63; 64] and breast tumors [65; 66; 67], where these specific target-directed therapies offer a therapeutic option that addresses some of the limitations associated with traditional cytotoxic therapies: chemotherapy and radiation therapy. Another frequent event in colon cancer initiation is the mutation of the APC tumor suppressor gene, occurring both in familial adenomatous polyposis and sporadic colon cancer cases [68]. Also, approximately 80% of colon cancers have mutations affecting at least one component of the TGF-β pathway [69].

Several other proteins are currently under investigation as prognostic factors in colorectal cancer. Among those we find nuclear proteins associated with tumor cell proliferation (PCNA, Ki-67), angiogenic stimulators (VEGF, CD31, CD34, anti-VIII factor), enzymes crucial for tumor invasion and metastasis (uPA, uPAR, and various MMPs), DNA replication, repair (thymidylate synthase), cell cycle regulation and apoptosis (p53), cell adhesion (DCC) [70].

A large proportion of colorectal cancers show chromosome-instability, which is thought to be the result of mutations that disrupt chromosome maintenance, but the

actual causative mutations are not always known. The most common numerical and structural chromosomal abnormalities in colorectal cancer are reviewed in [71; 72].

The five-year survival rates for colorectal cancer are the following; for Dukes stage A it is 85-95%, for stage B it is 60-80%, for stage C it is 30-60%, for stage D it is less than 5% [73].

1.1.4. Esophageal tumors

Esophageal cancer is one of the least studied and deadliest cancers worldwide. Worldwide, it is the sixth leading cause of death from cancer [74]. A similar TNM classification system applies to esophageal tumors that we use for colon tumors. Once esophageal cancer develops, it may spread rapidly; 14 to 21 percent of submucosal cancers (T1 lesions) and 38 to 60 percent of cancers that invade muscle (T2 lesions) are associated with spread to lymph nodes [75]. At the time of the diagnosis of esophageal cancer, more than 50 percent of patients have either unresectable tumors or radiographically visible metastases [76]. Most esophageal cancers are either squamous-cell carcinomas (SSCs) or adenocarcinomas, on rare occasions, melanomas, leiomyosarcomas, carcinoids, and lymphomas may develop in the esophagus as well. Approximately three quarters of all adenocarcinomas are found in the distal esophagus, whereas SSCs are more evenly distributed between the middle and lower third [75].

The pathogenesis of esophageal cancer is unclear. Oxidative damage from factors such as smoking or gastroesophageal reflux, which cause inflammation, esophagitis, and increased cell turnover, may initiate the carcinogenic process [77]. Frequent consumption of extremely hot beverages also appears to increase the incidence of SCC [78]. The genetic predisposition to esophageal cancer have been reported, nonepidermolytic palmoplantar keratoderma, a rare autosomal dominant disorder defined by a genetic abnormality at chromosome 17q25, is the only recognized familial syndrome that predisposes patients to squamous-cell carcinoma of the esophagus [79].

The overall survival rate at five years is poor, only 14% [76]. After complete surgical removal of the tumor, the five-year survival rate exceeds 95% for stage 0 disease, and is 50-80% for stage I disease, 30-40% percent for stage IIA disease, 10-

30% for stage IIB disease, and 10-15% for stage III disease, patients stage IV disease who are treated with palliative chemotherapy have a median survival of less than one year. [80; 81; 82].

1.1.5. Breast tumors

According to WHO data, breast cancer is the most frequent type of cancer in women, accounted for at least half a million deaths per year worldwide. Breast cancer is about a hundred times as frequent among women as among men, but survival rates are equal in both sexes. Breast cancer is also staged according to the TNM system, described above.

Several factors, including age, family history, age at first full-term pregnancy, early menarche, late menopause, postmenopausal obesity, use of postmenopausal hormones, alcohol consumption, and physical inactivity are associated with increased rick of breast cancer [83]. It is estimated that 5-10% of breast cancer cases result from inherited mutations or alterations in the breast cancer susceptibility genes BRCA1 and BRCA2 [84; 85]. Overexpression of another epidermal growth factor receptor, the HER2 (c-ErbB2, Neu) is typical to breast cancer, occurring in approximately 30% of breast carcinomas [86; 87]. Those tumors have a significantly less favorable prognosis as evidenced by a shorter recurrence-free survival and overall survival [88; 89].

1.2. The context of tumor microenvironment

Cell-stroma interactions are critical for the maintenance of tissue homeostasis. The ECM, which is a proteinaceous component of the stroma, regulates cell growth, survival, migration and differentiation through a repertoire of transmembrane receptors, of which integrins are the best characterized. At special sites of the cell membrane, called focal adhesions, integrins modulate cell fate by reciprocally transducing biochemical and biophysical cues between the cell and the ECM, facilitating processes essential in the life of a cell. As integrins span across the cell membrane they bind to

extracellular fibronectin; and at the inner surface of the membrane, they provide a focus to organize the attachment of actin microfilaments at focal adhesion contacts. As a result, ECM is indirectly linked to the actin cytoskeleton.

Loss of normal tissue cohesion is a pre-requisite of cancer cell spread. The ability of a cell to migrate is although not simply acquired by loss of adhesive properties. Instead, cell migration requires a dynamic pattern of adhesion contacts more complex than in a cell residing in a tissue. A single cell migrating through a tissue needs to adhere to the ECM to just the right extent, sufficiently tightly to pull itself through the tissue, but not so tightly as to become unable to extricate itself. Attachments need to be established at a leading edge and be broken at a trailing edge, and cytoskeletal contractions must be coordinated. However, it should be noted that some normal and tumor cells also move by a more amoeboid mode with less attachment and less activity of the actin cytoskeleton. In fact, carcinoma cells more often migrate as cell clusters, or even expand like cell sheets during fetal development. Nevertheless, cell migration requires reorganization of cell-cell and cell-matrix contacts and the cytoskeleton compared to cells in a resting tissue.

1.2.1. Collagens

The collagen superfamily of proteins comprises at least 29 members; the genes of which are dispersed throughout the nuclear genome. Being one of the most abundant proteins in the mammalian body, collagens are major structural components of the ECM. Members typically form supramolecular assemblies that contain at least one triple-helical collagenous domain with repeating $(Gly\text{-}X\text{-}Y)_n$ sequences, i.e. a glycine residue as every third amino acid, linked to predominantly proline and 4-hydroxyproline in the X and Y positions, respectively. Due to the extreme structural and functional diversity among collagen-built polymeric structures, the superfamily can be subdivided into nine different families: collagens that form fibrils (types I-III, V, and XI); fibril-associated collagens (types IX, XII, XIV, XVI, XIX, XX, and XXI); collagens that form hexagonal networks (types VIII and X); collagens that form beaded filament (type VI); basement membrane collagens (type IV) and basement membrane-associated collagens

(type VII); collagens with transmembrane domains (types XIII and XVII); and the family of type XV and type XVIII collagens [90].

After biosynthesis of fibrillar collagen precursors, as typical to secretory proteins, procollagens undergo extensive posttranslational modifications [91; 92]. Once outside the cells, hydroxylated and glycosylated procollagen molecules are proteolytically converted to collagen molecules [93]. Followed by fibril formation, collagens interact with non-collagenous and collagenous proteins. These interactions are essential in providing the tensile strength and mechanical stability of the collagen fibers and other supramolecular arrays [94], and are stabilized by numerous intra- and intermolecular covalent cross-links catalyzed by the family of lysyl oxidase enzymes [95; 96].

1.2.2. Elastin

Although not as widespread as collagens, elastin is present in large amounts, particularly in tissues with high elasticity and resilience; these are elastic ligaments, large blood vessels, tendons, lungs, and skin [97; 98]. In contrast to collagens, there is only one genetic type of elastin, although at least 11 variants arise by alternative splicing of the transcripts [97]. It is synthesized as a soluble monomer called tropoelastin that undergoes only minor posttranslational modifications; hydroxylation of proline residues occurs to a variable extent, though hydroxylysine and carbohydrate moieties are not present [97]. After secretion from the cell, certain lysyl residues of tropoelastin are oxidatively deaminated to aldehydes by lysyl oxidases, the same enzymes involved in this process in collagens [96; 99; 100]. In its mature, cross-linked form, elastin is highly insoluble and extremely stable. Elastin exhibits a variety of random coil conformations that permit the protein to stretch and recoil [101; 102].

1.2.3. Focal adhesion

Cell adhesions elicit a broad variety of signals within the cell. As key components of focal adhesions, integrins influence several pathways that define cell shape, mobility, growth, and survival, through various different adaptor proteins and protein kinases. In adherent cells, lack of attachment tends to cause anoikis, a specific kind of apoptosis. Alterations in signaling as a consequence of altered adhesion in carcinoma cells must therefore be compensated. This may explain why altered intracellular signaling is a common finding in cancers, or vice versa, abnormal activities of focal adhesion components might be responsible for anchorage-independent growth, one of the hallmarks of cancer cells [103]. Key molecular components of focal adhesions discussed below are frequently overexpressed and/or aberrantly activated in a variety of epithelial and non-epithelial cancers [104; 105; 106].

1.2.3.1. FAK

Focal adhesion kinase (FAK, pp125FAK, PTK2) is a 125 kDa non-receptor cytoplasmic protein tyrosine kinase; it signals the establishment of the focal adhesions [107]. A closely related kinase, proline-rich tyrosine kinase-2 (PYK2) shares a similar structure as well as common phosphorylation sites. However, FAK and PYK2 possess partially distinct signaling roles in the cells [108].

FAK has been implicated in a number of biological processes, including controlling the rate of cell migration and generating an antiapoptotic signal in response to cell adhesion [109]. In general, the activity of FAK is dependent on integrin-mediated cell adhesion and G protein-coupled receptors [110; 111]. Upon cell adhesion, FAK is recruited at an early stage to focal adhesions and activates itself by autophosphorylates at Tyr397. Active FAK creates a docking site for SH2 domains of various proteins, including Src family of non-receptor protein tyrosine kinases (SFKs) [112; 113; 114; 115], discussed below. The large C-terminal region of FAK has a key role targeting the kinase to focal adhesion sites [116] through interactions with cytoskeletal proteins talin [117] and paxillin [118], which are directly or indirectly associated with the actin cytoskeleton, respectively. The N-terminus has a complex role: it regulates FAK activity through an intramolecular interaction with the central kinase domain, and also

mediates FAK interactions with integrins. PDGF-, EGF-, or HGF-stimulated cell motility also works through FAK, as corresponding receptors are also linked to the amino end the kinase [119].

Besides the above mentioned, a total number of at least fifty different proteins have been identified as components of focal adhesions, some of these, such as SOCS [120], and SHP-2 [121] function as negative regulators of FAK activity [106]. *In toto*, FAK promotes cell survival by multiple pathways [122; 123; 124], and can promote tumorigenesis through stimulation of cell cycle progression [125; 126; 127] and cell migration [106].

1.2.3.2. Src

SFKs have pleiotropic functions in all metazoan cells. The family comprises at least twelve known enzymes (Src, Yes, Fyn, Fgr, Lck, Hck, Blk, Lyn, Frk, Brk, Srm, and Yrk). SFKs are subcellularly organized to the cytoplasm, plasma membrane or to the nucleus. They all share a basic multidomain structure with a high level of homology and are involved in such diverse processes as mitogenesis, cell survival, adhesion, motility, differentiation. SFKs have a key role in controlling signals from a set of cell surface receptors such as growth factor receptors, G protein-coupled receptors, antigen receptors, cytokine receptors, and integrins [128].

Src (c-Src, pp60c-Src), the founding member of the group [129] can be switched from an inactive to an active state through control of its phosphorylation state. The key regulatory element of Src is a short C-terminal domain that bears an inhibitory phosphorylation site (Tyr529) [130]. Src-mediated autophosphorylation of Tyr529 [131] inactivates Src through the interaction of pTyr529 with its SH2 domain, folding the entire peptide into a closed, inaccessible bundle [132; 133; 134]. In this inactivating process several lines of evidence also implicate the role of Csk [135; 136; 137] or its homolog Chk [138; 139] kinases.

Activation of Src occurs upon FAK activation. Active FAK binds the SH2 domain of Src, and triggers dephosphorylation of Src at Tyr529 leading to conformational change in Src to an open, accessible form [113; 115]. In addition, FAK

contains a binding site for the SH3 domain of Src that contributes to stabilization of the complex [140]. Conversely, active Src phosphorylates Tyr576, Tyr577, and Tyr925 in FAK, leading to further increased activity of FAK [141]. Besides active FAK, protein tyrosine phosphatases SHP-1 [142], RPTPα and CD45 [143; 144] also contribute to the Src molecule opening up to an active state. To acquire full catalytic activity, Src requires autophosphorylation within its kinase domain termed the activation loop (Tyr418) [145; 146], a step which occurs upon integrins directly binding to the SH3 domain of Src [147]. The mutually activated FAK/Src complex then initiates a cascade of phosphorylation events and protein-protein interactions to trigger several signaling pathways [106].

1.2.3.3. Paxillin

Paxillin was detected as a 68 kDa phosphotyrosine containing protein in RSV-transformed cells, and was later purified from smooth muscle cells [148; 149]. As a molecular adapter, it provides multiple docking sites at the plasma membrane for an array of intracellular signaling and structural proteins. Paxillin localizes to focal adhesions through its C-terminal domains, yet it is still unclear whether it directly or indirectly associates with integrin tails. Nevertheless, there is evidence for direct association of paxillin to growth factor receptors.

The active FAK/Src complex is known to interact and phosphorylate the N-terminus of paxillin (Tyr31 and Tyr118), that is cell adhesion to ECM via transmembrane integrins results in increased tyrosine phosphorylation of paxillin. Although it is not known as an actin-binding protein, paxillin activation is accompanied by the appearance of organized actin-containing stress fibers. This association of paxillin with filamentous actin occurs indirectly through vinculin and actopaxin proteins [150; 151]. Activation of paxillin allows recruitment of downstream effector molecules to facilitate cell motility [152; 153; 154]. In particular, phosphorylation of paxillin at Tyr118 by active FAK/Src complex allows paxillin to bind to Crk proteins that have been shown to be crucial in the regulation of cell migration [150; 155; 156; 157].

1.3. Mammalian amine oxidases

Amine oxidases, the major enzyme family of biogenic amine metabolism, are considered to be biological regulators, especially for cell growth and differentiation. Members of the amine oxidase superfamily catalyze oxidative deamination reactions, through which the amine substrate hydrolyses to an aldehyde, H_2O_2 and ammonia or amine (**Figure 1**).

$$R\text{-}CH_2\text{-}NH_2 + H_2O + O_2 = R\text{-}CHO + H_2O_2 + NH_3$$

Figure 1. The summarized oxidative deamination reaction catalyzed by amine oxidases.

Mammalian amine oxidases are divided into two groups based on their cofactors, which is either flavin-adenine dinucleotide (FAD) or a copper atom and a quinone cofactor (Table 1). Monoamine (MAOs) and polyamine oxidases (PAOs) are familiar examples to the group of FAD containing amine oxidases. MAOs are found bound to the outer membrane of mitochondria in most cell types, they inactivate neurotransmitters, catabolize monoamines ingested in food [158]. PAOs are principal enzymes in the process of biodegradation and in the back-conversion pathway of polyamines, such as spermine and spermidine [159]. Based on the type of quinone cofactor, there are two types of copper dependent quinine containing amine oxidases present: topaquinone (TPQ) and lysyltyrosyl quinone (LTQ) containing amine oxidases [160; 161; 162]. TPQ containing amine oxidases include diamine oxidase (DAO), semicarbizide-sensitive amine oxidase (SSAO) or vascular adhesion protein-1 (VAP-1). DAO catalyzes the degradation of compounds such as histamine [163]. SSAO circulates in the plasma, while its membrane-bound form, VAP-1 is found in various tissues and organs, with multiple functions [164]. The LTQ quinine containing copper amine oxidases are known as the lysyl oxidase enzyme family [9; 165].

Table 1 – Mammalian amine oxidases, their cofactors and substrates

Amine oxidase family	Cofactor	Substrate
MAO	FAD	arylalkyl amines
PAO	FAD	di- and polyamines
DAO	copper and TPQ	diamines
SSAO/VAP-1	copper and TPQ	monoamines
LOX and LOX-like	copper and LTQ	peptidyl lysines and hydroxylysines

1.3.1. Lysyl oxidases

Human lysyl oxidases form a multigene family comprising five known members: lysyl oxidase (LOX, LO, protein-lysine 6-oxidase), lysyl oxidase like protein (LOXL, LOL), lysyl oxidase like protein-2 (LOXL2, LOR-1), lysyl oxidase like protein-3 (LOXL3, LOR-2), and lysyl oxidase like protein-4 (LOXL4, LOXC) (**Figure 2**). Genes for these five enzymes are scattered throughout the genome. Based on the human genome data at Ensembl (http://www.ensembl.org), *lox* spans 11.9 kb on chromosome 5q23 with 7 exons; *loxl* spans 25.7 kb on chromosome 15q24 with 7 exons; *loxl2* spans 106.9 kb on chromosome 8p21 with 14 exons, *loxl3* spans 21.1 kb on chromosome 2p13 with 14 exons; and *loxl4* spans 20.6 kb on chromosome 10q24 with 15 exons.

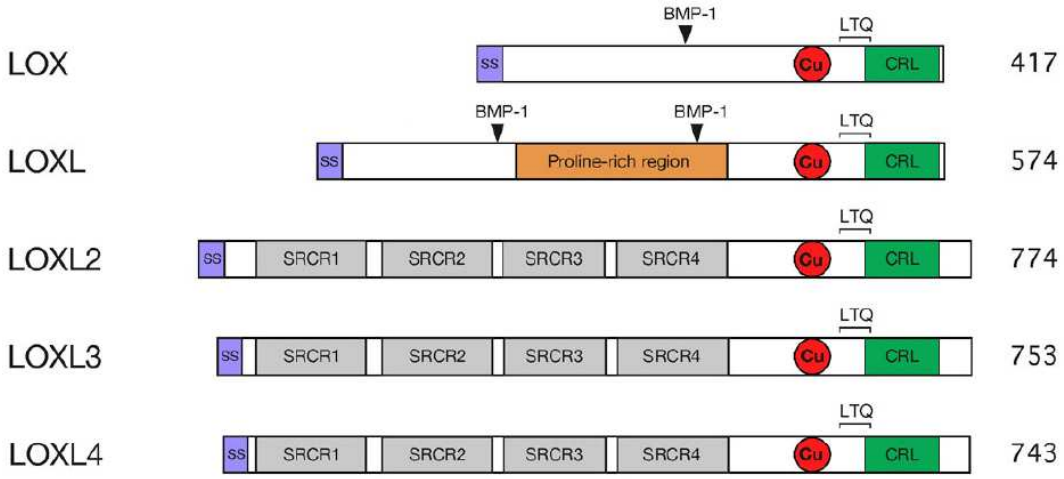

Figure 2. The basic structure of human lysyl oxidases. Predicted peptide domains are highlighted by different colors: signal peptides (purple), the proline-rich region (orange), SRCR domains (gray), copper-binding region (red), CRL domain (green). Formation of the unique LTQ cofactor is also shown. Predicted proteolytic processing sites by BMP-1 are indicated by arrows. The numbers of amino acids in each protein are denoted on the right.

Among all members of the family, the carboxyl termini share high degree of homology, including the cytokine-receptor like (CRL) domain. The CRL domain is named after its sequence homology to the class I superfamily of cytokine receptors [166]. However, the detailed function for the CRL domain in the lysyl oxidase family is yet to be elucidated. A recent report from our laboratory suggests that the CRL domain may stabilize interactions between lysyl oxidases and other proteins like fibronectin [167]. The catalytic domain containing copper- and quinine-cofactor binding sites is also a highly conserved among all lysyl oxidases. Copper binding is essential in the formation of the functional holoenzyme [168]. Atomic absorption spectroscopic studies have demonstrated that one tightly bound copper atom is present in each lysyl oxidase monomer [168; 169; 170]. The posttranslational modification of copper into lysyl oxidases occurs during protein trafficking through the endoplasmic reticulum and Golgi elements [171; 172]. The actual copper binding motif is considered to be a 14 amino acid long peptide segment, containing four histidine residues in conserved positions [173]. Aside from the main role of bound copper, that is electron transportation during oxidative deamination reactions [168], it has also been proposed that bound copper internally catalyses LTQ co-factor formation [174]. The LTQ structure is derived from the cross linking of the ε amino group of a peptidyl lysine (Lys304 bovine) with the modified side chain of a tyrosyl residue (Tyr 349 bovine) [175; 176]. The LTQ cofactor is unique to the lysyl oxidase family of enzymes, and the residues involved are highly conserved. Similar to copper binding, LTQ could be formed in the RER or Golgi [172]. The LTQ participates directly in the oxidation reaction [177], and it has been demonstrated that although bound copper is only partially [174], the LTQ is necessary for the lysyl oxidase catalytic activity [175; 176]; thus the C-terminal regions of lysyl oxidase correspond to their catalytic domains. Thus, enzymatically active lysyl oxidases oxidatively deaminate specific peptidyl lysine and hydroxylysine residues in their substrates, in the presence of molecular oxygen. As a side product, H_2O_2 and ammonia

is released (**Figure 3**). The ammonium ions can actually contribute to the formation of certain types of covalent crosslinks between the modified amino acid residues [178], and at the same they are reversible competitive inhibitors of lysyl oxidases [179]. Potential roles of H_2O_2 are discussed later in this chapter.

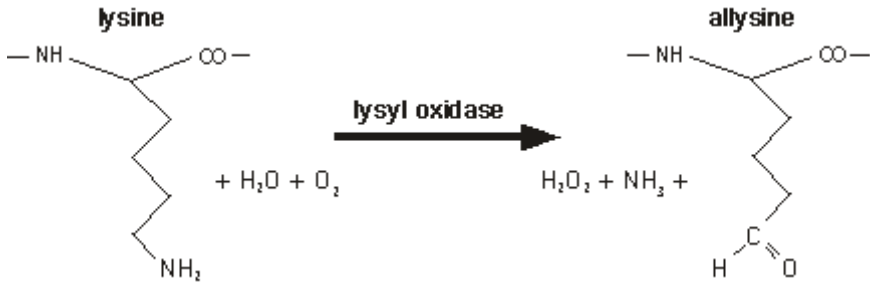

Figure 3. The oxidative deamination reaction catalyzed by lysyl oxidases. Active lysyl oxidases oxidatively deaminate peptidyl lysine to generate peptidyl allysine residues. The reactive aldehyde group of the allysine is then spontaneously able to react with another peptidyl lysine or allysine to form a covalent cross-link within or between proteins [180].

The amino termini of lysyl oxidases are more variable than their carboxyl termini. LOXL contains a unique proline-rich region, whereas LOXL2, LOXL3, and LOXL4 each contain four scavenger receptor cysteine-rich (SRCR) domains [181]. SRCR domains are typically found in cell membrane associated proteins with complex functions: SRCRs recognize, bind, and help the internalization of a wide range of negatively charged macromolecules, thus participating in cleaning up cellular debris, pathogenic microorganisms, or other potentially harmful compounds; or if SRCRs remain on the cell surface, they mediate cell adhesion [182]. SRCR domains in lysyl oxidases show occasional sequence variations [183; 184], which suggests differential substrate specificity among LOXL2, LOXL3, and LOXL4. However, the exact function of SRCR domains in lysyl oxidases remains to by elucidated. In LOX and LOXL, where SRCR domains are absent [185; 186; 187], the amino termini of the full length peptides have also been shown to determine substrate specificity [188]. Moreover, the N-terminal region of both LOX and LOXL3 contain a putative nuclear localization signal, which has not been described in other members of the family [189; 190]. The possible nuclear localization of LOX and LOXL3, and the observed nuclear localization

of LOX, LOXL, and LOXL3 further broadens the substrate palette of the oxidative deamination reaction catalyzed by lysyl oxidases [191; 192; 193; 194; 195].

Regardless of individual variety among family members, all lysyl oxidases contain a signal sequence for secretion at the very end their amino termini, indicating that all lysyl oxidases are potentially extracellular enzymes, where they first find the interacting substrates, and upon proteolytic activation they gain catalytic activity [9]. On the whole, due to the high degree of structural homology among family members, lysyl oxidases may share common biological functions.

1.3.1.1. LOX

The human LOX protein is translated as a 48 kDa preproenzyme with an N-terminal signal sequence of 21 amino acids. During protein trafficking in the endoplasmic reticulum and Golgi, the signal peptide is cleaved off, followed by an N-terminal N-linked glycosylation, increasing the molecular mass to 50 kDa [196]. A copper atom incorporates at the copper binding site [168; 171], which initiates the formation of the lysine tyrosylquinone (LTQ) cofactor derived from Lys314 and Tyr349 residues [162; 175]. As an inactive proenzyme, LOX then gets secreted into the extracellular space [197], where it is activated by a proteolytic cleavage between amino acids Gly168 and Asp169 (numbered according to the human sequence). The process is catalyzed by the type I procollagen C-proteinase/bone morphogenic protein-1 (BMP-1), and yields an active enzyme of 32 kDa [101; 196; 198; 199]. The activation is accomplished by the same protease that cleaves the C-terminal propeptide ends of procollagen triple helical molecules, a necessary event for subsequent collagen fiber assembly [200]. Although *in vitro* assays using purified recombinant enzymes identified other procollagen C-proteinases to productively cleave the LOX precursor at the correct physiological site; BMP-1 is 3-, 15-, and 20-fold more efficient than mammalian tolloid-like 1 (mTLL-1), tolloid-like 2 (mTLL-2), and tolloid (mTLD), respectively [201; 202]. However, very little is known about the conditions surrounding the *in vivo* proteolytic activation of LOX or the LOX-like enzymes.

Administration of the specific LOX inhibitor aminopropionitrile (BAPN) to growing animals results in a disease known as lathyrism [203]. Lathyrism is a pathological condition known to cause increased fragility of connective tissues and elevated solubility of collagen due to diminished cross-linking. It is known that chronic ingestion of the sweet pea (*Lathyrys odoratus*) results in lathyrism, directly caused by the agent β-(γ-glutamyl)-aminopropionitrile present in the seed, which is metabolized to BAPN [204; 205]. Therefore, the ability of BAPN to inhibit cross-link formation was recognized even before identification of lysyl oxidase activity *in vitro* [206; 207; 208]. BAPN was found to bind covalently to the active site, as an irreversible LOX inhibitor with an inhibitory constant (K_i) of about 3-5 μM [205; 209]. Since then, BAPN has been used experimentally to specifically inhibit activities of all lysyl oxidase isoenzymes. At low concentration (10^{-4}–10^{-6} M) it has higher affinity to bind to lysyl oxidases than to other family members [209]. Based on similarity in chemical structure, other potent LOX inhibitors were also found. Irreversible inhibitors, β-haloethylamines and β-nitroethylamine target the active site of LOX, with inhibition constants similar to that of BAPN [209; 210]. Vicinal diamines like cis-1,2- diaminocyclohexane and ethylenediamine are also potent irreversible LOX inhibitors [211]. Additionally, LOX is inhibited by heparin [212], tranylcypromine [213], homocysteine thiolactone and its selenium and oxygen analogs [214], N-(5-aminopentyl)aziridine [215]. In line with the studies above, investigations focusing on the effects of dietary copper deficiency on mammalian growth and development found that limited copper intake displayed phenotypes similar to lathyritic animals with decreased number of covalent crosslinks between collagens and elastin, and premature death due to ruptures of large blood vessels [216; 217; 218; 219; 220; 221; 222; 223]. Indeed, the defected enzyme was later identified and named LOX [208].

LOX is expressed in several different cells, including fibroblasts, aortic and lung smooth muscle cells, osteoblasts [201; 224; 225; 226; 227], myofibroblasts [3], endothelial cells [225; 228], chondrocytes [225; 229], biliary epithelial cells, liver parenchymal cells, spleen reticular cells, kidney tubular epithelial cells [225]. At the tissue level, LOX is abundantly expressed in fetal and adult aorta [101; 230], placenta, skin, and lung [230].

Other than collagens and elastin discussed above, numerous other binding partners and/or substrates for LOX have been identified, including histones H1 and H2 [192; 231], Ku antigen [232], 1,5-diaminopentane (cadaverine) [233; 234], basic fibroblast growth factor (bFGF) [235], cellular fibronectin [167], transforming growth factor-beta 1 (TGF-β1) [236].

1.3.1.2. LOXL2

The first report to describe LOXL2 localizes the *loxl2* gene at the chromosome region 8p21.2–21.3 came out from our laboratory [237]. Shortly after, the structure of the *loxl2* gene has also been described, and found LOXL2 to be expressed virtually in all tissue types, at high levels in reproductive tissues [238]. Knowing the complete sequence of the *loxl2* gene has revealed that the novel lysyl oxidase-like protein WS9-14, identified around the same time and found to be involved in cell adhesion and cellular senescence [239] is certainly unlikely to be derived from the *loxl2* gene due to a number differences in the two cDNA sequences.

Catalytic activity of LOXL2 has only been demonstrated *in vitro*, in cultures of ovary epithelial cells [240]. Different from that of LOX, BAPN had no effect on the catalytic activity of LOXL2, in a concentration range successfully inhibited LOX enzyme activity. Instead, D-penicillamine was found to inhibit enzyme activity of LOXL2 [240]. This finding is to be accepted only under protest, as D-penicillamine being a general copper chelator and in this respect could affect other mechanisms in the cell besides inhibiting LOXL2 activity.

Abundant LOXL2 expression was found to accompany replicative and stress-induced premature senescence of human diploid fibroblasts [241]. Interesting analogy, that WS9-14 mRNA levels were also highly expressed in senescent fibroblasts [239]. Further supporting the role of LOXL2 in cellular senescence, the same correlation was described for LOXL2 in lung fibroblasts from patients with emphysema [242]. A previous study from the same group showed reduced *in vitro* proliferation rate and number of population doublings of parenchymal lung fibroblasts from patients with emphysema and hypothesized that these findings could be related to a premature

cellular aging of these cells [243]. Besides, LOXL2 is also expressed in osteoblasts [227; 244], kidney epithelial cells [245; 246], and at the tissue level it is abundantly expressed in reproductive organs [238] and arteries [247].

1.3.1.3. Lysyl oxidases in tumor suppression

The tumor suppressor activity of LOX was discovered when the Ras-transformed phenotype of mouse NIH 3T3 cells was reversed after interferon treatment. A markedly down-regulated cDNA species, sensitive to interferon treatment, restored the non-tumorigenic, non-transformed phenotype. Thus, the cDNA was named as Ras-recision gene (*rrg*). When *rrg*-antisense RNA was applied on these Ras-transformed cells, the reappearance of the tumorigenic phenotype was observed. Comparing cDNA sequences of the mouse *rrg* and rat *lox*, they were subsequently found to be identical, indicating that *rrg* encodes LOX [248]. Expression of LOX was down-regulated in immortalized rat 208F fibroblasts after transformation by activated H-ras, and it was upregulated in spontaneous phenotypic revertants that continued to express the Ras oncogene [249; 250]. LOX inhibitory mechanism on Ras-mediated transformation is due to activation of signal pathways that prevent the activation of NFκB [251]. Extremely interesting data which may shift the direction of research to a new direction, yet confirms the tumor suppressor role for LOX, was reported recently; the 18 kDa N-terminal LOX propeptide itself, independent from lysyl oxidase activity has been noted to induce phenotypic reversion of Ras-transformed fibroblasts [252].

Several other studies support a potential tumor suppressor role for LOX. For instance, the *lox* gene was identified as a target for the anti-oncogenic transcription factor, interferon regulatory element-1 (IRF-1), which manifests tumor suppressor activity and its inactivation contributes to the development of human hematopoietic malignancies [253]. Another set of studies detected markedly decreased LOX activity in the medium of malignantly transformed cultured human cell lines, including fibrosarcoma, rhabdomyosarcoma, choriocarcinoma, melanoma, and SV40 transformed fetal lung cells, as a consequence of low transcriptional activity [254; 255]. Similarly, down-regulated LOX mRNA expression was detected in a mouse model for prostate

cancer, where LOX was expressed in normal prostate epithelium, but the expression was progressively lost in primary prostate cancer and associated metastatic lesions [256].

1.3.1.4. Lysyl oxidases in tumor promotion

Another study examining both LOX and LOXL2 mRNA levels in head and neck SCCs provided results that actually only partially support the tumor supressor hypothesis. The LOX mRNA levels in both cell lines and tissues of head and neck SCCs was markedly reduced as opposed to benign keratinocyte cell lines and mucosal tissue samples of the upper respiratory tract. Similar results were shown for LOXL2 mRNA levels in cell lines, although no reduction of LOXL2 mRNA levels were found in the malinantly transformed tissues [257]. Indeed, contrary to the tumor suppressor hypothesis above, several studies show evidence that elevated lysyl oxidase activity can enhance cell growth, perturb tissue organization, and promote cell migration and survival [5; 6; 7; 8]. As a prognostic histological parameter in breast and colorectal carcinomas, it was recognized that the transition from a localized to an invasive tumor is associated with the formation of fibrotic foci within the primary tumor [258; 259; 260]. Lysyl oxidases have been associated with fibrotic areas of various pre-malignant and malignant tissues [261; 262; 263; 264; 265; 266; 267]. Patients with high LOX-expressing human breast and head and neck tumors have poor distant metastasis-free and overall survivals, suggesting that LOX may be required to create a niche permissive for metastatic growth [268].

Based on the high degree of sequence homology, studies aiming to explore biological functions of the newly described family member hypothesized functional relevance of LOXL2 similar to the long-known relative, LOX. This approach was successful, and identified LOXL2 as being a key component of the molecular machinery regulating tumor progression [245; 246; 257; 263; 269; 270]. The process of epithelial–mesenchymal transition (EMT), through which cells of epithelial origin acquire characteristics of mesenchymal cells including higher invasive potential is a hallmark of aggressive carcinomas [271]. Increased LOXL2 expression was shown in

cultured immortalized kidney epithelial cells that had undergone EMT [245]. Furthermore, in embryonic and adult kidney cell cultures, LOXL2 has been found to interact with and increase stability of Snail, a transcription factor crucial in EMT [246]. Additional findings derived from studies on mammary gland epithelium are congruent with those listed above. Non-invasive MCF-7 breast carcinoma cells transfected with LOXL2 were reported to be locally invasive, when injected orthotopically into athymic nude mice [263]. Elevation of LOXL2 transcript levels were detected in highly invasive compared with poorly invasive breast cancer cell lines [246; 263; 269]. The same correlation was revealed for the LOXL2 protein in breast cancer cell cultures and tissue sections [246; 263].

Seemingly conflicting data we learned from studies listed above regarding the role of lysyl oxidases in the mechanism of tumor progression raise a substantial amount of questions. Our hypotheses and experimental design were aiming to elucidate at least a fragment of those problems, and the conclusions we have drawn are discussed at the end of recent thesis.

2. Objectives

In our research summarized in present thesis, we studied LOX and LOXL2 enzyme expression in various normal and malignantly transformed cell types and tissues. We explored possible genetic and epigenetic mechanisms underlying the particular expression patterns. Subsequently, we identified functional consequences to LOX and LOXL2 expressions in those various types of cells and tissues, and investigated molecular mechanisms behind the altered phenotypes. Ultimately our studies were addressed to identify possible molecular targets for future cancer prevention and therapy.

Study I

Specific aim 1: to characterize LOX expression pattern in normal tissues of the central nervous system and in neuroepithelial tumors.

a) To characterize our new anti-LOX antibody.
b) To evaluate normal and neoplastic brain tissue arrays for LOX expression *in vivo*, using immunohistochemistry combined with confocal laser microscopy.
c) To set up an *in vitro* model system that would enable further characterization LOX expression in those tissues.
d) To evaluate LOX expression by Western blot in a normal and malignant astrocytic cell culture model.
e) To establish whether LOX produced by astrocytes is catalytically active, utilizing *in vitro* lysyl oxidase activity assays.

Specific aim 2: to investigate the effects of LOX expression in context of astrocytic tumor progression.

a) To investigate the effect of active LOX expression on the migratory behavior of astrocytic tumor cells, using an *in vitro* cell migration assay.
b) To explore molecular mechanisms underlying the functional effects of active LOX expression, specifically focusing on focal adhesion components.

c) To develop a working hypothesis to model the role of LOX in neuroepithelial tumor progression.

Study II

Specific aim 1: to characterize LOXL2 expression pattern in the normal colon and esophagus, and in colon tumors and esophageal tumors.

a) To characterize our new anti-LOXL2 antibody.
b) To evaluate normal and neoplastic colon and esophagus tissue arrays for LOXL2 expression *in vivo*, using immunohistochemistry combined with confocal laser microscopy.
c) To set up an *in vitro* model system that would enable further characterization LOXL2 expression in those tissues.
d) To study LOXL2 expression by Western blot in a normal and malignant colon and esophagus cell culture model.

Specific aim 2: to investigate possible biological mechanisms controlling LOXL2 expression in the colon and the esophagus.

a) To identify possible genetic alterations affecting *loxl2* gene locus in colon and esophageal tumors, using loss of heterozygosity (LOH) analysis.
b) To characterize *loxl2* gene promoter.
c) To determine whether epigenetic mechanisms influence *loxl2* gene expression in colon and esophageal tumors.

Study III

Specific aim 1: to characterize LOXL2 expression pattern in the normal and malignant mammary epithelium.

a) To evaluate normal and neoplastic breast tissue arrays for LOXL2 expression *in vivo*, using immunohistochemistry combined with confocal laser microscopy.
b) To set up an *in vitro* model system that would enable further characterization LOXL2 expression in those tissues.

c) To study LOXL2 expression by Western blot in a normal and malignant mammary epithelial cell culture model.

Specific aim 2: to investigate the effects of LOXL2 overexpression on breast carcinoma.

a) To establish an *in vitro* model system that stably overexpresses LOXL2, using a lentiviral expression system.
b) To determine whether LOXL2 produced by breast epithelial cells is catalytically active, utilizing *in vitro* lysyl oxidase activity assays.
c) To investigate the effect of active LOX expression on the migratory behavior of astrocytic tumor cells, using an *in vitro* cell migration assay.

Specific aim 3: to investigate possible biological mechanisms controlling LOXL2 expression in the breast epithelium.

a) To determine whether epigenetic mechanisms influence *loxl2* gene expression in breast carcinomas.

3. Materials and methods

3.1. Cell lines and cell culture conditions

Normal human astrocyte (NHA) cell line was obtained from Cambrex Bio Science (Walkerville, MD, USA), and maintained according to the manufacturer's recommendations. U87 MG (hereafter U87) and U251 MG (hereafter U251) human primary astrocytoma cell lines were obtained from the American Type Culture Collection (ATCC) (Rockville, MD, USA). Human anaplastic astrocytoma cell line U343 MG-A (hereafter U343) was obtained from the Brain Tumor Research Center, University of California, San Francisco, CA, USA. All astrocytoma cell lines were routinely maintained in Alpha Minimal Essential Medium (Gibco BRL-Invitrogen, Carlsbad, CA, USA) supplemented with 10% fetal bovine serum (FBS; Lot# FB5351, Cellgro Mediatech, Herndon, VA, USA) and 100 U/mL penicillin G sodium (Sigma, St. Louis, MO, USA), 100 µg/mL streptomycin sulfate (Sigma), 0.25 µg/mL amphotericin B (Sigma). Normal human neonatal foreskin fibroblasts (Cambrex Bio Science) were maintained in high-glucose Dulbecco's Minimal Essential Medium (Gibco BRL-Invitrogen) supplemented with 10% FBS, 100 U/mL penicillin G sodium, 100 µg/mL streptomycin sulfate, 0.25 µg/mL amphotericin B.

HCT-116, DLD-1, and HCT-15 human colon carcinoma cell lines and CRL-1831 normal human fetal colon epithelial cell line were obtained from the ATCC and propagated under conditions designated by the manufacturer. The human esophageal moderately differentiated SCC cell lines WHCO1, WHCO3, WHCO5, and WHCO6 were developed at the University of Witwatersrand, Johannesburg, South Africa under the supervision and approval after approval from the local institutional review board, and grown in DMEM with 10% FBS. EcR-293 human embryonic kidney cells (Gibco BRL-Invitrogen) with Zeocin (Gibco BRL-Invitrogen), and 10% FBS according to the manufacturer's protocol.

MCF-10A immortalized non-transformed human breast epithelial cell line was purchased from the ATCC (Rockville, MD, USA) and maintained as previously described (Debnath et al., 2003). HMEC normal human mammary epithelial cell line

was obtained from Lonza (Allendale, NJ, USA), and grown in Mammary Epithelial Growth Medium (MEGM) according to the manufacturer's protocol. MCF-7, T47D, MDA-MB-231 (hereafter MB-231) and Hs578T human breast adenocarcinoma cell lines were obtained from ATCC and maintained in Royal Park Memorial Institute (RPMI) 1640 medium (Gibco BRL-Invitrogen) supplemented with 10% FBS, 10 mM HEPES buffer (Gibco BRL-Invitrogen), 10 mM L-glutamine (Sigma) and 100 U/mL penicillin G sodium, 100 µg/mL streptomycin sulfate, 0.25 µg/mL amphotericin B. 293FT human embryonic kidney epithelial cells (Gibco BRL-Invitrogen) were cultured according to the manufacturer's instructions.

All cells were kept cultured in T25, T75, and T150 flasks (Calbiochem, San Diego, CA, USA) under sterile conditions in a humidified incubator at 37 °C.

3.2. Chemicals

For treatment of cultured cells with the DNA methylation inhibitor 5-aza-dC (Sigma), cells were seeded 24 hours prior to treatment, and then grown for three days in fresh medium containing 0, 1 or 5 µM 5-aza-dC.

For co-treatment with the histone deacetylase inhibitor TSA (Cayman Chemical Co., Ann Arbor, MI, USA), cells were exposed to 500 nM TSA for 24 hours (Fong et al., 2007). RNA was harvested on the fourth day using TriReagent (Molecular Research Center, Inc., Cincinnati, OH, USA) according to the manufacturer's protocol.

To evaluate the effect of BAPN on cell migration, cells were pre-treated with 100 µM BAPN (Sigma) for 48 hours prior to protein extraction for Western blot, 24 hours prior to migration assays and an additional 4 hours during the assay.

For catalase (Sigma) treatment of cells, 200 U/mL final concentration was used for 48 hours prior to protein extraction for Western blot analysis, 24 hours prior to and 4 hours during the migration assay. These concentrations of BAPN and catalase were shown to have no cytotoxic effect on cells [269; 272].

Cultured breast epithelial cells were grown to 75% confluency prior to treatment with HALT protease inhibitor (PI) cocktail (Pierce). For those cells treated once with PI, fresh media with 0.5x PI was added to the cells on day 0. For those cells treated

twice with PI, fresh media with 0.5x PI was added to the cells on day 0 and day 2. The control cells did not receive any treatment. Protein was harvested on day 4.

3.3. Lentiviral vector construction and viral transduction of cells

Utilizing the ViraPower Lentiviral Expression System (Invitrogen, Carlsbad, CA, USA) we generated stable MCF-10A and MCF-7 cell lines that overexpress LOXL2. The system allows creation of a replication-incompetent, HIV-1-based lentivirus which can then be used to deliver and stably express our gene of interest in either dividing or non-dividing mammalian cells. Using the pLenti/V5 Directional TOPO Cloning Kit (Invitrogen) protocol, we subcloned full length *loxl2* cDNA (GenBank accession NM_002318) with and without a C-terminal V5 epitope tag, and transformed the clones into One Shot Stbl3 Escherichia coli cells to amplify up our plasmid constructs. For the cloning step, we designed special primers, including the CACC sequence necessary for directional cloning on the 5' end of the forward primer: hLOXL2ini 5'- CAC CAT GGA GAG GCC TCT GTG -3'; hLOXL2term 5'- TTA CTG CGG GGA CAG CTG G -3'; hLOXL2V5term 5'- CTG CGG GGA CAG CTG GTT -3'. To express our recombinant proteins (LOXL2, LOXL2-V5) we cotransfected the 293FT cell line with our constructs along with the optimized ViraPower Packaging Mix (Invitrogen) using Lipofectamine 2000 reagent (Invitrogen). At the transfection step we used the 293FT virus producer cells in adherent stage.

Virus-containing supernatants were collected, sterile filtered and titered. MCF-10A and MCF-7 cells were transduced in the presence of 6 µg/mL Polybrene (Sigma) to enhance viral transduction efficiency, and cultured in the presence of 5 µg/mL Blasticidin (Invitrogen) for 12 days to select for successfully transduced cells. Single cells were isolated using QuixellTM cell selection and automated transfer system (Stoelting; Wood Dale, IL, USA) to establish stable, monoclonal MCF-10A and MCF-7 cell lines that overexpress LOXL2. Results shown were obtained by summarizing individual data of quantitative and qualitative assays performed on at least three different monoclonal cell lines.

3.4. Southern blot analysis

PAC clone 17460, containing exons 3-13 of the *loxl2* gene, was obtained from Genome Systems (St. Louis, MO, USA). Purification of plasmid DNA followed manufacturer's protocol. Plasmid DNA was digested with *Eco*RI and *Bam*HI restriction enzymes, electrophoresed on a 0.8% agarose gel, transferred to Hybond-N+ membrane (Amersham, Piscataway, NJ, USA), and hybridized to a ^{32}P-labeled $(dCA)_{10}$ probe to detect (CA) repeat sequences. Sequence analysis was previously described in its details [238].

3.5. Microsatellite analysis

Primers flanking the novel microsatellite within intron 4 of the *loxl2* gene were designed: LOXL2ms1 5'-GCT GAG TAC AGA CGC TGA TGC-3'; LOXL2ms2 5'-GGT GAT GAG TGA TCG ACG GTC-3'. One primer was end-labeled with T4 polynucleotide kinase and 32P-γATP. PCR was performed in a final reaction volume of 25 µL with 50 mM KCl, 10 mM Tris-HCl (pH 8.3), 1.5 mM MgCl2, 20 ng genomic DNA, 1 µM each primer, 124 µM each dNTP, and 0.5 µM AmpliTaq (Applied Biosystems, Foster City, CA, USA). The termocycle profile was an initial denaturation step of 94 °C for 3 min, 30 sec each at 94, 55, and 72 °C for 30 cycles, and a final extension of 72 °C for 7 min. Labeled amplimers were denatured at 94 °C for 5 min, then subject to denaturing 6% PAGE. Autoradiography was performed with Fuji RX-U film (Fuji Medical Systems, Stanford, CA, USA) overnight at −80 °C.

Blood and tumor sample pairs that were homozygous for the microsatellite marker were uninformative. LOH was determined if one of the normal alleles was absent or at least diminished by ~ 50% in tumor DNA quantification using an image acquisition/analysis system (Ambis, San Diego, CA, USA). Allelic imbalance (AI) was determined if one of the alleles from tumor tissue was greater in intensity than the matching normal allele, or if the two alleles from tumor DNA differed in the ration of intensity, when compared to the alleles in normal DNA. Although AI can result from

either loss of an allele, amplification, of heterogeneity, we grouped LOH and AI as in our previous study [273], as they both indicate a contribution of this gene in tumor development.

3.6. Promoter analysis

The *Homo sapiens* chromosome 8 genomic contig sequence (NT023666) containing the entire *loxl2* gene spanning 107 kb of genomic sequence was used for genomic analysis. The entire sequence was analyzed for the presence of CpG islands using the GrailEXP CpG Island Locator (http://compbio.ornl.gov/grailexp/). Promoter analysis was performed on ~5 kb of sequence upstream of the predicted transcriptional start using Match and P-Match algorithms (http://www.gene-regulation.com) and Transcription Regulatory Regions Database (http://wwwmgs.bionet.nsc.ru/mgs/gnw/trrd/)[274].

3.7. Northern blot analysis

Total RNA was isolated from cultured cell lines grown to 80-90% confluency, using RNA STAT-60 (Tel-Test, Friendswood, TX, USA). Five micrograms of RNA for each esophageal cell line and from a normal esophagus tissue sample was electrophoresed though a 1.2% agarose gel containing 2.6 M formaldehyde, 20 mM MOPS, and 1 mM EDTA. Following hydrolysis, the RNA was transferred to Hybond-N+ membrane (Amersham) overnight with 20x saline-sodium citrate buffer. For the remainder of the cell lines, 10 µg of RNA from each sample was electrophoresed as above except that the gel contained 0.66 mM formaldehyde. A ^{32}P-random primer labeled human *loxl2* cDNA clone [238] was used for hybridization. The blots were washed and exposed to a phosphoimager plate. The blots were then re-probed with ^{32}P-labeled human *gapdh* cDNA control (Clontech, Mountain View, CA, USA).

3.8. Real time qPCR analysis

Total RNA was isolated from cells with Tri Reagent (Molecular Research Center Inc, Cincinnati, OH). 1 µg RNA was used to prepare cDNA, using Superscript II First-Strand Synthesis SuperMix (Invitrogen) with random hexamer primers following the manufacturer's standard protocol followed by RNase H treatment (37 °C, 20 min). PCR reactions were performed using DNA Engine Opticon 2 system (MJ Research-Biorad, Hercules, CA, USA) and SYBR Green qPCR Kit (New England Biolabs, Inc., Ipswich, MA, USA). A 368 bp LOX fragment was amplified using a forward primer 5'-GAT CCT GCT GAT CCG CGA CAA-3' and reverse primer, 5'-GGG AGA CCG TAC TGG AAG TAG CCA GT-3'. For LOXL2, a 364 bp fragment was amplified using forward primer 5'-GGA GGT GTT CAC CCA CTA TGA CC-3' and reverse primer 5'-CGC TGA AGG AAC CAC CTA TGT GG-3'. As control for RNA integrity and loading in cDNA reactions, a 268 bp GAPDH fragment was amplified using forward 5'-GGC TCT CCA GAA CAT CAT CCC TGC-3' and reverse 5'-GGG TGT CGC TGT TGA AGT CAG AGG-3' primers. Each reaction contained 1 µL cDNA, 12.5 µL 2x DyNAmo Hot Start SYBR Green qPCR mixture (New England Biolabs) and 1 µM of each primer in a 25 µL total volume. Initial denaturation occurred at 95 °C for 10 min. Each cycle consisted of a 94 °C 10 sec denaturation, 59 °C 30 sec annealing, and 72 °C 45 sec elongation, for 40 cycles. Fluorescence was measured at the end of every extension step at 81 °C for LOXL2, at 82 °C for GAPDH, and at 86 °C for LOX. Product specific amplification was confirmed by melting curve analysis, at a range from 65 °C to 92 °C by 0.2 °C steps. Linear amplification started between cycles 15 and 30. The cycle threshold line was established at the linear portion of the log scale curve using DNA Engine Opticon 2 system (MJ Research-Biorad). The ratio of LOX and LOXL2 to GAPDH was calculated using the $2^{-\Delta\Delta C}{}_{T}$ method [275]. Reactions were done in triplicates, statistical analysis was performed using Student's t-test and Prism 4, version 4.0b (GraphPad Software, San Diego, CA, USA) software.

3.9. Western blot analysis

For experiments using conditioned cell media (CCM), cells were grown to confluent, complete growth medium was aspired, cells were washed with PBS/TBS, and incubated with serum-free, phenol-red-free media supplemented with MITO+ serum extender (BD Biosciences, San Jose, CA, USA) for 2-3 days. The CCM was then centrifuged at 3,000 rpm for 10 minutes to pellet any remaining cells, and transferred to a fresh tube and kept on ice until used. To concentrate total protein from the CCM, StrataClean Resin (Stratagene, La Jolla, CA, USA) was added, samples were then vortexed, and mixed for 30 min at 4 °C. After centrifugation at 14,000 rpm for 1 min the supernatant was aspirated and resin was resuspended in Laemmli buffer (125 mM Tris-HCl (pH 6.8), 4% SDS, 20% glycerol, 100 mM DTT). The sample was boiled for 5 min and kept on ice until analyzed by Western blotting.

For experiments using the cell lysate fraction (CL), cells were grown to confluency, rinsed with PBS/TBS, and incubated with the cocktail of M-PER mammalian protein extraction reagent (Pierce, Rockford, IL, USA) supplemented with HALT protease inhibitor cocktail for 5 min on ice. When needed, phosphatase inhibitors Na_3VO_4 (1 mM, Sigma) and NaF (10 mM, Sigma) were also added. Cell lysed were then centrifuged at 10,000 rpm for 10 minutes. The insoluble M-PER pellets, representing insoluble membrane-bound and membrane-associated proteins, were collected (ISCL; insoluble cell lysate) and the soluble M-PER fraction, representing cytoplasmic and nuclear proteins, was acetone-precipitated and centrifuged (APSCL; acetone precipitated soluble cell lysate). Desired amounts of CCM, ISCL and APSCL protein samples were reconstituted in Laemmli buffer, boiled for 5 min and kept on ice until analyzed by Western blotting. For experiments looking at intracellular phosphorylation, cell layer was rinsed with TBS as PBS can interfere with phospho-specific antibody targeting.

Protein concentration measurements were performed with Bradford analysis using Polarstar Optima microplate reader (BMG Labtechnologies; Durham, NC, USA), as well as Ponceau S staining (Sigma) of the membranes to ensure equal loading. Typically, each protein sample contained 20 µg total protein per lane when resolved in the polyacrylamide gel. The protein samples were size separated on NuPAGE 4-12% Bis-Tris polyacrylamide gels (Invitrogen), using XCell SureLock Mini-Cell system. MagicMarkXP, SeeBlue Plus2 (Invitrogen), or NEB Broad Range Marker (New

England Biolabs, Inc.) were used for protein molecular weight standards. Proteins from the gels were transferred onto a methanol pretreated Immobilion-P PVDF membrane (Fisher, Billerica, MA, USA) using wet transfer XCell II Blot Module system. All equipments used for protein electrophoresis were purchased from Invitrogen. After protein transfer, membranes were blocked with 5% non-fat dry milk in PBST/TBST overnight at 4 °C. Membranes were washed in PBST/TBST, and the primary antibody diluents were applied on the membranes for 1 hour at room temperature.

The following antibodies were used: affinity purified rabbit polyclonal anti-LOX (1:1000, Covance Research Products, Denver, PA, USA)(characterized in Study I); affinity purified rabbit polyclonal anti-LOXL2 (1:1000 - 1:2500, Zymed Laboratories, South San Francisco, CA, USA)(characterized in Study III); goat polyclonal anti-GAPDH (1:1000, Abcam, Cambridge, MA, USA); rabbit anti-BMP-1 (1:3000, Affinity Bioreagent, Golden, CO, USA); mouse anti-fibronectin (1:1000, Molecular Probes-Invitrogen, Carlsbad, CA, USA); rabbit anti-FAK(pTyr576) (1:1000, Biosource Inc., Camarillo, CA, USA); rabbit anti-paxillin(pTyr118) (1:1000, EMD Biosciences Calbiochem, San Diego, CA, USA); chicken anti-GFAP (1:100,000, EnCore Biotechnology, Alachua, FL, USA); mouse monoclonal anti-V5 (1:5000, Invitrogen), goat anti-GAPDH (1:1000, Abcam, Cambridge, MA). Following incubation with primary antibodies, membranes were washed in PBST/TBST and incubated with anti-rabbit, anti-mouse (1:2500 – 1:5000, Amersham), anti-chicken and anti-goat (1:10,000 Jackson Immuno Research, Baltimore, PA, USA) horseradish peroxidase conjugated secondary antibodies for chemiluminescent detection. Subsequently, membranes were washed in PBST/TBST and PBS/TBS and incubated with ECL plus Western blot reagent mix (Amersham). To ensure even sample loading and gel transfer PVDF membranes were stripped (100 mM β-mercaptoethanol (Sigma), 2% SDS, 62.5 mM Tris-HCl pH 6.7, 55 °C, 30 min) and reprobed for internal controls based on a previously described method [276].

3.10. Immunocytochemical and immunohistochemical analyses

Astrocytes were grown on glass coverslips in tissue culture plates. Growth media were aspired, cells washed with PBS and fixed in 4% paraformaldehyde-PBS for 10 min. Fixed cells were permeabilized with 0.5% Triton X-100 (Sigma) and rinsed in PBS prior to the immunostaining procedure. Formalin-fixed and paraffin-embedded normal human brain tissue sample macroarrays were purchased from Novagen (San Diego, CA, USA). Tissue arrays containing human brain tumor tissue specimens were purchased from Cybrdi Inc. (Frederick, MD, USA) and contained grade I-IV astrocytic neoplasms, and normal brain tissue samples from male and female individuals aged 15-64 years. These included specimens from 21 individuals, 16 of which were from patients with different grades of astrocytic tumors. The array typically represented three sections from each patient specimen. There was a single sample from a grade I patient; five grade II patient samples; six grade III patient samples; and five grade IV patient samples. The samples were classified by a neuropathologist at Cybrdi Inc., according to the WHO classification guidelines. Sections were sequentially deparaffinized in xylene and rehydrated through steps of graded ethanol. Citrate buffer antigen retrieval method was applied as needed. Slides with tissue sections were rinsed with PBS and permeabilized with 0.5% Triton X-100. In immunocyto- and immunohistochemical detections, prior to adding primary antibodies, 0.1% bovine serum albumin (BSA)-PBS blocking was applied for 30 min to reduce unspecific staining. Primary antibodies were diluted in 1% BSA-PBS and applied on slides for 2 hours. The following primary antibodies were used: affinity purified rabbit anti-LOX in 12:1000 dilution (described in Kirschmann 2002), chicken anti-GFAP (EnCore Biotechnology, Alachua, FL, USA) in 1:5000 dilution; non-immunized rabbit and chicken IgG (Zymed) in 1:250 dilution, as negative controls. Cells or sections were washed several times in PBS and incubated with secondary antibodies: anti-rabbit Alexa Fluor 488 and anti-chicken Alexa Fluor 594 conjugated antibodies (Molecular Probes-Invitrogen) in 1:400 dilutions for 40 min. To visualize the cytoskeleton of astrocytes, phalloidin-red (Molecular Probes-Invitrogen) was applied to cells for 20 min following secondary antibody incubation. Cells and sections were mounted by Vectashield mounting medium that contained DAPI (Vector Laboratories, Burlingam, CA, USA) to label nuclei. Samples were analysed with Zeiss LSM 5 Pascal Confocal Inverted Microscope (Thornwood, NY, USA). The tissue sections were evaluated for LOX and GFAP expression by counting

positively stained cells in random multiple fields in each tissue section for each tumour grade. Scores were 1-5, based on the percentage of stained cells: 1 for samples with less than 20% and 5 for those over 80% of cells positively stained. Evaluation was performed by two individuals independently, and data were analysed using Student's t-test and Graphpad Prism software.

Formalin-fixed and paraffin-embedded histoarray slides containing tissue sections from 52 colorectal cancer samples, 50 esophageal cancer samples, and 58 normal colon samples were obtained from Imgenex Corporation (San Diego, CA, USA). In addition, macroarray slides containing normal colon and esophagus tissue were obtained from Novagen (La Jolla, CA, USA). Sections were deparaffinized, rehydrated, and antigen retrieval was performed by immersion in 0.1 M citrate buffer and heating in a microwave oven at high, medium, and low power for 5 min each. The sections were blocked with normal goat serum (NGS, Pierce) for 30 min, primary antibodies were diluted in 1% NGS-PBS and applied for 2 hours: either the rabbit anti-LOXL2 antibody (**described in Study II**) in 1:300 dilution, or 4 µg/mL rabbit IgG (Zymed) as negative control. Alexa Fluor 488-labeled goat anti-rabbit IgG secondary antibody (Molecular Probes, Eugene, OR, USA) was diluted 1:200 in 1% NGS-PBS and applied for 45 min. The sections were mounted with Vectashield Mounting Medium for fluorescence with DAPI (Vector Laboratories, Burlingame, CA, USA). Images were obtained using Zeiss LSM 5 Pascal confocal inverted microscope (Carl Zeiss, Thornwood, NY, USA) and the LSM 5 Pascal software, version 3.0. The tumor tissue slides were evaluated under a 63x objective. The maximum number of LOXL2 expressing cells per field were evaluated on two separate occasions, and scored as follows: 0, no LOXL2 expressing cells noted; 1, 1-5 LOXL2 expressing cells/field; 2, 6-10 LOXL2 expressing cells/field; 3, 11-20 LOXL2 expressing cells/field; 4, 21-40 LOXL2 expressing cells/field; and 5, more than 41 LOXL2 expressing cells/field. Statistical analysis was done using GraphPad Prism 3.0 (GraphPad Software, San Diego, CA, USA). Three-way analysis was performed using Kruskal-Wallis test and two-way analysis was performed using the Mann-Whitney test. A p value <0.05 was considered statistically significant.

A formalin-fixed, paraffin-embedded histoarray slide containing human tissue sections from various cancers and normal adjacent tissues, including 1 normal human

breast tissue sample and 1 infiltrating ductal carcinoma tissue sample, were obtained from Imgenex (San Diego, CA). Sections were deparaffinized, rehydrated, blocked with 5% normal goat serum (NGS; Pierce; Rockford, IL) for 30 min, then incubated with either the LOXL2 antibody (1:300, Fong et al, 2007) or rabbit IgG (4 lg/ml; Zymed; negative control) in 1% NGS for 2 h, followed by Alexa Fluor 488-labeled goat anti-rabbit IgG secondary antibody (1:200; Molecular Probes) in 1% NGS for 45 min. The sections were mounted with Vectashield Mounting Medium for Fluorescence with DAPI (Vector Laboratories, Burlingame, CA). Images were obtained using the Zeiss LSM 5 Pascal (Carl Zeiss) and the LSM 5 Pascal software, version 3.0.

3.11. Lysyl oxidase activity assay

The lysyl oxidase enzyme activity assay was measured with the Amplex Red fluorescence assay kit (Molecular Probes, Eugene, OR, USA), using a previously described method [234], which we adapted for use in a microplate format. The assay detects the presence of H_2O_2, produced by the activity of any amine oxidase, using urea and borate buffers to optimize activity of the lysyl oxidase family members. Briefly, cells were grown to 3-day post-confluency, washed with PBS, and incubated with serum-free, phenol-red-free media for another 3 days. The CCM was centrifuged at 3,000 rpm for 10 minutes to pellet any remaining cells and concentrated using 10,000 molecular weight cut-off Amicon Ultra centrifugal filter units (Millipore, Bedford, MA, USA). Aliquots of CCM containing a total of 100 µg protein were added to the reaction mixture of 50 mM sodium borate (pH 8.2), 1.2 M urea, 50 µM Amplex Red, 0.02 U/mL horseradish peroxidase (Sigma), and 10 mM 1,5-diaminopentane (cadaverin) substrate (Sigma). The reaction mix was incubated at 37 °C, in the presence or absence of 500 µM BAPN. The fluorescent product was excited at 560 nm, and the emission was read at 590 nm every 5 min for 2 hours, using Polarstar Optima plate reader. The lysyl oxidase activity was calculated as the increase in fluorescent units over time above that of the BAPN controls. Triplicate samples were used to decrease experimental error. Statistical analysis was performed using Prism 4, version 4.0b (GraphPad Software, San Diego, CA). In case of breast epithelial cells, two-way analysis comparing clonal cell

lines to parental cell lines was performed using the Mann–Whitney test. A p-value <0.05 was considered statistically significant and a p value <0.01 was considered statistically very significant. CCM fractions of normal human neonatal foreskin fibroblasts served as positive controls.

3.12. Cell migration assay

To evaluate *in vitro* cell motility, we utilized the MICS (Membrane Invasion Chamber System) assay [277]. Equal amounts (5 x 10^4/well) of cells were suspended in serum-free media and seeded onto a gelatin coated polycarbonate membrane with pores of 10 µm in diameter. For astrocytes, serum-free media were supplemented with G5 Supplement (Invitrogen). The bottom chambers of the device had complete serum-containing growth medium as chemoattractant. After 4-6 hours running the assay non-migratory cells from the top surface of the membrane were wiped away, cells that invaded through the membrane were fixed in methanol for 5 min, subsequently stained with the Hema-3 Stain Kit (Fisher Scientific, Houston, TX, USA) and counted. The whole membrane was scored under a phase contrast microscope and the assay was performed six times for each cell line. Statistical significance was established if $p<0.05$, a p value <0.01 was considered statistically very significant. Data were calculated using Prism 4.0b. For breast epithelial cells, two-way analysis comparing clonal cell lines to parental cell lines was performed using the Mann–Whitney test.

3.13. Patient population

Colon tumor samples, collected by Muhlenberg Hospital and Robert Wood Johnson Medical School, New Jersey, USA, of normal (whole blood) and tumor tissue were obtained from consenting patients undergoing surgery for colon cancer, with no obvious family history, after approval from the local institutional review board. After standard histological assessment, representative tissue samples were frozen in liquid nitrogen and stored at −80 °C. DNA isolation was performed for blood [278] and tissue

(QIAamp Tissue Kit; Qiagen Inc., Valencia, CA, USA). The composition of the 65 patient panel was 54% female and 46% male, between 35 and 89 years of age, with an average of 70.6 years (standard deviation of 11.5 years). All tumors were adenocarcinoma, with 30% removed from the proximal colon and the remainder from the distal colon. The majority of the tumors were Stage B (73%), followed by Stage C (14%), Stage A (9%), and Stage D (4%).

Esophageal tumor panel samples were collected by the University of Cape Town, South Africa, and were obtained by endoscopy, from the tumor and normal portion of the esophagus, from consenting patients, after local institutional review board approval. Biopsies were frozen in liquid nitrogen and stored at −80 °C until DNA extraction [279]. The 62 patient panel was 22.6% female and 77.4% male, in this male-predominant disease. The ethnic composition was 74.2% black, 22.6% colored, and 3.2% white. The age range was 38-85 years, with an average of 60.4 years (standard deviation of 11.3 years). All esophageal tumors were SCC, located at the middle third of the esophagus. The majority of the tumors were Stage 3 (83%), followed by Stage 4 (9%), Stage 2 (4%), Stage 1 (2%), and Stage 0 (2%).

4. Results

Study I

4.1. LOX antibody characterization

Affinity-purified rabbit anti-LOX antibody was generated using a peptide sequence that corresponded to the last 20 amino acids of human LOX (residues 398–417: CDIRYTGHHAYASGCTISPY, Covance Research Products, Denver, PA, USA). The sequence is conserved in both mouse and rat LOX, and it is unique among the LOX-like enzyme family. Furthermore, the antibody did not cross-react with other recombinant LOX family members (data not shown). On Western blots of CL and CCM fractions of cultured neonatal foreskin fibroblasts, the antibody detected the predicted 48-, 50- and 30-kDa protein bands (not shown).

4.2. LOX is expressed by normal and malignant astrocytes *in vivo*

To determine LOX expression pattern in the CNS, we first performed LOX and GFAP co-immunostaining on a normal human brain tissue set. The array comprised formalin fixed paraffin embedded samples from six different regions of the normal human brain. LOX expression alone was detected in various regions of the brain parenchyma, in a punctate, likely extracellular fashion. Abundant LOX staining was present in walls of blood vessel too (not shown). LOX was also detected in certain cell types of the cerebellum; in cells of the granular and molecular layers, and in Purkinje cells. LOX and GFAP co-staining was observed in the areas of corpus callosum, cerebellum, cerebral cortex, and mesencephalon (**Figure 4. A, B, C, D**). In the area of corpus callosum, and in general, in areas of white matter, the predominant form of astrocyte is the fibrous astrocyte, characterized by the presence of abundant amounts of GFAP intermediate filaments in the cytoplasm. Fibrous astrocytes in the corpus

callosum showed strong LOX expression as well, associated with glia fibrils (**Figure 4. A**).

Subsequently, to investigate LOX and GFAP expression pattern in astrocytic tumors, we stained a second tissue array containing normal and grade I–IV astrocytic tumor samples. In this array, location from where the sample was isolated was not specified, only the age and the gender of the patients were stated. In the normal brain tissue sections, the same staining pattern was noted as in the previous tissue set, with similar occurrence for LOX-GFAP co-staining. Grade I tumor samples demonstrated faint GFAP positivity within astrocytes, some of those co-expressing LOX, detected as dense, evenly distributed intracellular staining. The ECM also showed punctate immunoreactivity for LOX (**Figure 4. E**). In grade II tumor samples, perinuclear LOX staining was present in tumor, simultaneously stained for GFAP (**Figure 4. E**). Some of the grade II tumor samples demonstrated fibrotic bundles, and in these samples, LOX staining was distributed mostly along fibrous structures (not shown). In grade III tumors, LOX staining was present mostly in the cytoplasm of tumor cells and in certain groups of cells LOX co-stained with diminished GFAP (**Figure 4. G**). In some grade III tumor samples, in areas of high cell density LOX staining was very intense within cells and appeared to fill cell bodies. In grade IV tumor sections, GFAP was either greatly diminished or undetectable, whereas LOX expression was observed in almost all tumor cells as intense perinuclear staining, strong staining within the cytoplasm and processes of astrocytes, and as abundant punctate staining that appeared to be in the ECM (**Figure 4. H**).

Evaluation of these tissue sections for LOX protein expression revealed that LOX immunoreactivity was significantly higher in all tumor grades compared with normal CNS sections. In contrast, GFAP expression was significantly diminished with increasing tumor grade.

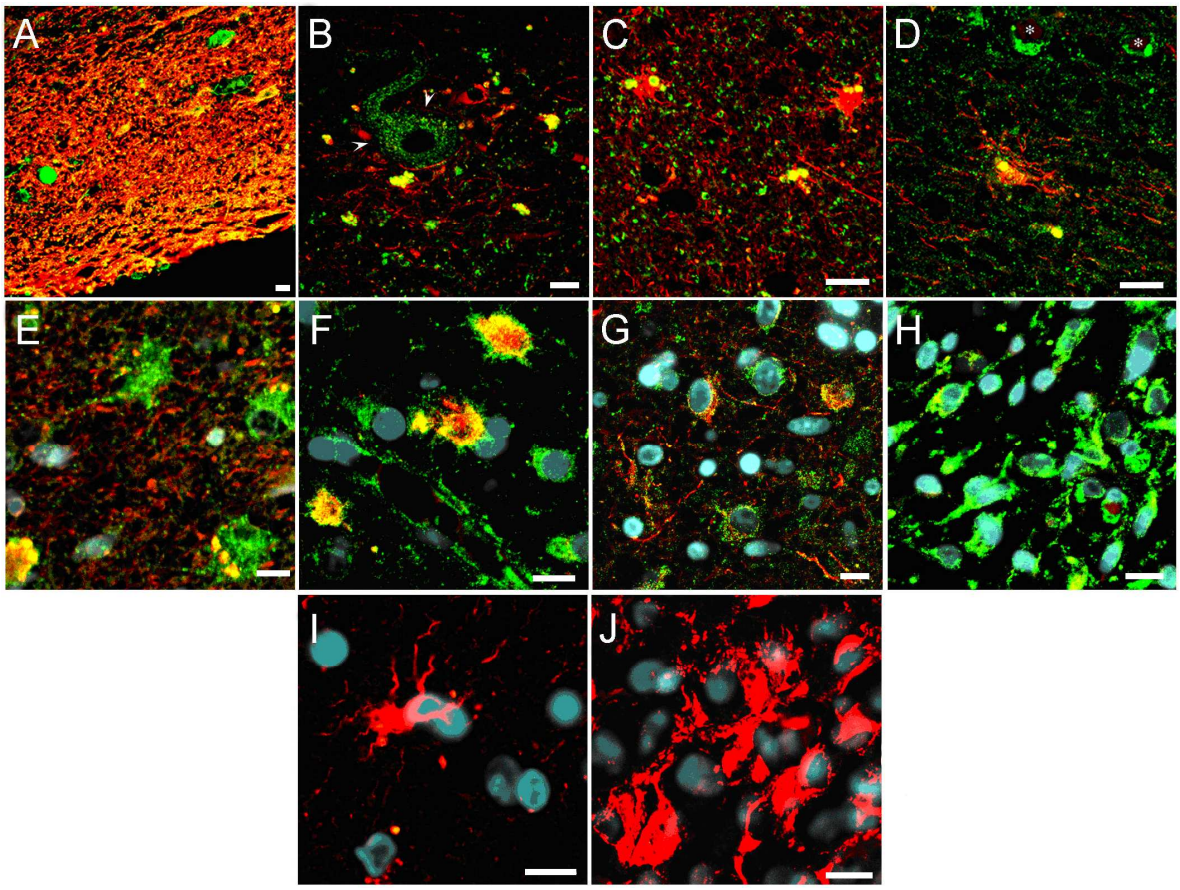

Figure 4. Immunohistochemical analysis of LOX and GFAP expression in normal tissue and astrocytic tumors of the human brain. Representative immunofluorescent stainings show co-localization of LOX and GFAP in various regions of a normal human brain and astrocytoma tissue sections: A – corpus callosum; B – cerebellum (arrowheads point at a Purkinje cell); C – cerebral cortex; D – mesenchephalon (stars mark lumens of blood vessels); E – grade I astrocytoma; F – grade II astrocytoma; G – grade III astrocytoma; H – grade IV astrocytoma; I – negative control for LOX stainings (isotype control rabbit IgG) on normal brain and J – on astrocytic tumor tissue sections. Colors correspond to LOX (green), GFAP (red). Co-localization of LOX and GFAP is detected in yellow. Nuclei were counterstained with DAPI (blue). Pictures were taken with an LMS Pascal 5 Confocal microscope (Zeiss). Scale bars represent 10 μm.

4.3. LOX is expressed in normal and malignant astrocytes *in vitro*

To be able to *in vitro* further characterize the role of LOX expressed in normal and malignantly transformed astrocytes, we were testing four cell lines for *in vitro* LOX and GFAP expression. First, we performed immunocytochemistry of normal human astrocytes (NHA), and three astrocytoma cell lines, U87 (grade III) (35,36), U251 (grade IV) (37), and U343 (graded III/IV)(35). LOX immunoreactivity was detected within both normal and neoplastic cells as faint dispersed immunostaining, with stronger appearance in association with intracellular fibrillar structures (**Figure 5, top panels**). GFAP immunoreactivity was detected in all cell lines, in U87 cells in slightly reduced amounts. In U251 and U343 cells displayed a great degree of variability in GFAP staining intensity (**Figure 5, bottom panels**). However, results obtained from immunocytochemistry stainings are not so convincing towards our hypothesis suggested by previous immunohistochemical data regarding positive correlation between LOX levels and tumor grade and negative correlation between GFAP levels and tumor grade. Latter correlation was already supported by the literature [55; 280], so we conceived our semi-inconsistent data as a result of immunocytochemistry being a rather qualitative than quantitative tool. Utilizing a more quantitative method, we went ahead and further investigated our chosen cell lines, searching for an appropriate model system to study biological effects of LOX in astrocytes. Nevertheless, Western blot data are also informative on the process of proteolytic activation of the LOX zymogen.

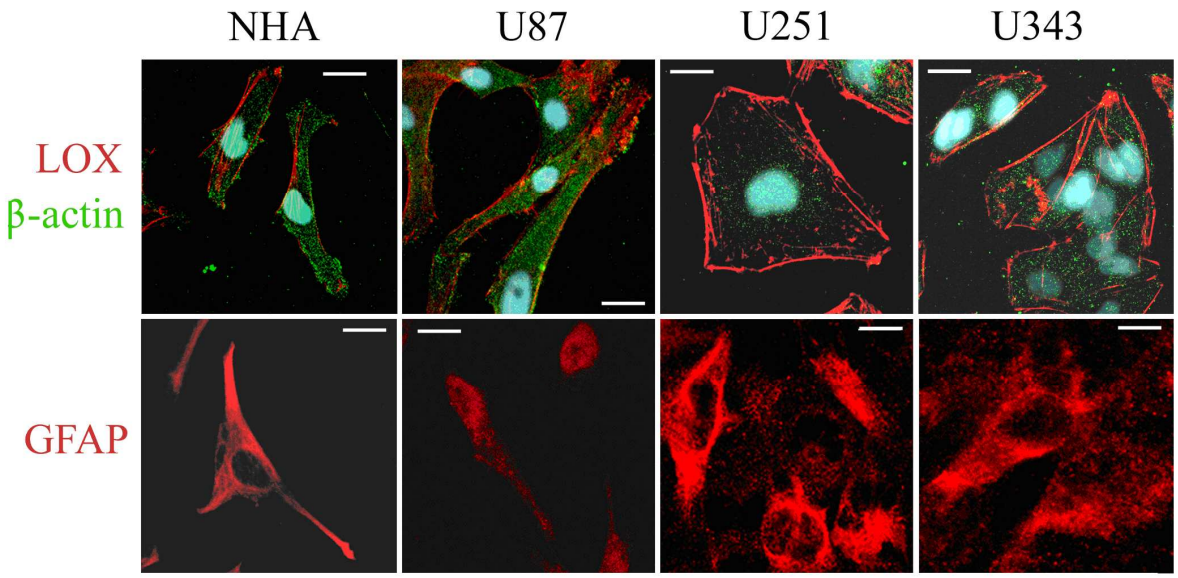

Figure 5. Immunocytochemical analysis of LOX and GFAP expression in normal astrocytes and astrocytic tumor cell lines. Representative immunofluorescent stainings show co-expression of LOX and GFAP in cultured normal and malignant astrocytes. LOX staining appeared to be associated with cytoskeletal fibrils, and was detected in all cell lines. GFAP immunoreactivity is present in all astrocytic cell lines, with reduced expression in U87 cells. Colors correspond to LOX (red, on the top panels), GFAP (red, on the bottom panels), and β-actin (green, on the top panels). Nuclei were counterstained with DAPI (blue). Pictures were taken with an LMS Pascal 5 Confocal microscope (Zeiss). Scale bars represent 20 μm.

4.4. LOX enzymatic activity positively correlates with astrocytic tumor grade

Secretion and proteolytic processing are critical steps for LOX activation. As our purified rabbit anti-LOX antibody was designed against an epitope present in both in the unprocessed and the active secreted enzyme, it was impossible to determine whether LOX detected by immunofluorescent microscopy was active or not. Consequently, we analyzed LOX expression pattern in our cultured cell lines using Western blot method. We separately collected CL and CCM from post-confluent cultures and studied both intracellular and extracellular LOX proteins. The expectation that LOX might be expressed at significantly higher levels in growth arrested post-confluent cell cultures is supported by the literature. Fibroblasts deriving from subjects with Werner syndrome or normal fibroblasts with late-passage number have an elevated expression level of LOX [281]. Markedly increased LOX expression is also found in pulmonary, arterial, dermal, and liver fibrosis, pathologies that are often associated with aging [265]. Therefore, we collected samples at 24-, 48-, and 72-hour post-confluent stages. Western blot data for each cell line are shown for 72-hour post-confluency (**Figure 6**). To confirm equal loading of protein samples we used GFAP for CL fractions, while for CCM samples PVDF membranes were stained with Ponceau dye.

LOX was detected as bands of 48 and 50 kDa that correspond to the known full length and glycosylated forms of LOX, in cell extracts in each cell line at each stage of confluency. In CCM fractions of normal astrocytes and U87 cells, however, the processed active form of LOX was not detectable. In contrast, a strong signal for active LOX was present in the media fractions of U251 and U343 cells (**Figure 6**). For

successful LOX activation, expression of active BMP-1 is needed, so we evaluated BMP-1 expression levels in these cells. We detected the active 75 kDa form of BMP-1 [282] in normal astrocytes and all three astrocytoma cell lines. Particularly in U251 cells, an increased amount of active BMP-1 was present, when compared with all other cell lines (**Figure 6**). These results indicated that all four cell lines have the capability to activate LOX. A previous study from our laboratory noted, that cellular fibronectin (FN) can act as a positive regulator for LOX processing and activation by BMP-1 [167]. Therefore, we also tested whether fibronectin is whether fibronectin is expressed and may contribute to LOX activation in higher-grade astrocytoma cells. Data we gained from these Western blots demonstrated that normal astrocytes did not, but all three astrocytoma cell lines produced cellular fibronectin, and the grade IV U251 cells had the highest amount present in their conditioned matrices (**Figure 6**).

Parallel with the detections above, we also looked for GFAP expression in cultured astrocytes. In normal astrocytes, a 48 kDa form was abundantly expressed in, while in dedifferentiated higher grade astrocytoma cells only faint expression of GFAP could be detected, in a slightly smaller size of 48 kDa. (**Figure 6**). In summary, results we obtained from astrocytic cell cultures supported our hypothesis that LOX exhibits increased expression in astrocytomas, which are also characterized by reduced GFAP production.

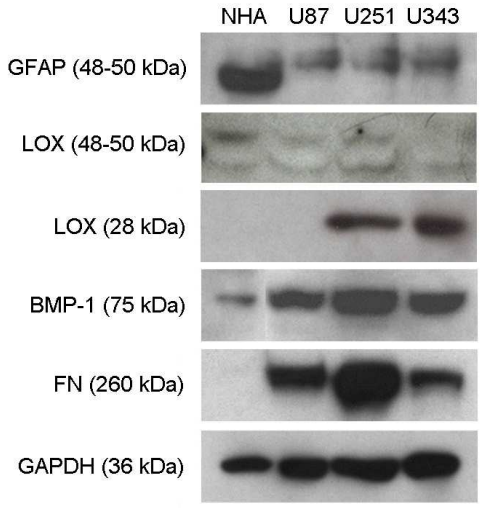

Figure 6. Western blot analysis for GFAP, LOX, BMP-1, and FN in cultured astrocytes. CL and CCM fractions of 3-day postconfluent astrocyte cultures were analyzed for GFAP, full

length LOX, active LOX, active BMP-1 and cellular fibronectin protein expression. GAPDH expression was measured for loading control in all experiments; representative GAPDH bands shown were obtained by stripping and reprobing blots.

Next we confirmed that LOX catalytic activity was elevated in high grade astrocytomas, suggested by Western blot data. Measurements using protein samples from CCM in the presence and absence of a specific LOX inhibitor, BAPN, demonstrated statistically significant increase in lysyl oxidase activity in the highest-grade U251 cells compared with normal astrocytes (**Figure 7**). The low activity value in normal and U87 astrocytes may be due to the presence of small amounts of active LOX in these cells that we noted only after overnight exposure on Western blots. Result from lysyl oxidase activity measurements nicely correspond with elevated levels of cFN expression in high grade astrocytomas, as a positive regulatory factor for LOX activation [167].

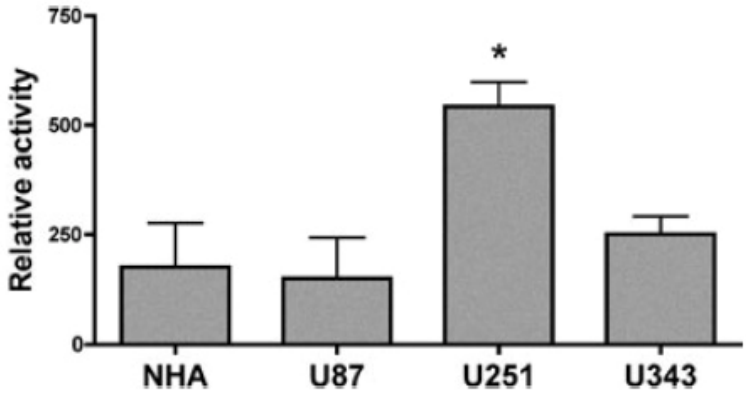

Figure 7. Lysyl oxidase activity measured in CCM fractions of NHA, U87, U251 and U343 cells in comparison to BAPN containing parallel samples. Bars represent BAPN inhibitable amine oxidase activity in each sample. Unpaired t-tests were used to compare activity in U87, U251 and U343 cells with NHA activity using data from six independent experiments. Error bars show standard deviation. Asterisk (*) marks statistically significant difference ($p = 0.0093$) between activities measured in NHA and U251 cell media fractions.

4.5. Active LOX contributes to astrocytic migration

High grade astrocytomas possess increased migratory potential. To test our hypothesis that the presence of active LOX in U251 and U343 high grade malignant astrocytes correlates with increased migratory ability, we performed cell migration assays using the membrane invasion chamber system. As U87 cells lacked processed active LOX and showed very low expression and amine oxidase activity, we did not test these further. Normal astrocytes had low migratory ability while U251 and U343 cells demonstrated significantly increased migration compared with normal cells (**Figure 8**). Application of a specific LOX inhibitor BAPN that targets its active site, allowed us to directly address the role of the active LOX on cell migration. Inhibition of LOX by BAPN significantly inhibited cell migration in both U251 and U343 cells (90% inhibition compared with untreated cells). BAPN-treated normal astrocytes showed somewhat diminished migration, but this was not statistically significant.

Previous reports noted that in monocytes [283], in smooth muscle cells [284], and in our study, in invasive breast tumor cells [285], cell migration depends on H_2O_2 generated during the catalytic reaction of active LOX with a substrate. To determine whether astrocyte migration was also mediated by LOX-generated hydrogen, we used catalase in the cell migration assays to deplete H_2O_2 by converting it to water and oxygen. In our migration assays, we used 200 U/mL catalase, as this concentration was reported to efficiently influence cellular behavior without toxicity [272; 285]. There was a decrease in migratory ability in the presence of catalase both in U251 (70% decrease) and in U343 cells (95% decrease) compared with untreated cells, while the migration of normal cells was not inhibited. These results were consistent with the presence of the processed active form of LOX we detected on Western blots, and the increased LOX activity that we measured in the U251 and U343 cells.

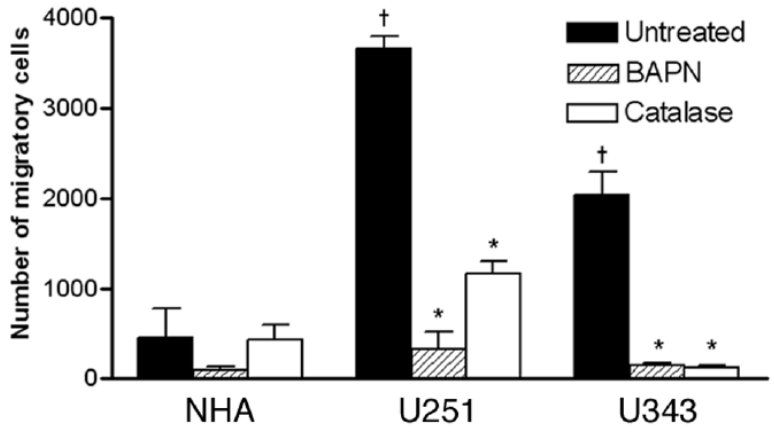

Figure 8. Enzymatically active LOX promotes astrocytic cell migration. *In vitro* quantitative evaluation of migratory phenotype of NHA and malignant astrocytes in the presence of active LOX, under conditions to inhibit LOX activity by BAPN, and deplete hydrogen peroxide by catalase. Results are means of 3–6 data points for each cell line, error bars represent standard deviation, asterisk (*) represents significance in the migratory behavior of treated cells vs. their untreated counterparts ($p < 0.05$), and dagger (†) represents significance in the migratory phenotype among the untreated NHA and U251 and U343 cells ($P < 0.05$). For statistical analysis, Anova and Scheffe's test were used.

4.6. Active LOX promotes astrocytic cell migration by facilitating FAK(Tyr576) and paxillin(Tyr118) phosphorylation

A study from our research group has previously demonstrated that active LOX induced FAK(Tyr576) phosphorylation in invasive breast tumor epithelial cells and that this was mediated through LOX generated H_2O_2 [285]. To determine whether FAK(Tyr576) phosphorylation correlated with the presence of significant amount of active LOX in invasive U251 astrocytes, we evaluated FAK(Tyr576) phosphorylation in untreated cells and cells treated with LOX activity inhibitor BAPN; subsequently we tested whether depleting H_2O_2 by catalase would affect FAK(Tyr576) phosphorylation in these cells. Western blot analysis revealed that FAK(Tyr576) was phosphorylated in U251 astrocytes. Addition of BAPN resulted in the reduction of phosphorylated FAK-(Tyr576), while catalase treatment almost completely diminished the amount of phosphorylated FAK(Tyr576) in these cells (**Figure 9**). The amount of total FAK did not change following BAPN treatment of cells (data not shown). Phosphorylation of

FAK(Tyr576) leads to paxillin(Tyr118) phosphorylation [286], subsequent binding of FAK and paxillin, localization to the focal adhesion complex and promotion of cell migration [287]. Paxillin activation is further promoted by H_2O_2 [288]. In U251 cells, we indeed detected phosphorylated paxillin(Tyr118), and both LOX activity inhibition by BAPN and depleting H_2O_2 by catalase significantly reduced the amount of phosphorylated paxillin(Tyr118) (**Figure 9**). These results were consistent with the presence of catalytically active LOX in U251 cells, the strong migratory ability of these cells, and inhibition of cell migration by both BAPN and catalase.

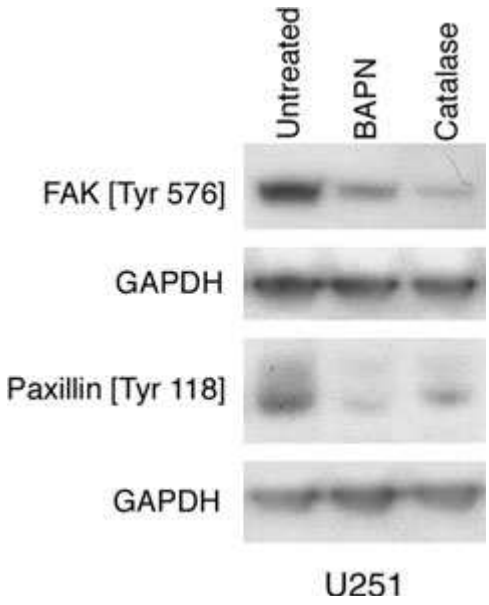

Figure 9. Western blot analysis of FAK(Tyr576) and paxillin(Tyr118) phosphorylation in cultured U251 cells using protein extracts from untreated, BAPN- and catalase-treated cells. BAPN was used to inhibit lysyl oxidase (LOX) catalytic activity and catalase to deplete hydrogen peroxide. For loading control, GAPDH is shown.

Study II

4.7. LOXL2 antibody characterization

To perform immunochemical analysis and detect LOXL2 protein expression, we designed a rabbit polyclonal antibody against the carboxyl terminus (EHFSGLLNNQLSPQ) of the human LOXL2 protein, and it was made by Zymed

Laboratories (San Francisco, CA, USA). The sequence is unique among the LOX protein family, with some similarity with LOXL3. Antibody specificity was tested against recombinant proteins expressed *in vitro*. Full-length human cDNAs were subcloned into the pIND/V5-His inducible expression vector (Invitrogen) to generate LOXL2 and LOXL3 with or without a V5-His carboxyl terminal epitope tag. Each construct was transfected into EcR-293 cells using Lipofectamine 2000 following the manufacturer's protocol. Expression was induced with 5 µM ponasterone A (Invitrogen) in serum-free medium for 20–24 h.

The antibody specifically recognized recombinant LOXL2 protein of 95 kDa when expressed in EcR-293 cells, but not the closely homologous recombinant LOXL3 (**Figure 10. A**). This size was larger than the 87 kDa protein predicted by sequence analysis and produced by *in vitro* translation, and may be due to post-translational modifications, as there are three potential N-linked glycosylation sites within LOXL2 [239]. In addition, the antibody detected a 63 kDa peptide in the culture medium. To determine whether this band was derived from the 95 kDa peptide, we expressed LOXL2 fused to a V5-His epitope tag. A similar band pattern was detected using an antibody against the V5 epitope; therefore we concluded that the 63 kDa peptide is a derivative of the larger 95 kDa protein. These two protein forms of LOXL2 have also been detected in the culture medium of transfected CHO and MCF-7 cells [240; 263], as well as the highly invasive breast cancer cell lines MB-231 (**Study III**) and Hs578T (data not shown), although the 63 kDa protein was not detected in the normal fetal colonic epithelial cell line CRL-1831. The 63 kDa protein, which has only been detected in culture medium, may represent an extracellularly proteolytically processed form of LOXL2, as other LOX family members, namely LOX and LOXL, have been characterized as proteins that are processed extracellularly into their functional forms [289; 290]. The polyclonal LOXL2 antibody was used in immunohistochemical analyses to determine the expression pattern of LOXL2 protein in normal colon and esophageal tissue, and colon adenocarcinoma and esophageal SCC tissue.

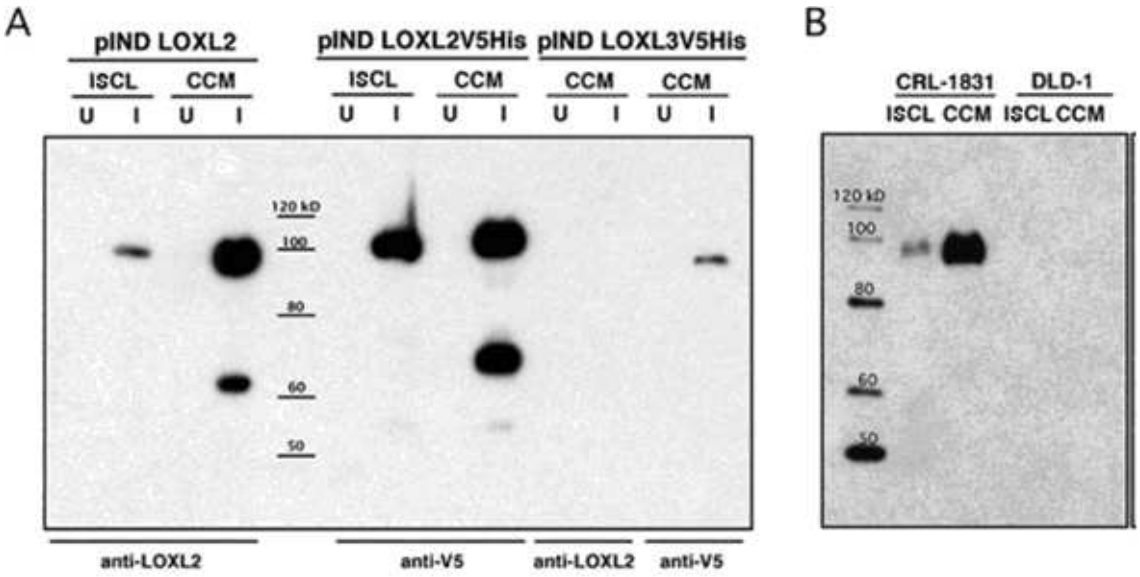

Figure 10. Western blot analysis of LOXL2 antibody specificity and LOXL2 protein expression in colon cell lines. Proteins collected from the ISCL and CCM were used for Western blot analysis. (A) Recombinant LOXL2 and LOXL3 protein expression. The vector is noted above and the primary antibody is noted below. Proteins were collected from uninduced (U) cells or from cells induced (I) with ponasterone A. LOXL2 expression is detected only in proteins isolated after induction using the LOXL2 antibody (left) or V5 antibody (right). (B) A Western blot containing proteins isolated from the human fetal colonic epithelial cell line CRL-1831 and the colon carcinoma cell line DLD-1 was analyzed using the LOXL2 antibody.

4.8. Increased LOXL2 expression is associated with less differentiated colon tumors

Analysis of an array of normal human colon tissues using immunohistochemistry and the LOXL2 antibody revealed that, in the colonic mucosa, LOXL2 was expressed in scattered single cells comprising a small percentage of the total cells (**Figure 11. A**), a histological pattern that is unique to only one of the four intestinal cell lines, enteroendocrine cells [291; 292; 293]. There are more than a dozen different types of enteroendocrine cells, also referred to as diffuse neuroendocrine cells or APUD cells (amine precursor uptake and decarboxylation cells). No staining was detectable in the normal colon tissue samples using control rabbit IgG as the primary antibody (not shown). LOXL2 expression was absent from the mitotically active crypt

base cells, which give rise to aberrant crypt foci, the precursor of adenomatous polyps and carcinomas [294]. Immunohistochemical analysis of the colon adenocarcinoma tissue array showed the presence of LOXL2-expressing tumor cells in 83% (43/52) of the samples (**Figure 11. B**). The number of LOXL2-expressing cells per field were scored and evaluated for correlation with tumor stage, tumor differentiation, and tumor site. There was a statistically significant correlation (P = 0.03) noted in the number of LOXL2-expressing tumor cells observed in the well-differentiated colon tumors (score = 0.9, SD = 1.0) compared to the moderately-differentiated (score = 2.1, SD = 1.6), poorly-differentiated, and mucinous tumors (score = 2.7, SD = 1.7). There was no significant correlation between tumor stage (Stage II: score = 2.1, SD = 1.8; Stage III: score = 1.8, SD = 1.6; Stage IV: score = 1.6, SD = 1.5) nor tumor site (right colon: score = 2.0, SD = 1.5; transverse colon: score = 2.0, SD = 1.9; left colon: score = 2.0, SD = 1.6) and number of LOXL2-expressing cells.

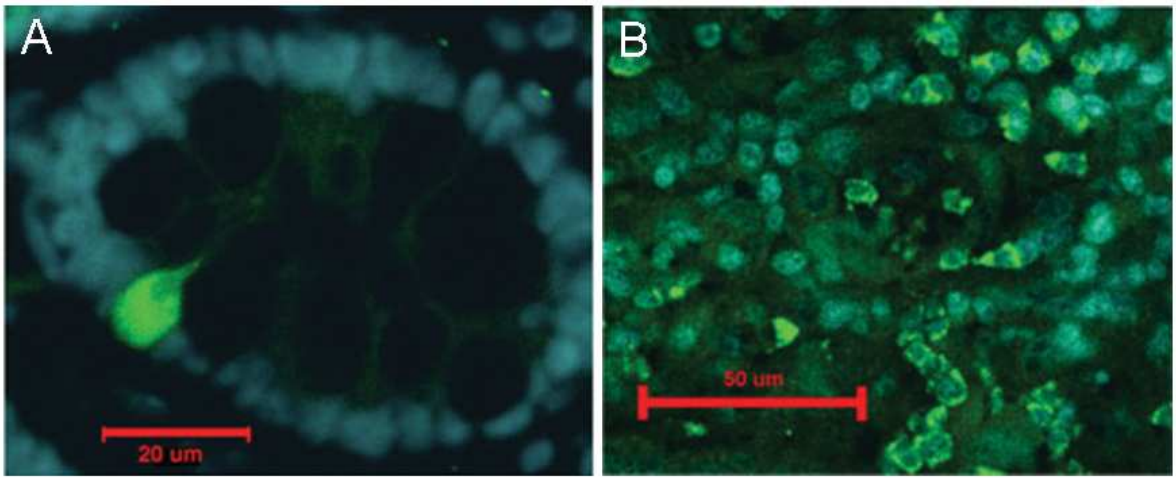

Figure 11. Immunohistochemical analysis of LOXL2 in normal tissue and tumors of the colon. One normal colon tissue array slide and one colon cancer tissue array were subject to immunohistochemical analysis using LOXL2 antibody (1:300) and Alexa Fluor 488, resulting in green fluorescence. Nuclei were counterstained with DAPI, shown in blue color. (A) Cross-section of a tubular gland of the colonic mucosa reveals LOXL2 localization to enteroendocrine cells. (B) LOXL2-expressing tumor cells in colon adenocarcinoma. Images were captured using LMS Pascal 5 Confocal microscope (Zeiss). Scale bars represent (A) 20 μm and (B) 50 μm.

4.9. Increased expression of LOXL2 in esophageal tumors

Analysis of tissue array slides containing normal human esophagus tissue revealed that LOXL2 localized to the outer layer of stratified squamous epithelium of the esophageal mucosa (**Figure 12. A**). No staining was detectable in the normal esophagus tissue samples using control rabbit IgG as the primary antibody (not shown). As with the colon, LOXL2 expression was absent from the proliferative cells in the basal layer of the esophageal mucosa, which may give rise to basal cell hyperplasia, preneoplastic dysplastic lesions, and SCC [295]. Immunohistochemical analysis of the esophageal SCC array demonstrated the presence of LOXL2-expressing tumor cells in 92% (46/50) of the samples (**Figure 12. B**). The number of LOXL2-expressing cells per field were scored and evaluated. There was no significant correlation found for tumor stage (Stage II: score = 2.9, SD = 1.7; Stage III: score = 2.7, SD = 1.6; Stage IV: score = 2.5, SD = 3.5) nor tumor differentiation (poor: score = 2.6, SD = 1.8; moderate: score = 2.7, SD = 1.8; well: score = 3.0, SD = 1.5).

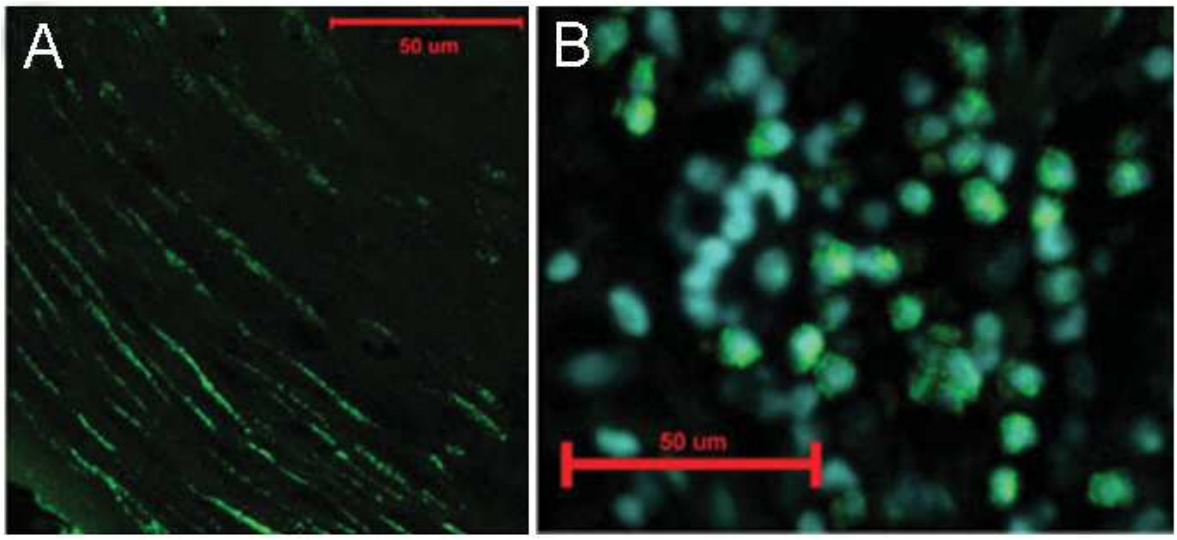

Figure 12. Immunohistochemical analysis of LOXL2 in normal tissue and tumors of the esophagus. Tissue array slides of normal esophagus tissue and one esophageal cancer tissue array were subject to immunohistochemical analysis using LOXL2 antibody (1:300) and Alexa Fluor 488, resulting in green fluorescence. In Panel B, nuclei were counterstained with DAPI, resulting in blue fluorescence. (A) In normal esophagus tissue, LOXL2 localizes to the stratified squamous epithelium, and is more prominent toward the outer layers (toward bottom left of

picture). (B) LOXL2-expressing tumor cells in esophageal SCC. Images were captured using LMS Pascal 5 Confocal microscope (Zeiss). Scale bars represent 50 μm.

4.10. LOH analysis of the *loxl2* gene in colon and esophageal tumors

Although there was no significant correlation, in general, the number of LOXL2-expressing cells decreased with increasing cancer stage in both the colon and esophageal cancers. This indicates that there could be possible loss of the *loxl2* gene and expression in these cancers. To address this possibility, we evaluated the presence of LOH of the *loxl2* gene to determine if the *loxl2* gene was one of the genes affected by the reported loss of 8p21.2–p21.3 in colon and esophageal cancers [296; 297; 298]. A CA-repeat microsatellite was detected by Southern blot analysis of PAC clone 17,460, containing exons 3–13 of the *loxl2* gene (data not shown). Sequence analysis revealed this microsatellite to be within intron 4 of the *loxl2* gene. Comparison to the GenBank database indicated a previously unidentified microsatellite within the complete sequence of human chromosome 8 clone RP11 177H13. We determined this microsatellite to be polymorphic and used it for the LOH studies in our panel of colon and esophageal tumor samples. Of the individuals in the colon tumor panel who were informative for the *loxl2* microsatellite, 33.3% (17/51) demonstrated LOH or AI. Only Stages B and C demonstrated LOH or AI. No LOH or AI was detected in Stage A tumors, and Stage D tumors were non-informative for this microsatellite marker. The 33.3% LOH of the *loxl2* gene that we observed in colon tumors is less than the previously reported 48–57.9% LOH of 8p21 in colon tumors [296; 298]. That our panel is an appropriate representation of sporadic colon cancer was demonstrated by the status of microsatellite D5S346, located between the apc and mcc genes, that we previously evaluated [273] in a panel that included the present panel in its entirety. The 36.0% (22/65) LOH that we observed for D5S346 is consistent with previous reports of sporadic colon cancer [299; 300]. In addition, there have been reports of tumor suppressor gene candidates at chromosome 8p21, including EXTL3, DLC-1, and KIAA1456 [301; 302; 303]. Thus, the *loxl2* gene is unlikely to be the tumor suppressor gene thought to reside at this chromosomal locus. Of the individuals in the esophageal tumor panel who were

informative for the microsatellite, 32.5% (13/40) demonstrated LOH or AI. Of the Stage 3 and Stage 4 tumors, 31% (9/29) and 25% (1/4), respectively, demonstrated LOH or AI. One Stage 1 tumor exhibited LOH, but none were observed in Stage 2 tumors. No Stage 0 tumors were informative for this microsatellite marker. The 32.5% LOH of the *loxl2* gene is similar to the previously reported 28% in a South African population [297], while these authors noted much higher LOH (up to 55%) in other chromosomal loci. Considering the gain of LOXL2 expression in 92% of esophageal tumors by immunohistochemical analysis, *loxl2* gene loss does not appear to play a major role. However, in 8% of the esophageal tumors, no LOXL2-expressing cells were noted. This lack of expression may be due to LOH accompanied by loss of the remaining allele. To determine if tumors with LOH of the *loxl2* gene are more likely to have absent or low expression of LOXL2 protein, tissues of five esophageal tumors demonstrating LOH were evaluated. Of these five, two samples had LOXL2-expressing tumor cells (scored 2 and 5). The other three samples lacked LOXL2 expression, which was a much higher proportion (3/5) than the esophageal SCC tissue array (4/50).

4.11. Characterization of the *loxl2* CpG island and promoter

In both normal colon and esophageal tissue, LOXL2 was not expressed in the mitotically active cells that are thought to be the origin of dysplastic and subsequently, cancerous cells. However, in colon and esophageal tumors, 83 and 92% of the tumor tissues, respectively, contained tumor cells expressing LOXL2 protein. LOX, a member of the same family as LOXL2, has been shown to be regulated by methylation of its CpG island in gastric, lung, colon, and ovarian carcinomas [304; 305]. To determine if an epigenetic mechanism was responsible for this activation of LOXL2 expression in the tumor cells, we analyzed the genomic sequence contig NT023666, which contains the *loxl2* gene, by GrailEXP CpG Island Locator. This revealed a single predicted CpG island of 1150 bp, starting from 176 bases upstream of the predicted transcriptional start of the *loxl2* gene and extending into intron 1, with an observed CpG/expected CpG ratio of 0.82 and a GC content of 67.6%. The location of the CpG island through 5'flanking region, exon 1 and intron 1 of the *loxl2* gene, was consistent with other 50 CpG islands

[23], including *lox* [305]. However, there was no significant sequence homology between the CpG islands of *lox* and *loxl2*. The location of the predicted *loxl2* CpG island indicated that the predicted transcriptional start was likely correct. A previous promoter analysis on the *loxl2* gene [238] used a truncated gene sequence that began with exon 4, and thus erroneously reported promoter elements within intron 3. Our analysis revealed no typical TATA or CCAAT box sequences in the *loxl2* promoter close to the transcriptional start sequence. This is not unexpected as about half of promoters with CpG islands lack a typical TATA box [306]. The location of putative transcription factor binding sites within the *loxl2* promoter region, including AP1, NFκB, and WT1, are shown in Table 2.

Table 2 – Putative transcription factor binding sites in the *loxl2* promoter

Transcription factor	Putative binding sites
AP1	−1156, −1561, −2258, −2762, −3451, −3677, −3596, −3801
REL	−160, −262, −1715
ELK1	−472, −716
EVI1	−1200, −4227
FOXD3	−4311
GATA1	−320, −957, −1639, −1839, −2133, −2242, −2297, −3234, −4054
HNF1	−3201, −4232, −4618
HNF3b	−511
HNF4	−1182, −1816
NFE2	−4965
NFkB	−265, −1012, −1481, −1715, −2621, −2777, −2913, −4140, −4455
NFY	−4293
PAX4	−2386, −3173, −4789
SP1	−76, −116, −146, −202, −341, −381, −465, −512, −552, −746, −948, −1136, −1526, −2341, −2476, −3095, −3323, −3749, −4133, −4898
WT1	−214

4.12. Activation of *loxl2* gene expression by 5-aza-dC treatment

To evaluate if demethylation of the LOXL2 CpG island could be responsible for activation of loxl2 gene expression, we characterized colon and esophageal cancer cell lines to identify cell lines that did not express LOXL2 mRNA. Northern blot analysis revealed that all of the esophageal SCC cell lines as well as the normal esophageal tissue (positive control) expressed LOXL2 mRNA (**Figure 13. A**). However, we identified three colon cancer cell lines, HCT-116, HCT-15, and DLD-1, which lacked LOXL2 mRNA expression (**Figure 13. B**), compared to the normal fetal colonic epithelial cell line CRL-1831 (positive control from Western blot analysis, **Figure 10. B**). DLD-1 was confirmed not to have LOXL2 protein expression by Western blot analysis (**Figure 10. B**). As the HCT-15 and DLD-1 cell lines are from the same genetic origin [307], only HCT-116 and DLD-1 were used for evaluating the role of DNA methylation of the CpG island in regulating LOXL2 expression.

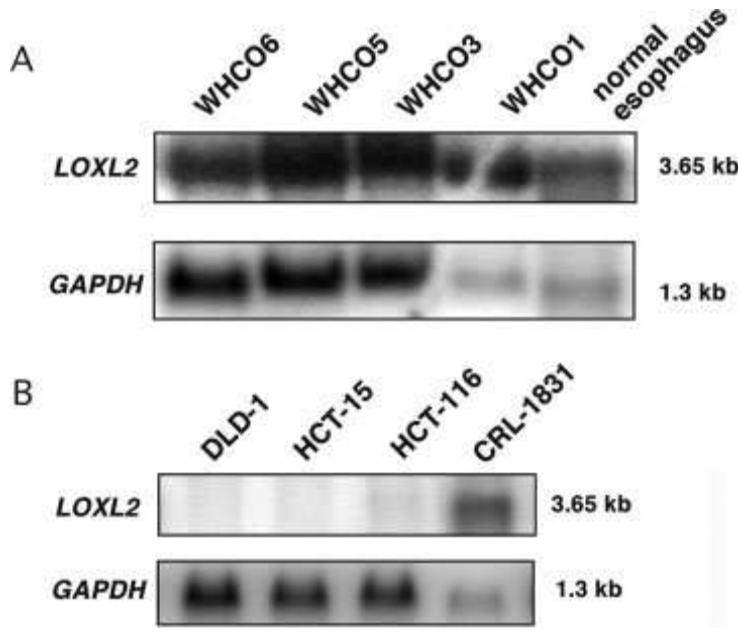

Figure 13. Northern blot analysis of LOXL2 mRNA expression in human esophageal and colon cell lines. (A) A Northern blot containing 5 μg of total RNA isolated from cultured human esophageal SCC cell lines, WHCO6, WHCO5, WHCO3, and WHCO1, and from normal esophagus tissue. (B) A Northern blot containing 10 μg of total RNA isolated from colon carcinoma (DLD-1, HCT-15, and HCT-116) and normal fetal colonic epithelial cells (CRL-

1831). The upper panels demonstrate the single 3.65 kb LOXL2 mRNA The lower panels are of the same blot hybridized to a GAPDH cDNA probe.

After treatment with 5-aza-dC, LOXL2 mRNA expression was upregulated in both HCT-116 and DLD-1 cell lines, a 40-fold induction over baseline in the DLD-1 cell line, and a smaller increase in HCT-116. The possible contribution of histone modifications was determined by co-treatment with TSA, which, in the DLD-1 cell line, up-regulated LOXL2 expression more than 5-azadC alone (**Figure 14.**).

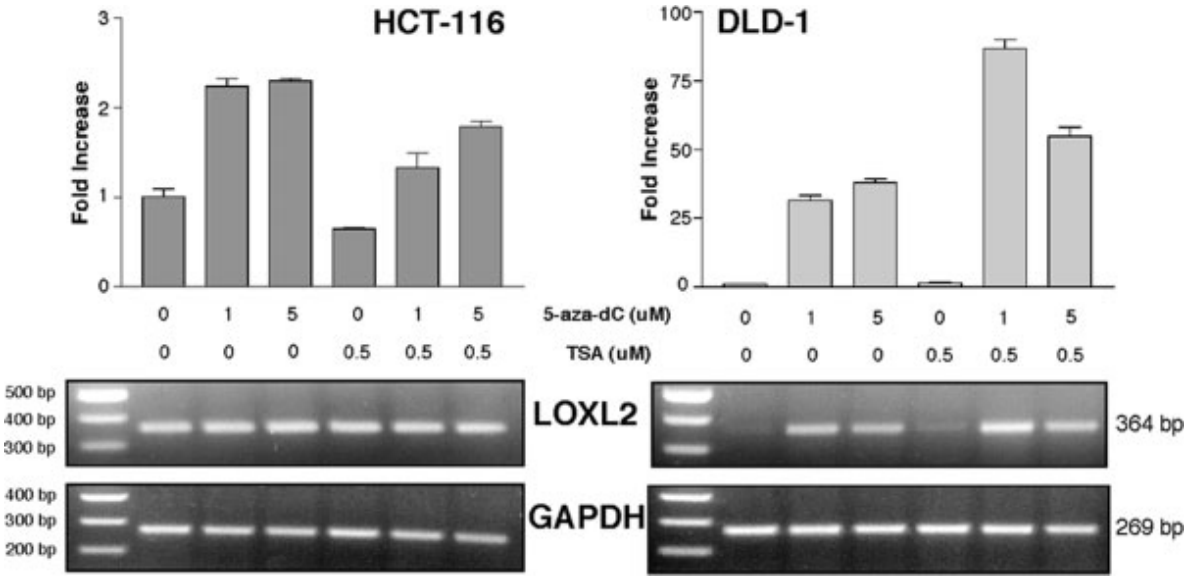

Figure 14. Effect of 5-aza-dC and TSA treatment on LOXL2 mRNA expression. The colon carcinoma cell lines HCT-116 and DLD-1 were treated with increasing concentrations of 5-aza-dC, without (first three lanes) or with (latter three lanes) TSA. LOXL2 mRNA expression levels were measured by real-time PCR and standardized to GAPDH expression. The upper panels depict the fold-increase of LOXL2 expression. Note that the scales are different. The lower panels depict the amplicons in the linear phase of amplification, following agarose gel electrophoresis. The markers are noted on the left and the amplicon sizes are noted on the right.

Study III

4.13. Characterization of LOXL2 expression in stably transduced cell lines

We have previously determined that the non-invasive, non-metastatic breast cancer lines MCF-7 and T47D lack LOXL2 mRNA expression; whereas the highly invasive, metastatic breast cancer cell lines MB-231 and Hs578T express high levels of LOXL2 mRNA [269]. To analyze the role of LOXL2 in tumor cell behavioral changes during the transition from a non-invasive to an invasive phenotype, we have developed 8 stably-transduced MCF- 7 breast cancer cell clones without a V5 tag, and 2 clones (V5-1 and V5-2) with a V5-tag. LOXL2 mRNA and protein expression in these cells was analyzed using RT-PCR and Western blot analysis of cultured cell media, respectively. All clones expressed the LOXL2 mRNA (**Figure 15. A**). Varying amounts of the 95 kDa peptide of LOXL2 was detected in all clones after 72 h of culturing (**Figure 15. B**). MCF-7 LOXL2 clones 1, 3–9 and V5-1 (appearing larger due to the V5-tag) also expressed a 63 kDa form of LOXL2, possibly resulting from posttranslational modifications and/or processing similarly reported for other LOX proteins [289; 290] but not yet characterized for LOXL2. On the Western blot, the amount of the 63 kDa band appeared proportional to the amount of the 95 kDa peptide, and the two clones with absent 63 kDa peptide also had the lowest 95 kDa peptide levels. A subsequent time course analysis of MCF-7 LOXL2 clone V5-1 demonstrated that the 63 kDa peptide (+V5 tag) was detectable within 24 h, and that there was a gradual increase of the signal during days 1–4 in samples derived from the cell media (**Figure 16. A**). This time course of accumulation of the 63 kDa form is consistent with processing. This was confirmed by protease inhibitor treatment of MCF LOXL2 clone V5-1, which resulted in decrease of the 63 kDa peptide accompanied by increase in the 95 kDa peptide with a single PI treatment (**Figure 16. B**). Cells treated twice with PI had decreased growth, yielding a decrease in the 95 kDa peptide compared to single treatment, accompanied by loss of the 63 kDa peptide. These experiments indicated that the 63 kDa peptide is a proteolytically processed product of the 95 kDa LOXL2.

In the five stably transduced LOXL2-expressing MCF-10A clones that we have also developed, increased LOXL2 mRNA expression was detected in all clones over the

parental cell line (**Figure 15. A**). Protein extracts from the media fractions were analyzed on Western blots. The parental MCF-10A line only expressed the 95 kDa peptide, while the clones expressed both the 95 and the 63 kDa peptide (**Figure 15. B**). The lack of the 63 kDa peptide in the MCF-10A parental line may be due to low expression of the 95 kDa peptide, similar to what we detected with MCF-7 LOXL2 clones 2 and V5-2. Time course and protease inhibitor experimentation using MCF-10A LOXL2 clone 3 revealed slight increase in the 63 kDa peptide over time (**Figure 16. C**), and gradual loss of the 63 kDa peptide with increasing exposure to protease inhibitors (**Figure 16. D**), indicating that proteolytic processing was present in both normal and breast cancer cell line media.

As LOX has also been implicated in promoting mammary epithelial cell migration and invasion [308] we also evaluated possible changes in LOX mRNA expression in all clones by quantitative real-time PCR and confirmed that there was no significant increase in LOX expression (**Figure 15. C**). Most cell lines demonstrated even a slight decrease in LOX mRNA expression. Because the clones did not have significant changes in LOX mRNA levels and there was no evidence to suggest that increase in LOXL2 would significantly alter other LOX family members, we presumed that any change in amine oxidase activity and/or cell behavior would be due to the increase in LOXL2 protein and/or activity in the clonal cell lines.

The variable expression of LOXL2 in our clones allowed for comparison of the amount of LOXL2 expressed relative to the different cell behavior observed. These results confirmed that our cell model was suitable to evaluate the possible roles of LOXL2 in invasive-promoting cell behavior.

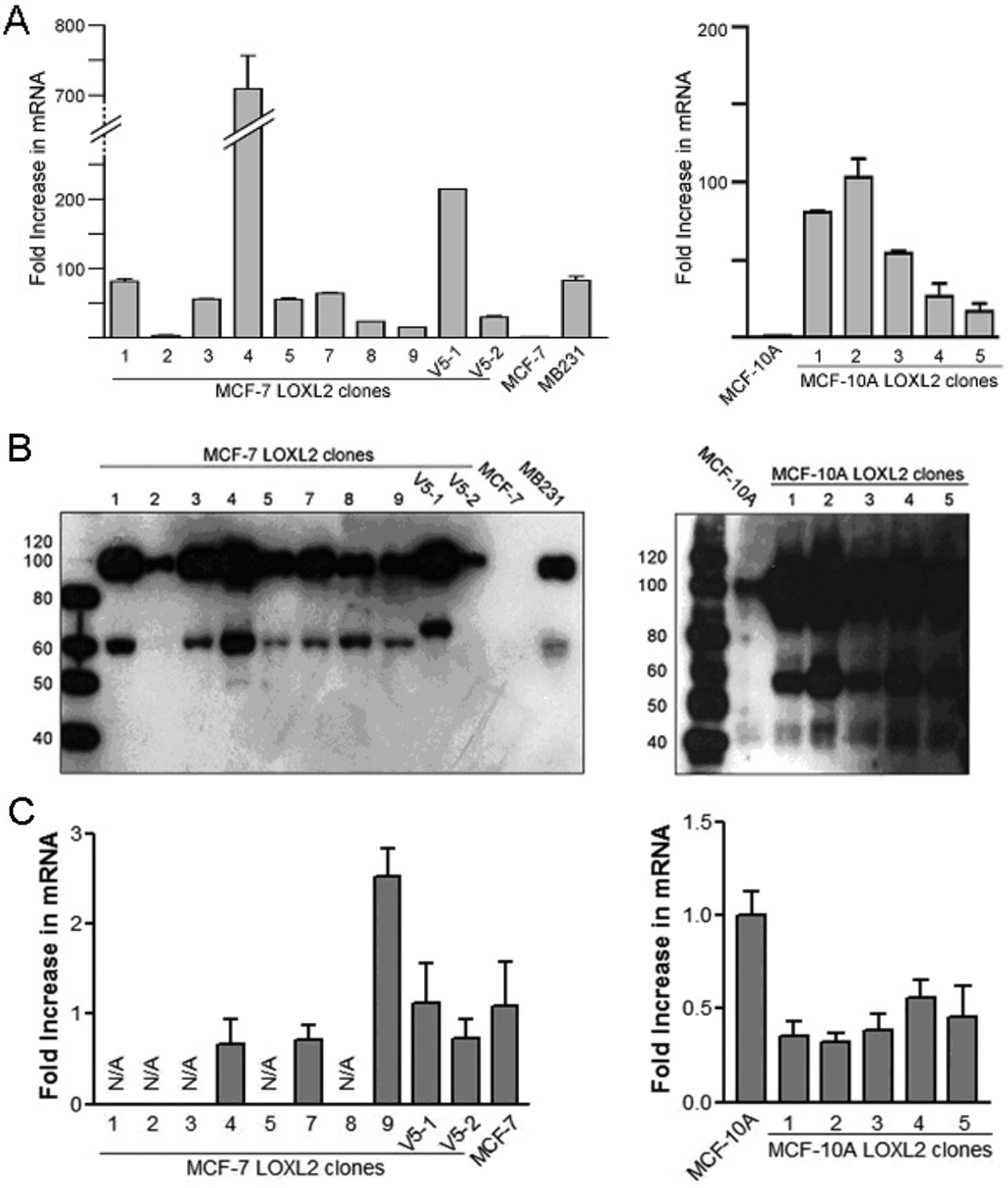

Figure 15. Expression analysis of mammary epithelial cell lines stably transduced with full-length LOXL2. (A) MCF-7 and MCF10-A cells, and their LOXL2 overexpressing clones (with or without a V5 tag), and MB-231 cells were evaluated for LOXL2 mRNA expression levels by quantitative real-time PCR, standardized to GAPDH expression and shown as fold-increase over expression in parental cells. For the parental MCF-7 cell line the average absolute LOXL2 mRNA copy number was 4,400, for the parental MCF-10A cell line it was 54,700. (B) Western analysis for LOXL2 from CCM collected after three days of exposure to serum-free

media, from cells listed above. (C) For negative control, cells listed above were also evaluated for LOX mRNA expression levels by quantitative real-time PCR. Results here were also standardized to GAPDH expression and are shown as fold-increase over expression in parental cells.

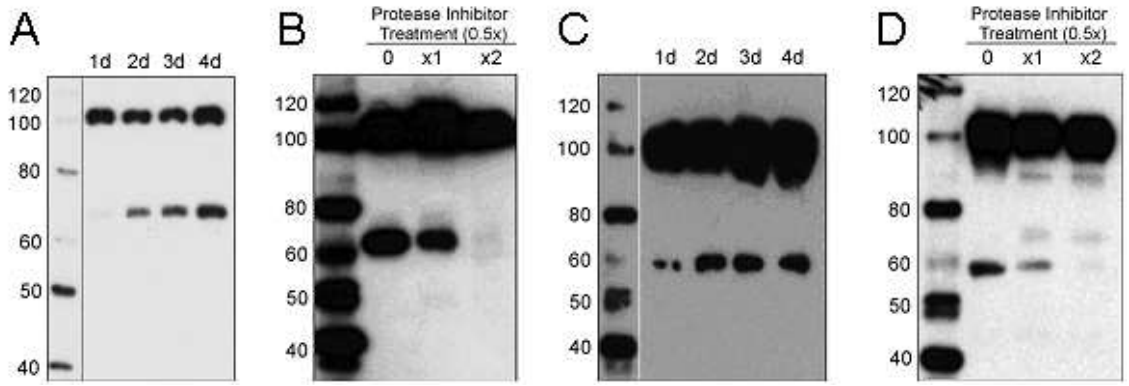

Figure 16. Secreted LOXL2 is proteolytically processed as detected by Western analysis. (A) LOXL2 detected from the CCM of MCF-7 LOXL2 clone V5-1, collected every 24 hours after exposure to serum-free media and (B) collected after four days of exposure to none, one, or two treatments with 0.5x HALT protease inhibitor cocktail. (C) LOXL2 detected from the CCM from MCF-10A LOXL2 clone 3, collected after every 24 hours after exposure to serum-free media and (D) collected after four days of exposure to none, one, or two treatments with 0.5x HALT protease inhibitor cocktail.

4.14. Overexpression of LOXL2 induces a mesenchymal-like phenotype in MCF-7 and MCF-10A clones

Clonal MCF-7 and MCF-10A cell lines overexpressing LOXL2 demonstrated a change in phenotype towards a more mesenchymal-like appearance compared to the parental cell lines (**Figure 17**). MCF-7 LOXL2 clones showed a decreased tendency to grow in tight clusters and had short, spiked protrusions. The MCF-10A LOXL2 clones did not form ‘‘cobblestone’’ clusters typical of epithelial cells, but acquired a more elongated, spindle-like morphology. This morphology was most pronounced in MCF-10A LOXL2 clones 1 and 2, which also had the highest level of LOXL2 expression.

Upon LOXL2 overexpression, both MCF-7 and MCF-10A cells exhibited a scattering, which is a possible response towards EMT. These cell phenotype changes are consistent with the role of LOXL2 in the promotion of invasive potential [263; 309]. The clones with the most LOXL2 expression – MCF-7 LOXL2 clone 4 and MCF-10A LOXL2 clones 1 and 2 – were also the slowest growing, consistent with previous observations [263].

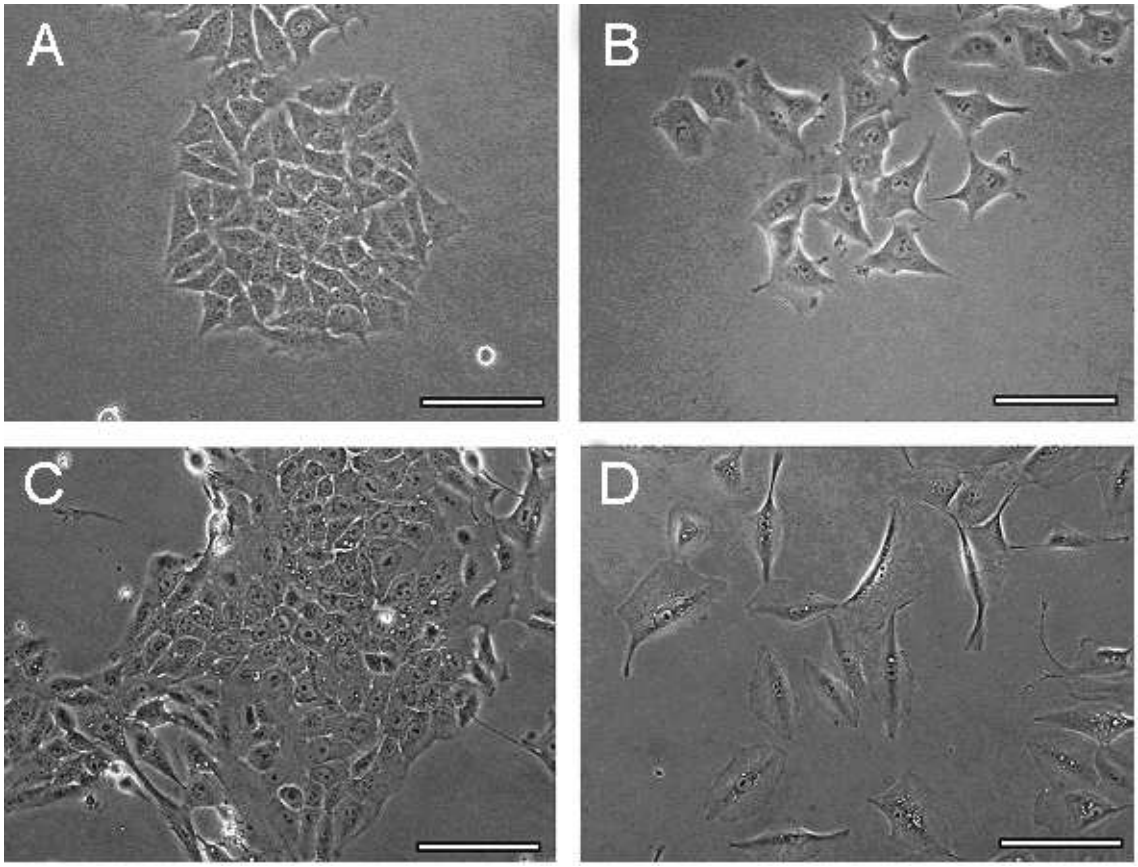

Figure 17. LOXL2 overexpression in MCF-7 and MCF-10A cells induces phenotype change. Morphology was observed in phase-contrast microscopy of cultured representative clones. (A) MCF-7, (B) MCF-7 LOXL2 clone 9, (C) MCF-10A and (D) MCF-10A LOXL2 clone 1. Scale bars represent 100 μm.

4.15. LOXL2 overexpression promotes migratory ability in MCF-7 but not in MCF-10A cells

To evaluate whether the morphologic changes in the LOXL2 overexpressing clones were associated with increased migratory ability, we performed migration assays testing seven of the eight MCF-7 LOXL2 clones and one of the two MCF-7 LOXL2-V5 clones. MCF-7 LOXL2 clone 8 and V5-2 were not included in the panel, as they did not have consistent LOXL2 expression levels over several passages as monitored by real-time PCR. Except for clones 1 and 2, all MCF-7 overexpressing LOXL2 became significantly more migratory than the parental MCF-7 line (**Figure 18. A**). MCF-7 LOXL2 clone 2, which was significantly less migratory than parental MCF-7, expressed the least amount of LOXL2 and had no detectable processed 63 kDa LOXL2 peptide on Western analysis (**Figures 18. A and 15. A, B**). MCF-7 LOXL2 clone 4 that expressed the highest levels of both the 95 and 63 kDa LOXL2 peptides had highly significant increase in migratory ability (**Figures 15. B and 18. A**). MCF-7 LOXL2 clone 5 had less migratory ability than clone 9, although clone 5 expressed more LOXL2 mRNA (**Figures 18. A and 15. A**). However, on Western blot, clone 9 demonstrated somewhat higher level of the processed 63 kDa LOXL2 than MCF-7 LOXL2 clone 5 (**Figure 15. B**). These results suggested a possible correlation between the 63 kDa LOXL2 and cell migratory ability. Migration assays were also performed on MCF-10A LOXL2 clones 1 and 2 (**Figure 18. B**) that expressed the highest levels of LOXL2 mRNA detected by quantitative real-time PCR (**Figure 15. A**) and had the most pronounced phenotypic changes (**Figure 17. D**). In contrast to the effect of LOXL2 overexpression in MCF-7 clones, overexpression of LOXL2 in clones of the normal mammary cell line MCF-10A resulted in a decreased migratory ability compared to the parental cell line (**Figure 18. B**), despite the prominent change we observed in cell phenotype. In these cells, there appeared to be no correlation between the presence of the 63 kDa LOXL2 and cell migratory ability.

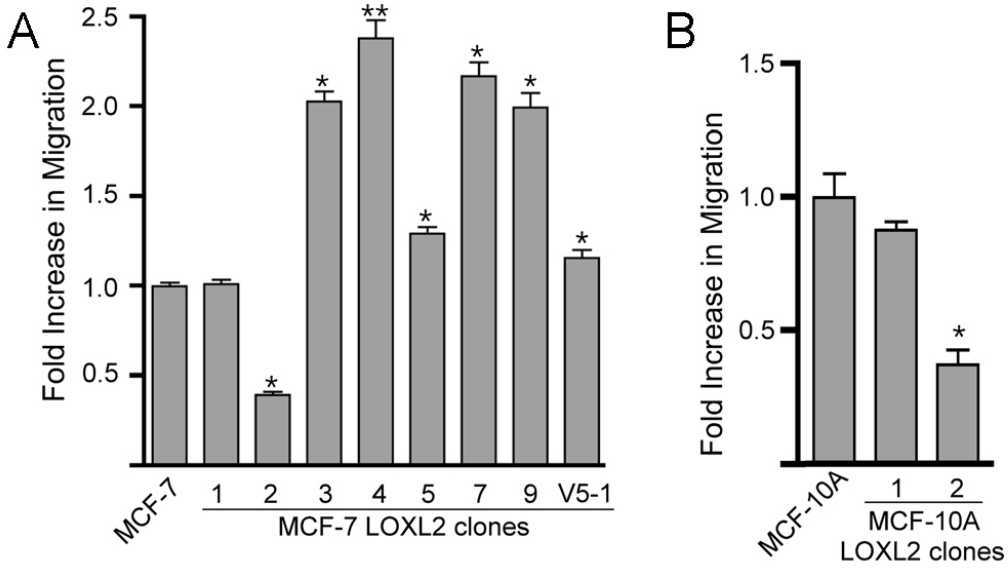

Figure 18. Effect of LOXL2 overexpression in MCF-7 and MCF-10A cells on cell migration. (A) Eight MCF-7 clones expressing LOXL2 (clones 1–5, 7, 9, V5-1) and (B) two MCF-10A clones (clones 1, 2) were evaluated for migratory ability. Fold increase in migratory ability of the clones over that of the parental line was calculated. The average number of migrating cells for the parental cell lines was 224 cells for MCF-7 and 1,120 cells for MCF-10A. *$p < 0.05$; **$p < 0.01$.

4.16. LOXL2 is catalytically active in both MCF-7 and MCF-10A cells

As we reported that the cell migratory ability of LOX was linked to its catalytic activity [269; 285] we determined whether the LOXL2 expressed in the MCF-7 and MCF-10A clonal cell line media was also catalytically active. Amine oxidase activity measurements were performed on parental MCF-7 and MCF-7 LOXL2 clones 7 and 9 that had the most migratory ability and LOXL2 expression profiles similar to that detected in the highly invasive and metastatic breast cancer cell line MB-231. In these assays, media fractions of both MCF-7 LOXL2 clones 7 and 9 had significantly higher amine oxidase activity than the parental MCF-7 (**Figure 19**). Amine oxidase activity measurements were also performed for MCF-10A LOXL2 clones 3, 4 and 5, along with the parental MCF-10A cells. MCF-10A LOXL2 clones 1 and 2 were slow growing and we could not obtain enough CCM proteins for activity measurements. MCF-10A

LOXL2 clones 3, 4 and 5, had similar protein expression profiles (**Figure 15. B**) and similar phenotype changes, and all three clones had significantly higher amine oxidase activity than the parental MCF-10A cells (**Figure 19**). The measured activities were not inhibitable by BAPN, indicating that LOX, LOXL and LOXL4 did not contribute to the measured activity, and that the overexpressed LOXL2 in these cells was catalytically active.

The activity data showed that both the normal and breast cancer cell lines contain catalytically active LOXL2. The MCF-7 parental cell line had lower activity than the MCF-10A parental cell line, corresponding to its lower level of LOXL2 expression (**Figures 19 and 15. B**). Although LOXL2 is not detectable in MCF-7 cells by Northern [269] and Western (**Figure 15. B**), real-time PCR demonstrated approximately 4,400 absolute mRNA copy numbers in MCF-7, compared to 54,700 absolute copy numbers for MCF-10A (GAPDH mRNA copy numbers similar in the two samples). The levels of activity in MCF-10A cells compared to MCF-7 activity (lower than 10-fold increase) did not exactly mirror the amount of mRNA detected. This may be due to differences in the amount of protein translated and the presence of LOXL2 forms that are catalytically active. Regardless, because all the cell lines demonstrated amine oxidase activity, it was unlikely that the presence of increased migratory ability of the MCF-7 LOXL2 clones and the absence of migratory ability of the MCF-10A LOXL2 clones was due to amine oxidase activity. We hypothesized that the difference in migratory ability between MCF-7 and MCF-10A LOXL2-overexpressing clones may be a consequence of other mechanisms, including different ability of these cells to compensate for processes that promote migratory cell behavior; different processing and functionally different forms of LOXL2 in normal breast epithelial and tumor cells; and/or potentially different substrates or interacting proteins for LOXL2 present in the ECM of these cells. To evaluate the latter hypothesis and to better understand the functional differences of LOXL2 in normal and tumor cells and tissues, we tested if the localization of LOXL2 was different between normal and cancerous tissues.

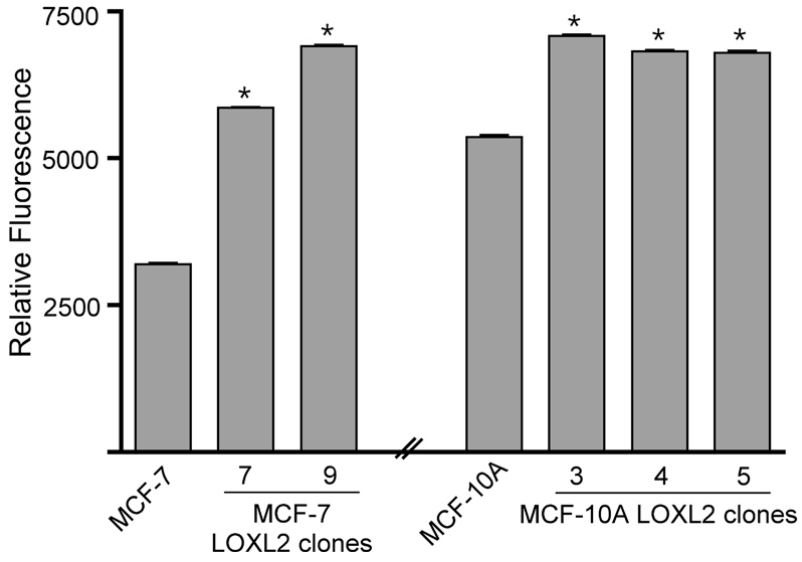

Figure 19. Effect of LOXL2 overexpression in MCF-7 and MCF-10A cells on amine oxidase activity. Two MCF-7 LOXL2 clones (7 and 9), and three MCF-10A LOXL2 clones (3–5) were evaluated for amine oxidase activity. CCM from these clones and the parental MCF-7 and MCF-10A were collected, concentrated and evaluated for fluorescence using the Amplex Red assay. *$p < 0.05$.

4.17. Altered localization of LOXL2 in breast tumor tissue

Previous examinations in our laboratory demonstrated LOXL2 expression in various tissue types known to have a secretory function, these were prostate glands, gastric glands, kidney tubules, type II cells of the lung that secrete surfactant (data not shown), colonic enteroendocrine cells that secrete peptide hormones **(study II).** Immunohistochemical analysis of an array containing various normal and cancerous tissues using the LOXL2 antibody also showed LOXL2 production in epithelial cells of mammary glands (**Figure 20**). LOXL2 was closely associated with the cell membrane facing the lumen in mammary glands (**Figures 20. A**) and the cell membrane in type II cells of the lung (data not shown). However, in breast and lung cancer cells, localization of the increased LOXL2 was generally more cytoplasmic (**Figure 20. B**). This cytoplasmic localization of LOXL2 was also seen in colon and esophageal cancer cells (**Study II**). Although immunohistochemistry does not indicate if LOXL2 is secreted in

tissues, data generated using the highly invasive breast cancer cell lines MB-231 (**Figure 15. B**) and Hs578T (data not shown), and results from this study indicate that LOXL2 protein is secreted. As LOXL2 is found on the lumenal surface of normal mammary glands (**Figure 20. A**) as well as normal gastric glands and kidney tubules (data not shown), secreted LOXL2 likely does not interact with the stromal ECM. However, in cancers arising from these cells, the tissue architecture is disorganized [310] and LOXL2 has the potential to interact with the matrix component of the surrounding stroma. Indeed, our yeast-two hybrid screen has identified several ECM proteins that potentially interact with LOXL2, including fibronectin (unpublished data not shown). Fibronectin has been demonstrated to regulate adhesion and migration [311], has increased expression in infiltrating breast cancer [312; 313] has been shown to regulate the activity of the homologous LOX protein [167] and has the potential to also regulate LOXL2.

The immunolocalization of LOXL2 to the lumenal surface of mammary and gastric glands, and kidney tubules, also indicated that LOXL2, whether secreted or not, may associate closely with the cell membrane. In this case, we would neither be able to detect this membrane-associated LOXL2, nor the possibly cytoplasmic LOXL2, in the media collected from our cultured cell lines. To evaluate the possibility of different processing and functionally different forms of LOXL2 not found in the media, we analyzed the CL fractions of all our clonal cell lines.

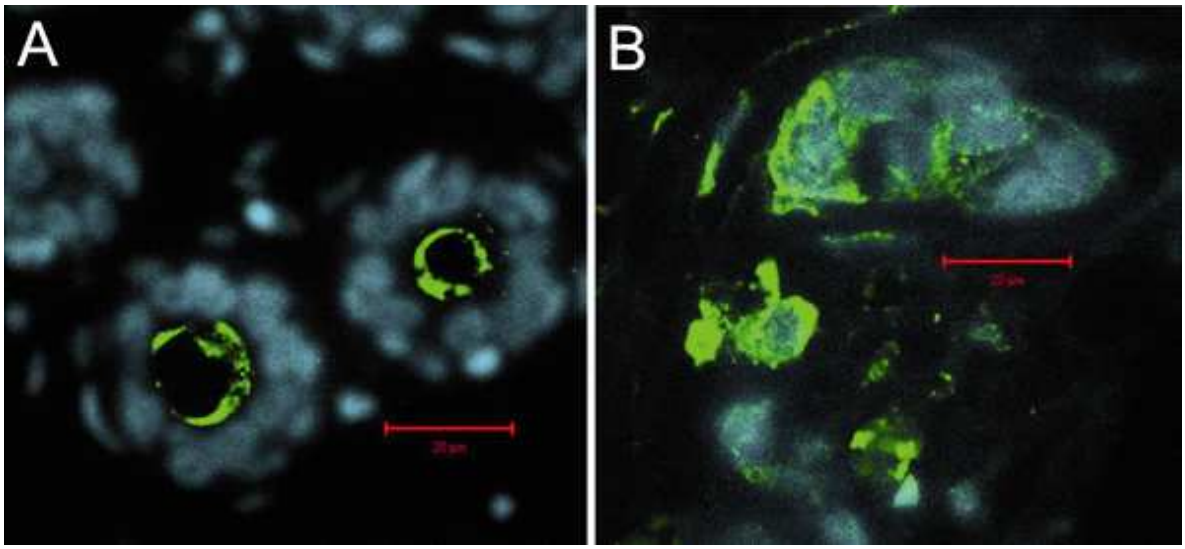

Figure 20. Immunohistochemical analysis of LOXL2 in normal and malignantly transformed human breast tissues. Histoarray slides containing normal breast and breast cancer tissues were subject to immunohistochemical analysis using the LOXL2 antibody (1:300) and Alexa Fluor 488, resulting in green fluorescence. Nuclei were counterstained with DAPI, visible in blue color. (A) In normal breast tissues, LOXL2 appears to mainly localize to the apical cell surface of epithelial cells. (B) In breast cancer tissues, increased LOXL2 expression appears more cytoplasmic. Pictures were taken with an LMS Pascal 5 Confocal microscope (Zeiss). Scale bars represent 20 μm.

4.18. Altered localization and size of LOXL2 in breast cell lines

All the stably transduced MCF-7 LOXL2-overexpressing clones expressed the 95 kDa LOXL2 peptide in the soluble cell fraction (**Figure 21. A**) and most in the insoluble cell fraction as well (**Figure 20. B**). There was no processed 63 kDa LOXL2 peptide found in the CL fraction of these clones. This pattern was consistent with the highly invasive, metastatic cell line MB-231, and indicated that for these breast cancer cells, the processed 63 kDa form was only found in the media (**Figures 15. B and 21**). However, for the stably transduced MCF-10A LOXL2-overexpressing clones, there were two peptides, sized 105 kDa and 95 kDa in both soluble and insoluble cell fractions (**Figures 21. C, D**). The 105 kDa LOXL2 peptide may represent a glycosylated form of LOXL2, as three potential N-linked glycosylation sites have been previously identified [239]. There was no 63 kDa peptide in either CL fractions, indicating that this form of LOXL2 may be specific to the media in both normal and cancerous breast cells. However, there was a 50 kDa peptide found in all MCF-10A clones and the parental line in the insoluble cell fraction (**Figure 21. D**), consisting of membrane-associated, membrane-bound and other insoluble proteins. This 50 kDa peptide has not been reported before. To evaluate if the 50 kDa peptide is a processed form of LOXL2, time course and protease inhibitor experiments were performed for MCF-10A LOXL2 clone 3. There was a gradual decrease of signal of the 105 kDa and 95 kDa in both CL fractions over time (**Figure 21. E, F**), accompanied by an increase in the 50 kDa peptide (**Figure 21. F**). Treatment with protease inhibitor resulted in

dramatic decrease in the 50 kDa peptide (**Figure 21. H**), accompanied by gain of the unprocessed LOXL2 in both CL fractions (**Figure 21. G, H**). These experiments indicated that the 50 kDa peptide is a proteolytically processed product of the 105 kDa and 95 kDa LOXL2.

The 50 kDa peptide was least abundant in MCF-10A LOXL2 clones 1 and 2 (**Figure 21. D**), despite these clones having the highest LOXL2 mRNA expression levels (**Figure 15. A**). Instead clones 1 and 2 had the most abundant 105 kDa and 95 kDa peptides in the soluble cell fraction. Overall, these two clones, which also had the most prominent phenotype change of the five MCF-10A LOXL2 clones, had a profile most similar to the pattern seen in the breast cancer cell lines. This change in localization, from insoluble membrane-associated to soluble cytoplasmic, nuclear and secreted, is consistent with our immunohistochemistry results (**Figure 20**). An alteration in LOXL2 processing and change in protein localization may be necessary for certain epithelial cells to transform from normal to cancerous.

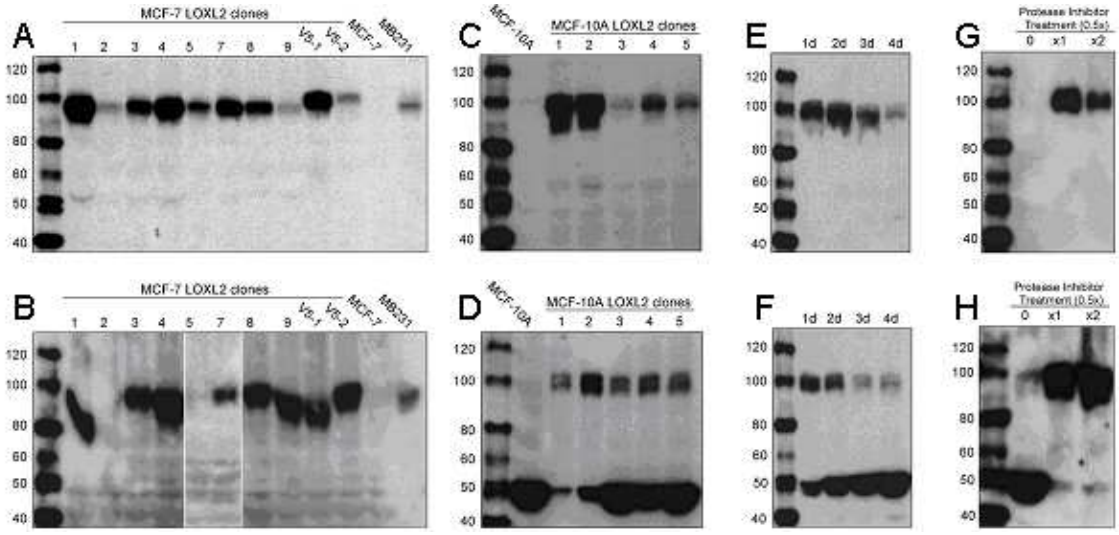

Figure 21. Alteration of LOXL2 localization in CL protein fractions isolated from the mammary cell lines stably transduced with full length LOXL2. Western analysis of (A) APSCL and (B) ISCL isolated from eight MCF-7 clones expressing LOXL2 without a V5 tag (1–5, 7–9) and two clones expressing LOXL2 with a V5 tag (V5-1, V5-2), parental MCF-7 and MB-231 cells. Western analysis of (C) APSCL and (D) ISCL isolated from parental MCF-10A and MCF-10A LOXL2 clones 1–5. Western analysis of (E) APSCL and (F) ISCL isolated from MCF10A LOXL2 clone 3 after 1–4 days of exposure to serum-free media. Western analysis of

(G) APSCL and (H) ISCL isolated from MCF-10A LOXL2 clone 3 after 4 days of exposure to 0, 1 or 2 treatments with 0.5x HALT protease inhibitor cocktail.

4.19. Activation of *loxl2* gene expression by 5-aza-dC and TSA treatment

Towards identifying the regulatory mechanisms responsible for the expression pattern differences of the *loxl2* gene in normal and tumor epithelial cells, we have previously demonstrated the presence of a single predicted CpG island of 1,150 bp, extending from upstream of the transcriptional start to intron 1 (**Study II**). To further evaluate if methylation of the *loxl2* CpG island or histone modification could contribute to the differential expression of LOXL2 seen in normal breast epithelial cells that express LOXL2 and the non-invasive and non-metastatic breast cancer cells that lack detectable LOXL2 by Western, we treated MCF-7, T47D, HMEC and MCF-10A cells with 5-aza-dC alone, or with TSA (**Figure 22**). Treatment with 5-aza-dC and TSA had no effect on LOXL2 expression in the normal, non-tumorigenic MCF-10A and HMEC cell lines, indicating that *loxl2* promoter methylation and histone deacetylation may not be a regulatory mechanism or that demethylation and histone acetylation have already occurred in these LOXL2 expressing cells (**Figure 22. A**). However, the epigenetic silencing mechanisms, methylation and/or histone deacetylation, may contribute to the suppressed LOXL2 expression in the tumorigenic, non-invasive MCF-7 and T47D cell lines. Indeed, treatment with 5-aza-dC caused a dose-dependent increase in *loxl2* gene transcription, and the effect was amplified by the addition of TSA (**Figure 22. B**). The susceptibility of the MCF-7 and T47D cell lines to epigenetic regulation may be related to their tumorigenicity, as the non-tumorigenic MCF-10A and HMEC cell lines were resistant. However, the fold-increase in *loxl2* gene expression in MCF-7 and T47D cells was still less than the 80-fold difference in LOXL2 expression between MCF-7 and MB-231 cells (**Figure 15. A**). For breast cancer cells to achieve the high level of LOXL2 expression seen in the highly invasive and metastatic MB-231 and Hs578T cells, it is likely that additional regulatory mechanisms are involved such as the actions of transcriptional enhancers and other factors that interact with transcription factor binding sites we have previously described in the promoter of the *loxl2* gene (**Study II**).

These may be induced by environmental factors such as hypoxia and increased cell density, which have been recently shown to upregulate LOXL2 [259].

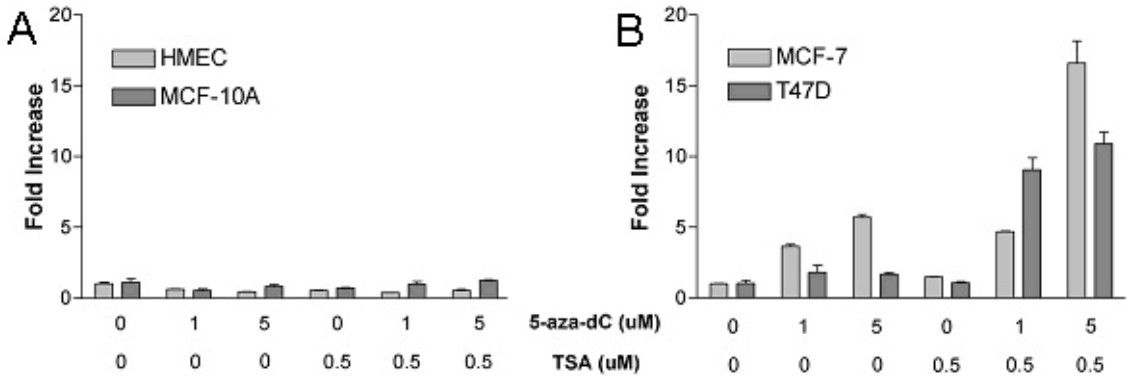

Figure 22. Effect of 5-aza-dC and TSA treatment on LOXL2 mRNA expression. (A) The normal breast cell lines, HMEC and MCF-10A, and (B) the poorly invasive breast cancer cell lines MCF-7 and T47D were treated with increasing concentrations of 5-aza-dC without (first three lanes in each graph), or with (latter three lanes) TSA. LOXL2 mRNA expression levels were measured by real-time PCR and standardized to GAPDH expression.

5. Discussion

During cancer progression, the ECM is dynamically altered such that its composition, turnover, processing and orientation change dramatically. These modifications influence cell shape, and modulate growth factor and hormonal responses to regulate processes including tissue morphogenesis and differentiation. Certain studies investigate potential role for lysyl oxidases in tumor progression by emphasizing the role of matrix stiffness. One side suggests that increased lysyl oxidase activity represents a possible host defense mechanism by stabilizing a scar-like peritumoral barrier, while lack of lysyl oxidase activity in the stroma favors tumor dispersion. For instance, myofibroblasts and myoepithelial cells in the stroma of *in situ* breast carcinomas express LOX at high levels, whereas a lack of LOX is associated with the loose stroma accompanying invading tumors [3]. The same group further confirmed this hypothesis, testing broncho-pulmonary carcinomas; a strong LOX expression was associated with the hypertrophic scar-like stromal reaction found at the front of tumor progression in SCCs, adenocarcinomas, large cell carcinomas, or at sites of initial extense in bronchiolo-alveolar carcinomas, tumors displaying a rather good prognosis. In contrast, little or no LOX expression was found within the stromal reaction of invasive carcinomas, small cell carcinomas, and neuroendocrine carcinomas [4].

Results we know from other studies propose a role for lysyl oxidases in tumor progression fundamentally conflict with the hypothesis above, in a sense that elevated lysyl oxidase activity causes a progressive stiffening of the stroma that can perturb tissue organization, promote cell growth and survival, enhance focal adhesion formation thus cell migration and tumor invasion [5; 6; 7; 8]. Both research groups used breast carcinoma as a model system, although latter one utilized *in vitro* cell cultures to establish their hypothesis.

A primary involvement of lysyl oxidases in cancer has also been explained by means of H_2O_2 production [314; 315]. H_2O_2 is released during lysyl oxidase mediated chemical reactions, which represents oxidative stress to cells. Increased ability of cells to migrate is a hallmark of tumor progression, and it has been shown that H_2O_2 produced by oxidative deamination promotes cell migration *in vitro* in human peripheral

blood mononuclear cells [283], vascular smooth muscle cells [284], and in invasive breast cancer cells [285]. In case of invasive breast cancer, the mechanism has been investigated in more its detail; it was accompanied by FAK/Src activation, and $p130^{Cas}$/Crk/Dock180 signaling complex formation with subsequent increase in Rac-GTP levels, which decreases actin stress fiber formation and increases formation of lamellipodia [316]. These results could nicely explain previous observations that increased LOX expression and enzymatic activity are exhibited by invasive breast carcinoma cells and were associated with their invasive properties [263; 269].

Study I

LOX-catalyzed oxidative reactions are known to use fibrillar collagen and elastin, and possibly other novel matrix proteins, as substrates. However, the nature of potential substrates and interactions of LOX with these substrates in the CNS has been poorly monitored. In addition to collagen type I [317] and type IV [318], invasive astrocytes are known to produce a large amount of tropoelastin [319]. These astrocyte-derived ECM components, in addition to being a potential adhesive media, may provide unusually high local substrate concentration for LOX, resulting in increased generation of hydrogen peroxide, subsequent hydrogen peroxide-mediated signaling and enhanced cell migration and invasion. It should be noted though, that tropoelastin synthesized by astrocytoma cells is susceptible to proteolytic trimming to the extent that it cannot be assembled into extracellular elastic fibers. However, endogenous tropoelastin degradation products generate signals in malignant astrocytoma cells leading to cell cycle progression thus exhibiting mitogenic activity [320].

Around the same time LOX has came in focus of CNS research in another aspect. Cumulative evidence indicates that after injury in the CNS, neurons possess innate ability to regenerate, although the ECM exerts prohibitive effects aborting the neuronal regeneration [321; 322]. An initial regenerative growth is allowed; however, within a short period of time, the new axonal sprouts stop growing, retract, and degenerate [323]. It has been proposed, that the early regenerative axonal sprouting is aborted as a consequence of a process with delayed activation, called injury-induced

astrocytic scar formation. In the disruptive process of scar formation the extracellular presence of LOX was noted, although the origin of secretion could not be identified. It has been suggested, that one of those cell types attracted to the site of injury would be responsible for LOX secreting and subsequent scar formation [53]. Later it was proved, that inhibition of LOX activity with BAPN accelerates functional recovery of neurons by reducing the physical barrier due to scar tissue formation [324; 325]. Our study identifies astrocytes as a potential source of active LOX production, thereby contributes to the theory that astrocytic scar formation generates an inhospitable environment and halts neuronal regeneration after CNS injury.

Our investigation on the role of LOX in invasive astrocytoma cell lines and primary brain tumors was based on our previous reports on the role of LOX in breast tumor cells. Those experiments demonstrated that the expression and catalytic activity of LOX were associated with invasive properties of breast tumor epithelial cells and were essential in inducing invasive and metastatic ability in breast tumors [269]. LOX overexpression resulted in increased adhesion, migration and invasion of non-invasive breast tumor cells, and this effect was due to LOX-generated H_2O_2 that mediated activation of the focal adhesion complex through Src(Tyr418), FAK(Tyr397) and FAK(Tyr576) phosphorylation [285]. In our study we were able to provide evidence for the same molecular mechanism leading to FAK(Tyr576) phosphorylation and we identified another step of the cascade being paxillin(Tyr118) phosphorylation, ultimately leading up to increased cell migration. Furthermore, cells that expressed active LOX had the highest level of fibronectin expression, thus a potential role for fibronectin in LOX activation in the CNS could be estimated, based on our previous finding [167].

Several studies indicate reactive oxygen species (ROS) as regulators of SFK activity, and hence cell migration. It has been reported, that exposure of several cell types (T-cells, B-cells, fibroblasts) to H_2O_2 (5 mM, 15 min) increases catalytic activity of Lck and induces autophosphorylation of the tyrosyl residue in the activation loop [326]. Inhibitory autophosphorylation at the C-terminal region was also induced after the H_2O_2 treatment; however, the activating autophosphorylation at the activation loop seemed to override the effect of inhibitory autophosphorylation. This inhibitory phosphorylation was most likely due to the inactivation of CD45 upon H_2O_2 treatment

(3 mM, 1 min) [327]. Another study using mesangial cells shows inhibition of c-Src kinase activity upon short treatment (2-5 min) with H_2O_2 (0.1-10 mM) suggesting phosphorylation of Y529 in the Src regulatory domain [328]. In a recent study, testing several cell types (endothelial-, embryonic kidney epithelial cells, fibroblasts) H_2O_2 at low to moderate concentrations (50-250 µM) could inactivate SFKs *in vivo* but not *in vitro* [329], although in a short time SFK kinase activity gradually returned to the basal level. This inactivation dislocated SFKs from the focal adhesion sites, which correlated well with a profound reduction in the tyrosine phosphorylation of focal adhesion proteins p130Cas and paxillin. It should be noted, that after reversion in SFK kinase activity to basal level, activated SFKs were mainly detected as big clusters in the cytoplasm, suggesting a sustained inactivation of SFKs localized to cell peripheral focal adhesion sites and the plasma membrane, at least in endothelial cells. The fact, that H_2O_2 does not directly inhibit SFKs *in vivo*, argues against the theory that phosphorylation of the activation loop conserved tyrosine is merely catalyzed by the kinase itself. Indeed, recent findings revealed a possible role of kinases other than SFK in the phosphorylation of the activation loop tyrosine [326; 330]. Therefore, according to the latest hypothesis, H_2O_2 may inhibit RTK activity through oxidizing these novel kinases [329]. There has been another regulatory mechanism described, may be involved in the inactivation of SFKs by H_2O_2 *in vivo*. CD45 and other protein tyrosine phosphatases can be reversibly oxidized and inactivated by ROS which may render SFKs to an inactive form [327; 331].

Study II

In previous studies, we reported that increased LOXL2 expression was associated with an invasive, metastatic phenotype in breast cancer cell lines [269] and metastatic squamous and spindle cell carcinomas [246]. It was also reported that non-invasive breast cancer cells transfected with LOXL2 were locally invasive in a mouse model [263]. Similarly, in our study, we have found that there is an increase in LOXL2 expression in colon and esophageal tumors, and that increased LOXL2 expression is significantly associated with poorly-differentiated colon tumors.

Immunohistochemistry of normal colon and esophageal tissue showed absence of LOXL2 in the mitotically active cells that are thought to be the origin of dysplastic and subsequently, tumor cells [294; 295]. Using colon and esophageal cancer tissue arrays, we determined that the majority of the tumors, 83 and 92%, respectively, expressed LOXL2. Moreover, there were significantly less LOXL2-expressing tumor cells in well-differentiated colon adenocarcinomas, compared to poorly differentiated adenocarcinoma and mucinous carcinoma. The latter two were grouped in this study due to similar characteristics including more aggressive behavior and high incidence of metastasis [332]. This is consistent with previous observations of increased LOXL2 protein and mRNA expression with breast cancer tumor grade [263] and invasive ability [246; 263; 269], respectively.

On the other hand, downregulation of LOXL2 has also been demonstrated in various cancer cell lines and tissues compared with normal cells and tissues. In head and neck SCCs, the mean LOXL2 expression was slightly lower in the cancer cells, but there was essentially no difference in cancer tissues [257]. In the ovarian tumor studies, expression of LOXL2 was present in normal ovarian surface epithelial cells [333], but downregulated in ovarian tumors [333; 334]. Normal breast epithelial cells also express LOXL2, detected by immunohistochemistry of breast tissue [263] and Western blot analysis of cultured normal human mammary epithelial cells (our unpublished data), but the poorly invasive, non-metastatic breast cancer cell lines, T47D and MCF-7, do not express LOXL2 [269]. The poorly invasive HCT-116 [335] and the HCT-15 and DLD-1 cell lines [336], also do not express LOXL2. In contrast, the majority of colon cancer tissues did express LOXL2, particularly those that are less differentiated.

Moreover, LOXL2 was found to be upregulated in epithelial to mesenchymal transition, which involves the loss of the epithelial phenotype and gain of a mesenchymal, motile phenotype [245]. This is consistent with our observation of absent LOXL2 expression in the epithelioid T47D, MCF-7, HCT-116, HCT-15, and DLD-1 cell lines, and presence in the highly invasive/metastatic breast cancer cell lines MB-231 and Hs578T, which are mesenchymal in phenotype [269]. In some tissues, like breast and ovary, there may be initial loss of LOXL2 expression followed by re-expression during tumor progression, perhaps in response to microenvironmental cues. Indeed, LOXL2 expression can be induced in MCF-7 cells by co-culture with

fibroblast-conditioned media [269]. Alternately, LOXL2 may behave similar to its family member LOX, which has been documented as having tumor suppressive and tumor promoting abilities, depending on cell type and transformation status [268; 269; 337].

To evaluate if epigenetic transcriptional regulation was a possible mechanism by which LOXL2 expression could be modulated, as documented for LOX [304; 305], we treated the colon carcinoma cell lines DLD-1 and HCT-116 with the demethylating agent 5-aza-dC, which resulted in increased expression of LOXL2. It was reported that colon cancer cell lines HCT-116 and HCT-15, and primary tumors had similar distribution and frequency of gene methylation [338]. Therefore, the gain of LOXL2 expression in later phases of colon tumor progression could certainly be due to promoter demethylation, and this mechanism may also be important for esophageal tumor development as well. These results, along with our observation that esophageal SCC samples that demonstrated LOH of the LOXL2 gene had a higher incidence of absent LOXL2 protein by immunohistochemistry, implies that both genetic and epigenetic mechanisms are likely involved in the modulation of LOXL2 gene expression during cancer progression.

This study is the first to evaluate the possible involvement of LOXL2 in colon and esophageal cancer pathogenesis, and the first to implicate demethylation as a possible mechanism of LOXL2 regulation. Modulation of expression may also be accomplished through transcriptional factors implicated in tumor progression and EMT, such as AP1, NFκB and WT1 [339; 340; 341]. We have recently reported that Snail, a protein crucial to the process of EMT, interacts with LOXL2 protein [246]. Overexpression of LOXL2, in collaboration with Snail, resulted in induction of EMT, while downregulation of LOXL2 in Snail-expressing metastatic carcinoma cells caused gain of E-cadherin expression and reduced expression of mesenchymal, invasive, and angiogenic markers. Moreover, LOXL2 increased Snail protein stability, and all these effects required the presence of two lysine residues in the N-terminal portion of Snail [246]. Although it is not known whether LOXL2 has catalytic activity against Snail, the importance of the interaction between LOXL2 and Snail in EMT supports a contribution of increased LOXL2 to tumor progression, particularly invasion and

metastasis, and indicate that in certain tumor types LOXL2 may be a potential marker for predicting metastatic potential, and a target for novel therapeutic intervention.

Study III

Catalytic activity for LOXL2 has previously been described only in transfected Chinese hamster ovary cells [240]. Our results with monoclonal cell lines that stably express high levels of LOXL2, demonstrated that LOXL2 secreted by both MCF-7 malignantly transformed and MCF-10A non-transformed human breast epithelial cells, is also catalytically active. Thus, LOXL2 has the potential to contribute to extracellular stromal stiffness and fibrosis, similar to its family members. However, there is evidence to suggest that LOXL2 has specific features. It is the only LOX family member whose catalytic activity is not inhibitable by BAPN [240]. It is also the only member that did not respond to BMP-2 treatment that induces osteoblast differentiation and type I collagen production that leads to collagen cross-linking in bone [227]. Moreover, there is evidence that LOXL2 functions intracellularly, as it has been reported that LOXL2 interacts with the transcription factor Snai1 [246]. In this study, we found LOXL2 secreted and in membrane-associated and cytoplasmic and nuclear compartments, and that there was differential localization and processing of the LOXL2 protein in normal and cancer tissues and cells. The functional relevance of these differences has yet to be characterized. Although LOXL2 overexpression resulted in a more mesenchymal appearance in all of our clones, LOXL2 only induced increased migration in the transformed and tumorigenic MCF-7, but not in normal mammary epithelial cells. We have noted similarly selective cell type-dependent response in our previous studies with LOX. Active LOX promoted migration in LOX overexpressing MCF-7 cells, but not in MCF-10A cells [285; 342]. Congruent findings on the behavior of these two members of the lysyl oxidase family support that increased expression and activity of LOX and LOXL2 alone is not sufficient to promote increased migration of normal mammary epithelial cells, but is highly effective in non-invasive tumor cells. We hypothesize that accessibility of substrate or interacting molecules within tissue matrices and within the cell may determine the effect of LOX family members in normal cell function, tumorigenesis and acquisition of invasive ability, including migration. We have noted

that cultured normal breast epithelial cells produce a processed 50 kDa peptide of LOXL2 that is likely processed extracellularly, and then associated with the extracellular membrane surface. In tissues, we have observed localization of LOXL2 to the lumenal surfaces of normal mammary and gastric glands and kidney tubules (data not presented for latter two). Alterations of tissue architecture in the progression of these normal tissues to cancer, would allow for the exposure of membrane-bound LOXL2 protein to the tumor matrix, possibly facilitating interactions between LOXL2 and ECM molecules to promote metastatic cell behavior. In cultured breast cancer cells, the processed form of LOXL2 is only found in the media, indicating a possible extracellular role. Several members of the LOX family are known to interact with and modify ECM proteins, but the role of LOXL2 in such extracellular interactions has not been characterized. We do have preliminary data to suggest that LOXL2 interacts with the extracellular protein, fibronectin, which has been described to have a role in adhesion and migration [311]. Besides the secreted form, immunohistochemistry on breast and lung cancer tissues, as well as our previous results with colon and esophageal cancer (**Study II**), revealed that LOXL2 appeared in the cytoplasm. It has been previously shown that LOXL2 interacts with the transcription factor Snail [246]. LOXL2 contains two protein domains that have the potential to interact with other molecules, a CRL domain and four SRCR domains. Other proteins containing these domains have been reported to be involved in cell adhesion and EMT, processes that facilitate cell migration and invasion. The LOXL2-CRL domain has homology to the receptors for growth hormone and prolactin [166], proteins that induce oncogenic transformation and a mesenchymal phenotype and affect breast cancer cell proliferation [343; 344; 345]. The SRCR superfamily contains highly conserved secreted or cell surface proteins [346], reported to be involved in cell adhesion and polarity [347; 348; 349], alterations of which can induce transformation and EMT [350; 351]. Besides the differences in localization of LOXL2 protein in normal and pathologic states, the amount of LOXL2 expression may be important as well. In mammalian cells, gene silencing is most often associated with hypermethylation of the promoter region and a tight chromatin conformation controlled by histone modifications [15; 48]. We identified CpG island methylation and histone deacetylation as two cellular mechanisms that contribute to the lack of LOXL2 expression in non-invasive, tumorigenic mammary

epithelial cell cultures. Notably, applying both treatments, 5-aza-dC for demethylation and TSA for histone acetylation, resulted in prominent re-expression of LOXL2 in the tumorigenic MCF-7 and T47D, consistent with the dynamic link of these two epigenetic events [16]. Along with our *in vitro* assay results, growing number of studies indicate that elevated LOXL2 expression levels correlate both with primary tumor development in tumorigenesis and with the aggressive nature of mammary carcinomas. Thus, identifying epigenetic regulatory mechanisms that affect LOXL2 expression in these cells offers a potential target in clinical tumor therapy in possibly inhibiting cancer growth and metastasis. Furthermore, our results indicate that the monoclonal cell lines we established are an appropriate model to further evaluate the role of LOXL2 in the progression of non-invasive breast cancer cells towards a metastatic phenotype.

6. Conclusions

In conclusion, results of present thesis on individual roles of LOX and LOXL2 in astrocytic-, colon-, esophageal-, and mammary tumors can be summarized as follows:

a) The LOX antibody we developed specifically recognizes LOX and can be used in immunocytochemical, immunohistochemical, and Western blot analyses.

b) LOX is produced by astrocytes and shows increased expression and activity in high grade astrocytoma tumor cells.

c) Increased LOX activity contributes to increased cell migration in high grade astrocytic tumor cells, facilitating focal adhesion formation by means of H_2O_2 release.

d) The LOXL2 antibody we developed specifically recognizes LOXL2 and can be used in immunocytochemical, immunohistochemical, and Western blot analyses.

e) Compared to normal colon tissue, LOXL2 shows increased expression in colon adenocarcinomas, where the positive correlation between LOXL2 expression and tumor grade is statistically significant.

f) Compared to normal esophagus tissue, esophageal SSC tumors show increased LOXL2 expression.

g) LOH affecting the *loxl2* locus can be detected in approximately one third of colon adenocarcinoma and esophageal SSC tumors.

h) Epigenetic gene silencing mechanisms could contribute to decreased LOXL2 expression in normal colon epithelial cells and low grade colon adenocarcinoma cells, compared to high grade colon adenocarcinoma cells.

i) LOXL2 produced by mammary epithelial cells is catalytically active.

j) LOXL2 overexpression in normal mammary epithelial cells and in non-invasive mammary adenocarcinoma cells causes loss of epithelial appearance and induces a more mesenchymal cell morphology.

k) LOXL2 overexpression stimulates cell migration only in transformed mammary epithelial cells, not in normal mammary epithelial cells, possibly because altered extracellular processing of LOXL2.

l) The 65 kDa and 50 kDa forms of LOXL2 are likely to be products of extracellular proteolytic processing.

m) The low level of LOXL2 expression typical in non-invasive transformed mammary epithelial cells may be due to promoter hypermethylation and histone deacetylation epigenetic silencing mechanisms.

Abstract

Lysyl oxidases are copper-dependent amine oxidases responsible for covalent cross-linking of collagen and elastin molecules in the extracellular matrix. The role of lysyl oxidases in tumor progression has been shown by multiple studies. Both LOX and LOXL2, two members of the family, have been implicated in both tumor suppression and tumor promotion. The aim of our studies was to investigate roles of LOX and LOXL2 enzyme expression in certain tumor types of epithelial and neuroepithelial origin. For our studies we generated and characterized two polyclonal antibodies specifically recognizing LOX and LOXL2. Our results provide evidence that enzymatically active LOX is produced by astrocytes and shows increased expression in high grade astrocytomas. Elevated LOX activity contributes to increased astrocytic cell migration, facilitating focal adhesion formation by means of H_2O_2 release. We also show that compared with normal colon tissue, LOXL2 shows increased expression in colon adenocarcinomas, where the positive correlation between LOXL2 expression and tumor grade is statistically significant. Similarly, compared to normal esophagus tissue, esophageal SSC tumors show increased LOXL2 expression. Loss of heterozygosity affecting the *loxl2* locus can be detected in approximately one third of these two tumor types. Furthermore, we identified promoter hypermethylation and histone deacetylation as two epigenetic gene silencing mechanisms contributing to decreased LOXL2 expression in normal colon epithelial cells and low grade colon adenocarcinoma cells, compared to high grade colon adenocarcinoma cells. We also show experimental evidence proving that LOXL2 produced by mammary epithelial cells is catalytically active. Overexpression of LOXL2 in normal mammary epithelial cells and in non-invasive mammary adenocarcinoma cells causes loss of epithelial appearance and induces a more mesenchymal cell morphology; and stimulates cell migration but only in transformed mammary epithelial cells, not in normal mammary epithelial cells, possibly due to altered extracellular processing of LOXL2. The low level of LOXL2 expression, typical in non-invasive transformed mammary epithelial cells, may also be explained by epigenetic silencing mechanisms. In summary, our results help to clarify some of the controversy around the biological importance of lysyl oxidases in tumor progression.

Összefoglaló

A lizil oxidázok réztartalmú amin oxidázok, fő funkciójuk a sejtközötti állomány elasztin és kollagén molekuláinak kovalens keresztkötése. Ezen túlmenően, számos tanulmány bizonyítja tumorprogresszióban betöltött szerepüket; daganattípustól függően mind a LOX, mind a LOXL2, a lizil oxidáz fehérjecsalád két tagja, bizonyítottan tumorszuppresszor és tumorpromóter funkciót is betölthet. Kísérleteinkkel a LOX és LOXL2 enzimek jelenlétének és aktivitásának különböző epiteliális és neuroepiteliális tumorokban betöltött szerepét kívántuk pontosítani. Ehhez LOX-ot és LOXL2-t specifikusan felismerő poliklonális ellenanyagokat terveztünk és gyártattunk. Eredményeink bizonyítják, hogy az asztrociták aktív LOX termelésére képesek és magas grádusú asztrocitómákban a LOX aktivitás megemelkedett, mely hidrogén-peroxid termelés révén fokális adhéziók kialakulásához vezet, ezzel a sejtek migrációs képességét növeli. Továbbá kimutattuk, hogy normál szövetekhez képest mind vastagbél adenokarcinómákban, mind nyelőcső laphámrákokban a LOXL2 termelés megemelkedett, mely a vastagbél adenokarcinómák esetén statisztikailag jelentős mértékben pozitív összefüggést mutat a tumor grádusával. A *loxl2* gén lókuszát érintő deléció – heterozigótaság elvesztése – a vizsgált tumorok egyharmadában volt azonosítható. Ezen túlmenően promóter hipermetilációt és hiszton deacetilációt, két epigenetikai géncsendesítési folyamatot sikerült azonosítanunk, melyek hozzájárulnak a LOXL2 normál vastagbél és alacsony grádusú vastagbél adenokarcinóma szövetekben tapasztalt alacsony szintű expressziójához. Bebizonyítottuk, hogy az emlő epiteliális sejtek által termelt LOXL2 enzimatikusan aktív, és hogy LOXL2 túltermelés hatására ezek a sejtek egy kevésbé differenciálódott, inkább mezenchimális jellegű morfológiát mutatnak. Normál emlő epiteliális sejtekkel szemben a LOXL2 túltermelésnek sejtmigrációt fokozó hatása csak a transzformálódott emlő epiteliális sejteken volt, melynek hátterében feltételezhető, hogy egy megváltozott extracelluláris fehérjeérési folyamat rejlik. A nem-invazív emlő epiteliális sejtekre jellemző alacsony LOXL2 expresszió okozati tényezőjeként szintén epigenetikus génecsendesítési folyamatokat azonosítottunk. Összességében elmondhatjuk, hogy eredményeink olyan megállapításokat szögeznek le, melyek a lizil oxidázok tumorprogresszióban betöltött szerepét finomabb részleteiben engedik megérteni.

References

[1] N. Nagan, and H.M. Kagan, Modulation of lysyl oxidase activity toward peptidyl lysine by vicinal dicarboxylic amino acid residues. Implications for collagen cross-linking. J Biol Chem 269 (1994) 22366-71.

[2] L.I. Smith-Mungo, and H.M. Kagan, Lysyl oxidase: properties, regulation and multiple functions in biology. Matrix Biol 16 (1998) 387-98.

[3] S. Peyrol, M. Raccurt, F. Gerard, C. Gleyzal, J.A. Grimaud, and P. Sommer, Lysyl oxidase gene expression in the stromal reaction to in situ and invasive ductal breast carcinoma. Am J Pathol 150 (1997) 497-507.

[4] S. Peyrol, F. Galateau-Salle, M. Raccurt, C. Gleyzal, and P. Sommer, Selective expression of lysyl oxidase (LOX) in the stromal reactions of broncho-pulmonary carcinomas. Histol Histopathol 15 (2000) 1127-35.

[5] M.J. Paszek, and V.M. Weaver, The tension mounts: mechanics meets morphogenesis and malignancy. J Mammary Gland Biol Neoplasia 9 (2004) 325-42.

[6] M.J. Paszek, N. Zahir, K.R. Johnson, J.N. Lakins, G.I. Rozenberg, A. Gefen, C.A. Reinhart-King, S.S. Margulies, M. Dembo, D. Boettiger, D.A. Hammer, and V.M. Weaver, Tensional homeostasis and the malignant phenotype. Cancer Cell 8 (2005) 241-54.

[7] L. Kass, J.T. Erler, M. Dembo, and V.M. Weaver, Mammary epithelial cell: influence of extracellular matrix composition and organization during development and tumorigenesis. Int J Biochem Cell Biol 39 (2007) 1987-94.

[8] S. Kumar, and V.M. Weaver, Mechanics, malignancy, and metastasis: The force journey of a tumor cell. Cancer Metastasis Rev (2009).

[9] K. Csiszar, Lysyl oxidases: a novel multifunctional amine oxidase family. Prog Nucleic Acid Res Mol Biol 70 (2001) 1-32.

[10] S.I. Grewal, and D. Moazed, Heterochromatin and epigenetic control of gene expression. Science 301 (2003) 798-802.

[11] C. Wu, and J.R. Morris, Genes, genetics, and epigenetics: a correspondence. Science 293 (2001) 1103-5.

[12] K.D. Robertson, and P.A. Jones, DNA methylation: past, present and future directions. Carcinogenesis 21 (2000) 461-7.

[13] M.R. Rountree, K.E. Bachman, J.G. Herman, and S.B. Baylin, DNA methylation, chromatin inheritance, and cancer. Oncogene 20 (2001) 3156-65.

[14] S.B. Baylin, M. Esteller, M.R. Rountree, K.E. Bachman, K. Schuebel, and J.G. Herman, Aberrant patterns of DNA methylation, chromatin formation and gene expression in cancer. Hum Mol Genet 10 (2001) 687-92.

[15] T. Jenuwein, and C.D. Allis, Translating the histone code. Science 293 (2001) 1074-80.

[16] F. Fuks, W.A. Burgers, A. Brehm, L. Hughes-Davies, and T. Kouzarides, DNA methyltransferase Dnmt1 associates with histone deacetylase activity. Nat Genet 24 (2000) 88-91.

[17] M.R. Rountree, K.E. Bachman, and S.B. Baylin, DNMT1 binds HDAC2 and a new co-repressor, DMAP1, to form a complex at replication foci. Nat Genet 25 (2000) 269-77.

[18] K.E. Bachman, M.R. Rountree, and S.B. Baylin, Dnmt3a and Dnmt3b are transcriptional repressors that exhibit unique localization properties to heterochromatin. J Biol Chem 276 (2001) 32282-7.
[19] F. Fuks, W.A. Burgers, N. Godin, M. Kasai, and T. Kouzarides, Dnmt3a binds deacetylases and is recruited by a sequence-specific repressor to silence transcription. Embo J 20 (2001) 2536-44.
[20] A.D. Riggs, and P.A. Jones, 5-methylcytosine, gene regulation, and cancer. Adv Cancer Res 40 (1983) 1-30.
[21] S.J. Clark, J. Harrison, and M. Frommer, CpNpG methylation in mammalian cells. Nat Genet 10 (1995) 20-7.
[22] A.P. Bird, CpG-rich islands and the function of DNA methylation. Nature 321 (1986) 209-13.
[23] M. Gardiner-Garden, and M. Frommer, CpG islands in vertebrate genomes. J Mol Biol 196 (1987) 261-82.
[24] D. Takai, and P.A. Jones, Comprehensive analysis of CpG islands in human chromosomes 21 and 22. Proc Natl Acad Sci U S A 99 (2002) 3740-5.
[25] F. Antequera, and A. Bird, Number of CpG islands and genes in human and mouse. Proc Natl Acad Sci U S A 90 (1993) 11995-9.
[26] D.P. Barlow, Gametic imprinting in mammals. Science 270 (1995) 1610-3.
[27] K.D. Robertson, DNA methylation, methyltransferases, and cancer. Oncogene 20 (2001) 3139-55.
[28] K.D. Robertson, E. Uzvolgyi, G. Liang, C. Talmadge, J. Sumegi, F.A. Gonzales, and P.A. Jones, The human DNA methyltransferases (DNMTs) 1, 3a and 3b: coordinate mRNA expression in normal tissues and overexpression in tumors. Nucleic Acids Res 27 (1999) 2291-8.
[29] T.H. Bestor, The DNA methyltransferases of mammals. Hum Mol Genet 9 (2000) 2395-402.
[30] J.K. Christman, 5-Azacytidine and 5-aza-2'-deoxycytidine as inhibitors of DNA methylation: mechanistic studies and their implications for cancer therapy. Oncogene 21 (2002) 5483-95.
[31] D.V. Santi, A. Norment, and C.E. Garrett, Covalent bond formation between a DNA-cytosine methyltransferase and DNA containing 5-azacytosine. Proc Natl Acad Sci U S A 81 (1984) 6993-7.
[32] L.H. Li, E.J. Olin, H.H. Buskirk, and L.M. Reineke, Cytotoxicity and mode of action of 5-azacytidine on L1210 leukemia. Cancer Res 30 (1970) 2760-9.
[33] E. Flatau, F.A. Gonzales, L.A. Michalowsky, and P.A. Jones, DNA methylation in 5-aza-2'-deoxycytidine-resistant variants of C3H 10T1/2 C18 cells. Mol Cell Biol 4 (1984) 2098-102.
[34] J.K. Christman, N. Mendelsohn, D. Herzog, and N. Schneiderman, Effect of 5-azacytidine on differentiation and DNA methylation in human promyelocytic leukemia cells (HL-60). Cancer Res 43 (1983) 763-9.
[35] F. Creusot, G. Acs, and J.K. Christman, Inhibition of DNA methyltransferase and induction of Friend erythroleukemia cell differentiation by 5-azacytidine and 5-aza-2'-deoxycytidine. J Biol Chem 257 (1982) 2041-8.
[36] S.M. Taylor, and P.A. Jones, Mechanism of action of eukaryotic DNA methyltransferase. Use of 5-azacytosine-containing DNA. J Mol Biol 162 (1982) 679-92.

[37] A. Cihak, Biological effects of 5-azacytidine in eukaryotes. Oncology 30 (1974) 405-22.
[38] E. Kaminskas, A.T. Farrell, Y.C. Wang, R. Sridhara, and R. Pazdur, FDA drug approval summary: azacitidine (5-azacytidine, Vidaza) for injectable suspension. Oncologist 10 (2005) 176-82.
[39] M.A. Gama-Sosa, V.A. Slagel, R.W. Trewyn, R. Oxenhandler, K.C. Kuo, C.W. Gehrke, and M. Ehrlich, The 5-methylcytosine content of DNA from human tumors. Nucleic Acids Res 11 (1983) 6883-94.
[40] J.N. Lapeyre, M.S. Walker, and F.F. Becker, DNA methylation and methylase levels in normal and malignant mouse hepatic tissues. Carcinogenesis 2 (1981) 873-8.
[41] A.P. Feinberg, and B. Vogelstein, Alterations in DNA methylation in human colon neoplasia. Semin Surg Oncol 3 (1987) 149-51.
[42] S.E. Goelz, B. Vogelstein, S.R. Hamilton, and A.P. Feinberg, Hypomethylation of DNA from benign and malignant human colon neoplasms. Science 228 (1985) 187-90.
[43] S. Ribieras, X.G. Song-Wang, V. Martin, P. Lointier, L. Frappart, and R. Dante, Human breast and colon cancers exhibit alterations of DNA methylation patterns at several DNA segments on chromosomes 11p and 17p. J Cell Biochem 56 (1994) 86-96.
[44] M. Ehrlich, DNA methylation in cancer: too much, but also too little. Oncogene 21 (2002) 5400-13.
[45] P.A. Jones, The DNA methylation paradox. Trends Genet 15 (1999) 34-7.
[46] C. Nguyen, G. Liang, T.T. Nguyen, D. Tsao-Wei, S. Groshen, M. Lubbert, J.H. Zhou, W.F. Benedict, and P.A. Jones, Susceptibility of nonpromoter CpG islands to de novo methylation in normal and neoplastic cells. J Natl Cancer Inst 93 (2001) 1465-72.
[47] P.A. Jones, and P.W. Laird, Cancer epigenetics comes of age. Nat Genet 21 (1999) 163-7.
[48] P.A. Jones, and S.B. Baylin, The fundamental role of epigenetic events in cancer. Nat Rev Genet 3 (2002) 415-28.
[49] C.K. Glass, and M.G. Rosenfeld, The coregulator exchange in transcriptional functions of nuclear receptors. Genes Dev 14 (2000) 121-41.
[50] T. Kouzarides, Histone acetylases and deacetylases in cell proliferation. Curr Opin Genet Dev 9 (1999) 40-8.
[51] D.C. Drummond, C.O. Noble, D.B. Kirpotin, Z. Guo, G.K. Scott, and C.C. Benz, Clinical development of histone deacetylase inhibitors as anticancer agents. Annu Rev Pharmacol Toxicol 45 (2005) 495-528.
[52] S. Shankar, and R.K. Srivastava, Histone deacetylase inhibitors: mechanisms and clinical significance in cancer: HDAC inhibitor-induced apoptosis. Adv Exp Med Biol 615 (2008) 261-98.
[53] G.M. Gilad, H.M. Kagan, and V.H. Gilad, Lysyl oxidase, the extracellular matrix-forming enzyme, in rat brain injury sites. Neurosci Lett 310 (2001) 45-8.
[54] A. Paetau, and I. Virtanen, Cytoskeletal properties and endogenous degradation of glial fibrillary acidic protein and vimentin in cultured human glioma cells. Acta Neuropathol 69 (1986) 73-80.

[55] K. Fukuyama, K. Matsuzawa, S.L. Hubbard, P.B. Dirks, M. Murakami, and J.T. Rutka, Analysis of glial fibrillary acidic protein gene methylation in human malignant gliomas. Anticancer Res 16 (1996) 1251-7.
[56] J.T. Rutka, M. Murakami, P.B. Dirks, S.L. Hubbard, L.E. Becker, K. Fukuyama, S. Jung, A. Tsugu, and K. Matsuzawa, Role of glial filaments in cells and tumors of glial origin: a review. J Neurosurg 87 (1997) 420-30.
[57] D.N. Louis, H. Ohgaki, O.D. Wiestler, W.K. Cavenee, P.C. Burger, A. Jouvet, B.W. Scheithauer, and P. Kleihues, The 2007 WHO classification of tumours of the central nervous system. Acta Neuropathol 114 (2007) 97-109.
[58] R. Burt, Inheritance of Colorectal Cancer. Drug Discov Today Dis Mech 4 (2007) 293-300.
[59] F.J. Ramos, T. Macarulla, J. Capdevila, E. Elez, and J. Tabernero, Understanding the predictive role of K-ras for epidermal growth factor receptor-targeted therapies in colorectal cancer. Clin Colorectal Cancer 7 Suppl 2 (2008) S52-7.
[60] R.S. Herbst, and D.M. Shin, Monoclonal antibodies to target epidermal growth factor receptor-positive tumors: a new paradigm for cancer therapy. Cancer 94 (2002) 1593-611.
[61] M.W. Saif, and M. Shah, K-ras mutations in colorectal cancer: a practice changing discovery. Clin Adv Hematol Oncol 7 (2009) 45-53, 64.
[62] D.S. Salomon, R. Brandt, F. Ciardiello, and N. Normanno, Epidermal growth factor-related peptides and their receptors in human malignancies. Crit Rev Oncol Hematol 19 (1995) 183-232.
[63] P. Rieske, R. Kordek, J. Bartkowiak, M. Debiec-Rychter, W. Biernat, and P.P. Liberski, A comparative study of epidermal growth factor receptor (EGFR) and MDM2 gene amplification and protein immunoreactivity in human glioblastomas. Pol J Pathol 49 (1998) 145-9.
[64] A.J. Ekstrand, C.D. James, W.K. Cavenee, B. Seliger, R.F. Pettersson, and V.P. Collins, Genes for epidermal growth factor receptor, transforming growth factor alpha, and epidermal growth factor and their expression in human gliomas in vivo. Cancer Res 51 (1991) 2164-72.
[65] J.G. Klijn, P.M. Berns, P.I. Schmitz, and J.A. Foekens, The clinical significance of epidermal growth factor receptor (EGF-R) in human breast cancer: a review on 5232 patients. Endocr Rev 13 (1992) 3-17.
[66] R.A. Walker, and S.J. Dearing, Expression of epidermal growth factor receptor mRNA and protein in primary breast carcinomas. Breast Cancer Res Treat 53 (1999) 167-76.
[67] B. Bucci, I. D'Agnano, C. Botti, M. Mottolese, E. Carico, G. Zupi, and A. Vecchione, EGF-R expression in ductal breast cancer: proliferation and prognostic implications. Anticancer Res 17 (1997) 769-74.
[68] K.W. Kinzler, and B. Vogelstein, Lessons from hereditary colorectal cancer. Cell 87 (1996) 159-70.
[69] W.M. Grady, L.L. Myeroff, S.E. Swinler, A. Rajput, S. Thiagalingam, J.D. Lutterbaugh, A. Neumann, M.G. Brattain, J. Chang, S.J. Kim, K.W. Kinzler, B. Vogelstein, J.K. Willson, and S. Markowitz, Mutational inactivation of transforming growth factor beta receptor type II in microsatellite stable colon cancers. Cancer Res 59 (1999) 320-4.

[70] F. Graziano, and S. Cascinu, Prognostic molecular markers for planning adjuvant chemotherapy trials in Dukes' B colorectal cancer patients: how much evidence is enough? Ann Oncol 14 (2003) 1026-38.
[71] G. Bardi, T. Sukhikh, N. Pandis, C. Fenger, O. Kronborg, and S. Heim, Karyotypic characterization of colorectal adenocarcinomas. Genes Chromosomes Cancer 12 (1995) 97-109.
[72] H. Pirc-Danoewinata, J.P. Bull, I. Okamoto, J. Karner, S. Breiteneder, A. Liebhardt, A. Budinsky, and C. Marosi, Cytogenetic findings in colorectal cancer mirror multistep evolution of colorectal cancer. Wien Klin Wochenschr 108 (1996) 752-8.
[73] J.S. Macdonald, Adjuvant therapy of colon cancer. CA Cancer J Clin 49 (1999) 202-19.
[74] P. Pisani, D.M. Parkin, F. Bray, and J. Ferlay, Estimates of the worldwide mortality from 25 cancers in 1990. Int J Cancer 83 (1999) 18-29.
[75] J.R. Siewert, H.J. Stein, M. Feith, B.L. Bruecher, H. Bartels, and U. Fink, Histologic tumor type is an independent prognostic parameter in esophageal cancer: lessons from more than 1,000 consecutive resections at a single center in the Western world. Ann Surg 234 (2001) 360-7; discussion 368-9.
[76] P.C. Enzinger, and R.J. Mayer, Esophageal cancer. N Engl J Med 349 (2003) 2241-52.
[77] P. Terry, J. Lagergren, W. Ye, O. Nyren, and A. Wolk, Antioxidants and cancers of the esophagus and gastric cardia. Int J Cancer 87 (2000) 750-4.
[78] A. Garidou, A. Tzonou, L. Lipworth, L.B. Signorello, V. Kalapothaki, and D. Trichopoulos, Life-style factors and medical conditions in relation to esophageal cancer by histologic type in a low-risk population. Int J Cancer 68 (1996) 295-9.
[79] J.M. Risk, H.S. Mills, J. Garde, J.R. Dunn, K.E. Evans, M. Hollstein, and J.K. Field, The tylosis esophageal cancer (TOC) locus: more than just a familial cancer gene. Dis Esophagus 12 (1999) 173-6.
[80] M. Pera, V.F. Trastek, H.A. Carpenter, M.S. Allen, C. Deschamps, and P.C. Pairolero, Barrett's esophagus with high-grade dysplasia: an indication for esophagectomy? Ann Thorac Surg 54 (1992) 199-204.
[81] P.C. Enzinger, D.H. Ilson, and D.P. Kelsen, Chemotherapy in esophageal cancer. Semin Oncol 26 (1999) 12-20.
[82] J.R. Headrick, F.C. Nichols, 3rd, D.L. Miller, M.S. Allen, V.F. Trastek, C. Deschamps, C.D. Schleck, A.M. Thompson, and P.C. Pairolero, High-grade esophageal dysplasia: long-term survival and quality of life after esophagectomy. Ann Thorac Surg 73 (2002) 1697-702; discussion 1702-3.
[83] I.S. Fentiman, Fixed and modifiable risk factors for breast cancer. Int J Clin Pract 55 (2001) 527-30.
[84] D.T. Bishop, BRCA1, BRCA2, BRCA3 ... a myriad of breast cancer genes. Eur J Cancer 30A (1994) 1738-9.
[85] S. Fuller, F. Liebens, B. Carly, A. Pastijn, and S. Rozenberg, Breast cancer prevention in BRCA1/2 mutation carriers: a qualitative review. Breast J 14 (2008) 603-4.
[86] D.J. Slamon, G.M. Clark, S.G. Wong, W.J. Levin, A. Ullrich, and W.L. McGuire, Human breast cancer: correlation of relapse and survival with amplification of the HER-2/neu oncogene. Science 235 (1987) 177-82.

[87] D.J. Slamon, W. Godolphin, L.A. Jones, J.A. Holt, S.G. Wong, D.E. Keith, W.J. Levin, S.G. Stuart, J. Udove, A. Ullrich, and et al., Studies of the HER-2/neu proto-oncogene in human breast and ovarian cancer. Science 244 (1989) 707-12.
[88] M.F. Press, L. Bernstein, P.A. Thomas, L.F. Meisner, J.Y. Zhou, Y. Ma, G. Hung, R.A. Robinson, C. Harris, A. El-Naggar, D.J. Slamon, R.N. Phillips, J.S. Ross, S.R. Wolman, and K.J. Flom, HER-2/neu gene amplification characterized by fluorescence in situ hybridization: poor prognosis in node-negative breast carcinomas. J Clin Oncol 15 (1997) 2894-904.
[89] R. Seshadri, F.A. Firgaira, D.J. Horsfall, K. McCaul, V. Setlur, and P. Kitchen, Clinical significance of HER-2/neu oncogene amplification in primary breast cancer. The South Australian Breast Cancer Study Group. J Clin Oncol 11 (1993) 1936-42.
[90] J. Myllyharju, and K.I. Kivirikko, Collagens and collagen-related diseases. Ann Med 33 (2001) 7-21.
[91] K.I. Kivirikko, and T. Pihlajaniemi, Collagen hydroxylases and the protein disulfide isomerase subunit of prolyl 4-hydroxylases. Adv Enzymol Relat Areas Mol Biol 72 (1998) 325-98.
[92] K.I. Kivirikko, and J. Myllyharju, Prolyl 4-hydroxylases and their protein disulfide isomerase subunit. Matrix Biol 16 (1998) 357-68.
[93] D.J. Prockop, A.L. Sieron, and S.W. Li, Procollagen N-proteinase and procollagen C-proteinase. Two unusual metalloproteinases that are essential for procollagen processing probably have important roles in development and cell signaling. Matrix Biol 16 (1998) 399-408.
[94] N.D. Light, and A.J. Bailey, Polymeric C-terminal cross-linked material from type-I collagen. A modified method for purification, anomalous behaviour on gel filtration, molecular weight estimation, carbohydrate content and lipid content. Biochem J 189 (1980) 111-24.
[95] P. Bornstein, A.H. Kang, and K.A. Piez, The nature and location of intramolecular cross-links in collagen. Proc Natl Acad Sci U S A 55 (1966) 417-24.
[96] K.A. Piez, Cross-linking of collagen and elastin. Annu Rev Biochem 37 (1968) 547-70.
[97] B. Vrhovski, and A.S. Weiss, Biochemistry of tropoelastin. Eur J Biochem 258 (1998) 1-18.
[98] L. Debelle, and A.M. Tamburro, Elastin: molecular description and function. Int J Biochem Cell Biol 31 (1999) 261-72.
[99] E.J. Miller, G.R. Martin, C.E. Mecca, and K.A. Piez, The biosynthesis of elastin cross-links. The effect of copper deficiency and a lathyrogen. J Biol Chem 240 (1965) 3623-7.
[100] B.L. O'Dell, D.F. Elsden, J. Thomas, S.M. Partridge, R.H. Smith, and R. Palmer, Inhibition of the biosynthesis of the cross-links in elastin by a lathyrogen. Nature 209 (1966) 401-2.
[101] H.M. Kagan, C.A. Vaccaro, R.E. Bronson, S.S. Tang, and J.S. Brody, Ultrastructural immunolocalization of lysyl oxidase in vascular connective tissue. J Cell Biol 103 (1986) 1121-8.
[102] J. Rosenbloom, W.R. Abrams, and R. Mecham, Extracellular matrix 4: the elastic fiber. Faseb J 7 (1993) 1208-18.
[103] N.K. Zouq, J.A. Keeble, J. Lindsay, A.J. Valentijn, L. Zhang, D. Mills, C.E. Turner, C.H. Streuli, and A.P. Gilmore, FAK engages multiple pathways to

maintain survival of fibroblasts and epithelia - differential roles for paxillin and p130Cas. J Cell Sci 122 (2009) 357-67.
[104] J.M. Summy, and G.E. Gallick, Src family kinases in tumor progression and metastasis. Cancer Metastasis Rev 22 (2003) 337-58.
[105] A.B. Lassman, Molecular biology of gliomas. Curr Neurol Neurosci Rep 4 (2004) 228-33.
[106] J. Zhao, and J.L. Guan, Signal transduction by focal adhesion kinase in cancer. Cancer Metastasis Rev 28 (2009) 35-49.
[107] J.T. Parsons, Focal adhesion kinase: the first ten years. J Cell Sci 116 (2003) 1409-16.
[108] H. Avraham, S.Y. Park, K. Schinkmann, and S. Avraham, RAFTK/Pyk2-mediated cellular signalling. Cell Signal 12 (2000) 123-33.
[109] J.L. Guan, Role of focal adhesion kinase in integrin signaling. Int J Biochem Cell Biol 29 (1997) 1085-96.
[110] K. Malarkey, C.M. Belham, A. Paul, A. Graham, A. McLees, P.H. Scott, and R. Plevin, The regulation of tyrosine kinase signalling pathways by growth factor and G-protein-coupled receptors. Biochem J 309 (Pt 2) (1995) 361-75.
[111] D. Ilic, C.H. Damsky, and T. Yamamoto, Focal adhesion kinase: at the crossroads of signal transduction. J Cell Sci 110 (Pt 4) (1997) 401-7.
[112] M.D. Schaller, C.A. Borgman, B.S. Cobb, R.R. Vines, A.B. Reynolds, and J.T. Parsons, pp125FAK a structurally distinctive protein-tyrosine kinase associated with focal adhesions. Proc Natl Acad Sci U S A 89 (1992) 5192-6.
[113] M.D. Schaller, J.D. Hildebrand, J.D. Shannon, J.W. Fox, R.R. Vines, and J.T. Parsons, Autophosphorylation of the focal adhesion kinase, pp125FAK, directs SH2-dependent binding of pp60src. Mol Cell Biol 14 (1994) 1680-8.
[114] B.S. Cobb, M.D. Schaller, T.H. Leu, and J.T. Parsons, Stable association of pp60src and pp59fyn with the focal adhesion-associated protein tyrosine kinase, pp125FAK. Mol Cell Biol 14 (1994) 147-55.
[115] Z. Xing, H.C. Chen, J.K. Nowlen, S.J. Taylor, D. Shalloway, and J.L. Guan, Direct interaction of v-Src with the focal adhesion kinase mediated by the Src SH2 domain. Mol Biol Cell 5 (1994) 413-21.
[116] J.D. Hildebrand, M.D. Schaller, and J.T. Parsons, Identification of sequences required for the efficient localization of the focal adhesion kinase, pp125FAK, to cellular focal adhesions. J Cell Biol 123 (1993) 993-1005.
[117] H.C. Chen, P.A. Appeddu, J.T. Parsons, J.D. Hildebrand, M.D. Schaller, and J.L. Guan, Interaction of focal adhesion kinase with cytoskeletal protein talin. J Biol Chem 270 (1995) 16995-9.
[118] K. Tachibana, T. Sato, N. D'Avirro, and C. Morimoto, Direct association of pp125FAK with paxillin, the focal adhesion-targeting mechanism of pp125FAK. J Exp Med 182 (1995) 1089-99.
[119] D.J. Sieg, C.R. Hauck, D. Ilic, C.K. Klingbeil, E. Schaefer, C.H. Damsky, and D.D. Schlaepfer, FAK integrates growth-factor and integrin signals to promote cell migration. Nat Cell Biol 2 (2000) 249-56.
[120] E. Liu, J.F. Cote, and K. Vuori, Negative regulation of FAK signaling by SOCS proteins. Embo J 22 (2003) 5036-46.
[121] S. Manes, E. Mira, C. Gomez-Mouton, Z.J. Zhao, R.A. Lacalle, and A.C. Martinez, Concerted activity of tyrosine phosphatase SHP-2 and focal adhesion kinase in regulation of cell motility. Mol Cell Biol 19 (1999) 3125-35.

[122] H.C. Chen, P.A. Appeddu, H. Isoda, and J.L. Guan, Phosphorylation of tyrosine 397 in focal adhesion kinase is required for binding phosphatidylinositol 3-kinase. J Biol Chem 271 (1996) 26329-34.
[123] B.T. Hennessy, D.L. Smith, P.T. Ram, Y. Lu, and G.B. Mills, Exploiting the PI3K/AKT pathway for cancer drug discovery. Nat Rev Drug Discov 4 (2005) 988-1004.
[124] J. Luo, B.D. Manning, and L.C. Cantley, Targeting the PI3K-Akt pathway in human cancer: rationale and promise. Cancer Cell 4 (2003) 257-62.
[125] A.P. Gilmore, and L.H. Romer, Inhibition of focal adhesion kinase (FAK) signaling in focal adhesions decreases cell motility and proliferation. Mol Biol Cell 7 (1996) 1209-24.
[126] J.L. Sechler, and J.E. Schwarzbauer, Control of cell cycle progression by fibronectin matrix architecture. J Biol Chem 273 (1998) 25533-6.
[127] J.H. Zhao, H. Reiske, and J.L. Guan, Regulation of the cell cycle by focal adhesion kinase. J Cell Biol 143 (1998) 1997-2008.
[128] S.J. Parsons, and J.T. Parsons, Src family kinases, key regulators of signal transduction. Oncogene 23 (2004) 7906-9.
[129] H. Oppermann, A.D. Levinson, H.E. Varmus, L. Levintow, and J.M. Bishop, Uninfected vertebrate cells contain a protein that is closely related to the product of the avian sarcoma virus transforming gene (src). Proc Natl Acad Sci U S A 76 (1979) 1804-8.
[130] J.A. Cooper, K.L. Gould, C.A. Cartwright, and T. Hunter, Tyr527 is phosphorylated in pp60c-src: implications for regulation. Science 231 (1986) 1431-4.
[131] M. Osusky, S.J. Taylor, and D. Shalloway, Autophosphorylation of purified c-Src at its primary negative regulation site. J Biol Chem 270 (1995) 25729-32.
[132] F. Sicheri, I. Moarefi, and J. Kuriyan, Crystal structure of the Src family tyrosine kinase Hck. Nature 385 (1997) 602-9.
[133] J.C. Williams, A. Weijland, S. Gonfloni, A. Thompson, S.A. Courtneidge, G. Superti-Furga, and R.K. Wierenga, The 2.35 A crystal structure of the inactivated form of chicken Src: a dynamic molecule with multiple regulatory interactions. J Mol Biol 274 (1997) 757-75.
[134] W. Xu, S.C. Harrison, and M.J. Eck, Three-dimensional structure of the tyrosine kinase c-Src. Nature 385 (1997) 595-602.
[135] S. Nada, M. Okada, A. MacAuley, J.A. Cooper, and H. Nakagawa, Cloning of a complementary DNA for a protein-tyrosine kinase that specifically phosphorylates a negative regulatory site of p60c-src. Nature 351 (1991) 69-72.
[136] M. Bergman, T. Mustelin, C. Oetken, J. Partanen, N.A. Flint, K.E. Amrein, M. Autero, P. Burn, and K. Alitalo, The human p50csk tyrosine kinase phosphorylates p56lck at Tyr-505 and down regulates its catalytic activity. Embo J 11 (1992) 2919-24.
[137] A. Imamoto, and P. Soriano, Disruption of the csk gene, encoding a negative regulator of Src family tyrosine kinases, leads to neural tube defects and embryonic lethality in mice. Cell 73 (1993) 1117-24.
[138] I. Hamaguchi, N. Yamaguchi, J. Suda, A. Iwama, A. Hirao, M. Hashiyama, S. Aizawa, and T. Suda, Analysis of CSK homologous kinase (CHK/HYL) in hematopoiesis by utilizing gene knockout mice. Biochem Biophys Res Commun 224 (1996) 172-9.

[139] D. Davidson, L.M. Chow, and A. Veillette, Chk, a Csk family tyrosine protein kinase, exhibits Csk-like activity in fibroblasts, but not in an antigen-specific T-cell line. J Biol Chem 272 (1997) 1355-62.
[140] J.W. Thomas, B. Ellis, R.J. Boerner, W.B. Knight, G.C. White, 2nd, and M.D. Schaller, SH2- and SH3-mediated interactions between focal adhesion kinase and Src. J Biol Chem 273 (1998) 577-83.
[141] Y. Zhao, C. Min, S.R. Vora, P.C. Trackman, G.E. Sonenshein, and K.H. Kirsch, The lysyl oxidase pro-peptide attenuates fibronectin-mediated activation of focal adhesion kinase and p130Cas in breast cancer cells. J Biol Chem 284 (2009) 1385-93.
[142] C. Frank, C. Burkhardt, D. Imhof, J. Ringel, O. Zschornig, K. Wieligmann, M. Zacharias, and F.D. Bohmer, Effective dephosphorylation of Src substrates by SHP-1. J Biol Chem 279 (2004) 11375-83.
[143] J. Su, M. Muranjan, and J. Sap, Receptor protein tyrosine phosphatase alpha activates Src-family kinases and controls integrin-mediated responses in fibroblasts. Curr Biol 9 (1999) 505-11.
[144] A. Petrone, and J. Sap, Emerging issues in receptor protein tyrosine phosphatase function: lifting fog or simply shifting? J Cell Sci 113 (Pt 13) (2000) 2345-54.
[145] J.E. Smart, H. Oppermann, A.P. Czernilofsky, A.F. Purchio, R.L. Erikson, and J.M. Bishop, Characterization of sites for tyrosine phosphorylation in the transforming protein of Rous sarcoma virus (pp60v-src) and its normal cellular homologue (pp60c-src). Proc Natl Acad Sci U S A 78 (1981) 6013-7.
[146] H. Yamaguchi, and W.A. Hendrickson, Structural basis for activation of human lymphocyte kinase Lck upon tyrosine phosphorylation. Nature 384 (1996) 484-9.
[147] J.A. Cooper, and A. MacAuley, Potential positive and negative autoregulation of p60c-src by intermolecular autophosphorylation. Proc Natl Acad Sci U S A 85 (1988) 4232-6.
[148] C.E. Turner, J.R. Glenney, Jr., and K. Burridge, Paxillin: a new vinculin-binding protein present in focal adhesions. J Cell Biol 111 (1990) 1059-68.
[149] C.E. Turner, Paxillin: a cytoskeletal target for tyrosine kinases. Bioessays 16 (1994) 47-52.
[150] C.E. Turner, Paxillin interactions. J Cell Sci 113 Pt 23 (2000) 4139-40.
[151] E. Zamir, B.Z. Katz, S. Aota, K.M. Yamada, B. Geiger, and Z. Kam, Molecular diversity of cell-matrix adhesions. J Cell Sci 112 (Pt 11) (1999) 1655-69.
[152] F.J. Alenghat, B. Fabry, K.Y. Tsai, W.H. Goldmann, and D.E. Ingber, Analysis of cell mechanics in single vinculin-deficient cells using a magnetic tweezer. Biochem Biophys Res Commun 277 (2000) 93-9.
[153] M.C. Brown, J.A. Perrotta, and C.E. Turner, Identification of LIM3 as the principal determinant of paxillin focal adhesion localization and characterization of a novel motif on paxillin directing vinculin and focal adhesion kinase binding. J Cell Biol 135 (1996) 1109-23.
[154] S. Sachdev, Y. Bu, and I.H. Gelman, Paxillin-Y118 phosphorylation contributes to the control of Src-induced anchorage-independent growth by FAK and adhesion. BMC Cancer 9 (2009) 12.
[155] V. Petit, B. Boyer, D. Lentz, C.E. Turner, J.P. Thiery, and A.M. Valles, Phosphorylation of tyrosine residues 31 and 118 on paxillin regulates cell

migration through an association with CRK in NBT-II cells. J Cell Biol 148 (2000) 957-70.
[156] L. Lamorte, S. Rodrigues, V. Sangwan, C.E. Turner, and M. Park, Crk associates with a multimolecular Paxillin/GIT2/beta-PIX complex and promotes Rac-dependent relocalization of Paxillin to focal contacts. Mol Biol Cell 14 (2003) 2818-31.
[157] L.Y. Romanova, S. Hashimoto, K.O. Chay, M.V. Blagosklonny, H. Sabe, and J.F. Mushinski, Phosphorylation of paxillin tyrosines 31 and 118 controls polarization and motility of lymphoid cells and is PMA-sensitive. J Cell Sci 117 (2004) 3759-68.
[158] D.E. Edmondson, A. Mattevi, C. Binda, M. Li, and F. Hubalek, Structure and mechanism of monoamine oxidase. Curr Med Chem 11 (2004) 1983-93.
[159] N.J. Butcher, G.M. Broadhurst, and R.F. Minchin, Polyamine-dependent regulation of spermidine-spermine N1-acetyltransferase mRNA translation. J Biol Chem 282 (2007) 28530-9.
[160] D.M. Dooley, Structure and biogenesis of topaquinone and related cofactors. J Biol Inorg Chem 4 (1999) 1-11.
[161] M. Mure, Tyrosine-derived quinone cofactors. Acc Chem Res 37 (2004) 131-9.
[162] J.A. Bollinger, D.E. Brown, and D.M. Dooley, The Formation of lysine tyrosylquinone (LTQ) is a self-processing reaction. Expression and characterization of a Drosophila lysyl oxidase. Biochemistry 44 (2005) 11708-14.
[163] O. Chassande, S. Renard, P. Barbry, and M. Lazdunski, The human gene for diamine oxidase, an amiloride binding protein. Molecular cloning, sequencing, and characterization of the promoter. J Biol Chem 269 (1994) 14484-9.
[164] F. Boomsma, H. Hut, U. Bagghoe, A. van der Houwen, and A. van den Meiracker, Semicarbazide-sensitive amine oxidase (SSAO): from cell to circulation. Med Sci Monit 11 (2005) RA122-6.
[165] H. Ito, H. Akiyama, H. Iguchi, K. Iyama, M. Miyamoto, K. Ohsawa, and T. Nakamura, Molecular cloning and biological activity of a novel lysyl oxidase-related gene expressed in cartilage. J Biol Chem 276 (2001) 24023-9.
[166] J.F. Bazan, Structural design and molecular evolution of a cytokine receptor superfamily. Proc Natl Acad Sci U S A 87 (1990) 6934-8.
[167] B. Fogelgren, N. Polgar, K.M. Szauter, Z. Ujfaludi, R. Laczko, K.S. Fong, and K. Csiszar, Cellular fibronectin binds to lysyl oxidase with high affinity and is critical for its proteolytic activation. J Biol Chem 280 (2005) 24690-7.
[168] S.N. Gacheru, P.C. Trackman, M.A. Shah, C.Y. O'Gara, P. Spacciapoli, F.T. Greenaway, and H.M. Kagan, Structural and catalytic properties of copper in lysyl oxidase. J Biol Chem 265 (1990) 19022-7.
[169] H. Iguchi, and S. Sano, Cadmium- or zinc-binding to bone lysyl oxidase and copper replacement. Connect Tissue Res 14 (1985) 129-39.
[170] E.D. Harris, Copper-induced activation of aortic lysyl oxidase in vivo. Proc Natl Acad Sci U S A 73 (1976) 371-4.
[171] T. Kosonen, J.Y. Uriu-Hare, M.S. Clegg, C.L. Keen, and R.B. Rucker, Incorporation of copper into lysyl oxidase. Biochem J 327 (Pt 1) (1997) 283-9.
[172] R.B. Rucker, T. Kosonen, M.S. Clegg, A.E. Mitchell, B.R. Rucker, J.Y. Uriu-Hare, and C.L. Keen, Copper, lysyl oxidase, and extracellular matrix protein cross-linking. Am J Clin Nutr 67 (1998) 996S-1002S.

[173] C.J. Krebs, and S.A. Krawetz, Lysyl oxidase copper-talon complex: a model. Biochim Biophys Acta 1202 (1993) 7-12.
[174] C. Tang, and J.P. Klinman, The catalytic function of bovine lysyl oxidase in the absence of copper. J Biol Chem 276 (2001) 30575-8.
[175] S.X. Wang, M. Mure, K.F. Medzihradszky, A.L. Burlingame, D.E. Brown, D.M. Dooley, A.J. Smith, H.M. Kagan, and J.P. Klinman, A crosslinked cofactor in lysyl oxidase: redox function for amino acid side chains. Science 273 (1996) 1078-84.
[176] S.X. Wang, N. Nakamura, M. Mure, J.P. Klinman, and J. Sanders-Loehr, Characterization of the native lysine tyrosylquinone cofactor in lysyl oxidase by Raman spectroscopy. J Biol Chem 272 (1997) 28841-4.
[177] M. Akagawa, and K. Suyama, Characterization of a model compound for the lysine tyrosylquinone cofactor of lysyl oxidase. Biochem Biophys Res Commun 281 (2001) 193-9.
[178] H. Umeda, M. Takeuchi, and K. Suyama, Two new elastin cross-links having pyridine skeleton. Implication of ammonia in elastin cross-linking in vivo. J Biol Chem 276 (2001) 12579-87.
[179] H.M. Kagan, D.M. Soucy, C.G. Zoski, R.J. Resnick, and S.S. Tang, Multiple modes of catalysis-dependent inhibition and inactivation of aortic lysyl oxidase. Arch Biochem Biophys 221 (1983) 158-67.
[180] H.M. Kagan, and P. Cai, Isolation of active site peptides of lysyl oxidase. Methods Enzymol 258 (1995) 122-32.
[181] D. Resnick, A. Pearson, and M. Krieger, The SRCR superfamily: a family reminiscent of the Ig superfamily. Trends Biochem Sci 19 (1994) 5-8.
[182] Y. Yamada, T. Doi, T. Hamakubo, and T. Kodama, Scavenger receptor family proteins: roles for atherosclerosis, host defence and disorders of the central nervous system. Cell Mol Life Sci 54 (1998) 628-40.
[183] C. Jourdan-Le Saux, A. Tomsche, A. Ujfalusi, L. Jia, and K. Csiszar, Central nervous system, uterus, heart, and leukocyte expression of the LOXL3 gene, encoding a novel lysyl oxidase-like protein. Genomics 74 (2001) 211-8.
[184] J.E. Lee, and Y. Kim, A tissue-specific variant of the human lysyl oxidase-like protein 3 (LOXL3) functions as an amine oxidase with substrate specificity. J Biol Chem 281 (2006) 37282-90.
[185] P.C. Trackman, A.M. Pratt, A. Wolanski, S.S. Tang, G.D. Offner, R.F. Troxler, and H.M. Kagan, Cloning of rat aorta lysyl oxidase cDNA: complete codons and predicted amino acid sequence. Biochemistry 29 (1990) 4863-70.
[186] K. Kenyon, W.S. Modi, S. Contente, and R.M. Friedman, A novel human cDNA with a predicted protein similar to lysyl oxidase maps to chromosome 15q24-q25. J Biol Chem 268 (1993) 18435-7.
[187] Y. Kim, C.D. Boyd, and K. Csiszar, A new gene with sequence and structural similarity to the gene encoding human lysyl oxidase. J Biol Chem 270 (1995) 7176-82.
[188] L. Thomassin, C.C. Werneck, T.J. Broekelmann, C. Gleyzal, I.K. Hornstra, R.P. Mecham, and P. Sommer, The Pro-regions of lysyl oxidase and lysyl oxidase-like 1 are required for deposition onto elastic fibers. J Biol Chem 280 (2005) 42848-55.

[189] W. Li, K. Nellaiappan, T. Strassmaier, L. Graham, K.M. Thomas, and H.M. Kagan, Localization and activity of lysyl oxidase within nuclei of fibrogenic cells. Proc Natl Acad Sci U S A 94 (1997) 12817-22.
[190] J.M. Maki, and K.I. Kivirikko, Cloning and characterization of a fourth human lysyl oxidase isoenzyme. Biochem J 355 (2001) 381-7.
[191] K. Nellaiappan, A. Risitano, G. Liu, G. Nicklas, and H.M. Kagan, Fully processed lysyl oxidase catalyst translocates from the extracellular space into nuclei of aortic smooth-muscle cells. J Cell Biochem 79 (2000) 576-82.
[192] M. Giampuzzi, R. Oleggini, and A. Di Donato, Demonstration of in vitro interaction between tumor suppressor lysyl oxidase and histones H1 and H2: definition of the regions involved. Biochim Biophys Acta 1647 (2003) 245-51.
[193] H.M. Kagan, and W. Li, Lysyl oxidase: properties, specificity, and biological roles inside and outside of the cell. J Cell Biochem 88 (2003) 660-72.
[194] J. Molnar, K.S. Fong, Q.P. He, K. Hayashi, Y. Kim, S.F. Fong, B. Fogelgren, K.M. Szauter, M. Mink, and K. Csiszar, Structural and functional diversity of lysyl oxidase and the LOX-like proteins. Biochim Biophys Acta 1647 (2003) 220-4.
[195] K. Hayashi, K.S. Fong, F. Mercier, C.D. Boyd, K. Csiszar, and M. Hayashi, Comparative immunocytochemical localization of lysyl oxidase (LOX) and the lysyl oxidase-like (LOXL) proteins: changes in the expression of LOXL during development and growth of mouse tissues. J Mol Histol 35 (2004) 845-55.
[196] P.C. Trackman, D. Bedell-Hogan, J. Tang, and H.M. Kagan, Post-translational glycosylation and proteolytic processing of a lysyl oxidase precursor. J Biol Chem 267 (1992) 8666-71.
[197] D.L. Layman, A.S. Narayanan, and G.R. Martin, The production of lysyl oxidase by human fibroblasts in culture. Arch Biochem Biophys 149 (1972) 97-101.
[198] A.D. Cronshaw, L.A. Fothergill-Gilmore, and D.J. Hulmes, The proteolytic processing site of the precursor of lysyl oxidase. Biochem J 306 (Pt 1) (1995) 279-84.
[199] M.V. Panchenko, W.G. Stetler-Stevenson, O.V. Trubetskoy, S.N. Gacheru, and H.M. Kagan, Metalloproteinase activity secreted by fibrogenic cells in the processing of prolysyl oxidase. Potential role of procollagen C-proteinase. J Biol Chem 271 (1996) 7113-9.
[200] E. Kessler, K. Takahara, L. Biniaminov, M. Brusel, and D.S. Greenspan, Bone morphogenetic protein-1: the type I procollagen C-proteinase. Science 271 (1996) 360-2.
[201] M.I. Uzel, S.D. Shih, H. Gross, E. Kessler, L.C. Gerstenfeld, and P.C. Trackman, Molecular events that contribute to lysyl oxidase enzyme activity and insoluble collagen accumulation in osteosarcoma cell clones. J Bone Miner Res 15 (2000) 1189-97.
[202] M.I. Uzel, I.C. Scott, H. Babakhanlou-Chase, A.H. Palamakumbura, W.N. Pappano, H.H. Hong, D.S. Greenspan, and P.C. Trackman, Multiple bone morphogenetic protein 1-related mammalian metalloproteinases process pro-lysyl oxidase at the correct physiological site and control lysyl oxidase activation in mouse embryo fibroblast cultures. J Biol Chem 276 (2001) 22537-43.

[203] B.J. Geiger, H. Steenbock, and H.T. Parsons, Nutrition Classics. The Journal of Nutrition 6:427-442, 1933. Lathyrism in the rat. Beatrice J. Geiger, Harry Steenbock, and Helen T. Parsons. Nutr Rev 34 (1976) 240-1.
[204] J. Gross, C.I. Levene, and S. Orloff, Fragility and extractable collagen in the lathyritic chick embryo. An assay for lathyrogenic agents. Proc Soc Exp Biol Med 105 (1960) 148-51.
[205] A.S. Narayanan, R.C. Siegel, and G.R. Martin, On the inhibition of lysyl oxidase by -aminopropionitrile. Biochem Biophys Res Commun 46 (1972) 745-51.
[206] S.R. Pinnell, and G.R. Martin, The cross-linking of collagen and elastin: enzymatic conversion of lysine in peptide linkage to alpha-aminoadipic-delta-semialdehyde (allysine) by an extract from bone. Proc Natl Acad Sci U S A 61 (1968) 708-16.
[207] R.C. Siegel, and G.R. Martin, Collagen cross-linking. Enzymatic synthesis of lysine-derived aldehydes and the production of cross-linked components. J Biol Chem 245 (1970) 1653-8.
[208] R.C. Siegel, S.R. Pinnell, and G.R. Martin, Cross-linking of collagen and elastin. Properties of lysyl oxidase. Biochemistry 9 (1970) 4486-92.
[209] S.S. Tang, P.C. Trackman, and H.M. Kagan, Reaction of aortic lysyl oxidase with beta-aminopropionitrile. J Biol Chem 258 (1983) 4331-8.
[210] P.R. Williamson, and H.M. Kagan, Electronegativity of aromatic amines as a basis for the development of ground state inhibitors of lysyl oxidase. J Biol Chem 262 (1987) 14520-4.
[211] S.N. Gacheru, P.C. Trackman, S.D. Calaman, F.T. Greenaway, and H.M. Kagan, Vicinal diamines as pyrroloquinoline quinone-directed irreversible inhibitors of lysyl oxidase. J Biol Chem 264 (1989) 12963-9.
[212] P. Gavriel, and H.M. Kagan, Inhibition by heparin of the oxidation of lysine in collagen by lysyl oxidase. Biochemistry 27 (1988) 2811-5.
[213] M.A. Shah, P.C. Trackman, P.M. Gallop, and H.M. Kagan, Reaction of lysyl oxidase with trans-2-phenylcyclopropylamine. J Biol Chem 268 (1993) 11580-5.
[214] G. Liu, K. Nellaiappan, and H.M. Kagan, Irreversible inhibition of lysyl oxidase by homocysteine thiolactone and its selenium and oxygen analogues. Implications for homocystinuria. J Biol Chem 272 (1997) 32370-7.
[215] N. Nagan, P.S. Callery, and H.M. Kagan, Aminoalkylaziridines as substrates and inhibitors of lysyl oxidase: specific inactivation of the enzyme by N-(5-aminopentyl)aziridine. Front Biosci 3 (1998) A23-6.
[216] B.L. O'Dell, B.C. Hardwick, G. Reynolds, and J.E. Savage, Connective tissue defect in the chick resulting from copper deficiency. Proc Soc Exp Biol Med 108 (1961) 402-5.
[217] G.S. Shields, W.F. Coulson, D.A. Kimball, W.H. Carnes, G.E. Cartwright, and M.M. Wintrobe, Studies on copper metabolism. 32. Cardiovascular lesions in copper-deficient swine. Am J Pathol 41 (1962) 603-21.
[218] W.F. Coulson, and W.H. Carnes, Cardiovascular Studies on Copper-Deficient Swine. V. the Histogenesis of the Coronary Artery Lesions. Am J Pathol 43 (1963) 945-54.
[219] B. Starcher, C.H. Hill, and G. Matrone, Importance of Dietary Copper in the Formation of Aortic Elastin. J Nutr 82 (1964) 318-22.
[220] J.E. Savage, D.W. Bird, G. Reynolds, and B.L. O'Dell, Comparison of copper deficiency and lathyrism in turkey poults. J Nutr 88 (1966) 15-25.

[221] B.L. O'Dell, D.W. Bird, D.L. Ruggles, and J.E. Savage, Composition of aortic tissue from copper-deficient chicks. J Nutr 88 (1966) 9-14.
[222] D.W. Bird, J.E. Savage, and B.L. O'Dell, Effect of copper deficiency and inhibitors on the amine oxidase activity of chick tissues. Proc Soc Exp Biol Med 123 (1966) 250-4.
[223] W.S. Chou, J.E. Savage, and B.L. O'Dell, Role of copper in biosynthesis of intramolecular cross-links in chick tendon collagen. J Biol Chem 244 (1969) 5785-9.
[224] K. Csiszar, I. Entersz, P.C. Trackman, D. Samid, and C.D. Boyd, Functional analysis of the promoter and first intron of the human lysyl oxidase gene. Mol Biol Rep 23 (1996) 97-108.
[225] A. Di Donato, G.M. Ghiggeri, M. Di Duca, E. Jivotenko, R. Acinni, J. Campolo, F. Ginevri, and R. Gusmano, Lysyl oxidase expression and collagen cross-linking during chronic adriamycin nephropathy. Nephron 76 (1997) 192-200.
[226] P. Atsawasuwan, Y. Mochida, D. Parisuthiman, and M. Yamauchi, Expression of lysyl oxidase isoforms in MC3T3-E1 osteoblastic cells. Biochem Biophys Res Commun 327 (2005) 1042-6.
[227] M. Kaku, Y. Mochida, P. Atsawasuwan, D. Parisuthiman, and M. Yamauchi, Post-translational modifications of collagen upon BMP-induced osteoblast differentiation. Biochem Biophys Res Commun 359 (2007) 463-8.
[228] T. Fujimaki, Y. Hotta, H. Sakuma, K. Fujiki, and A. Kanai, Large-scale sequencing of the rabbit corneal endothelial cDNA library. Cornea 18 (1999) 109-14.
[229] K.E. Gregory, M.E. Marsden, J. Anderson-MacKenzie, J.B. Bard, P. Bruckner, J. Farjanel, S.P. Robins, and D.J. Hulmes, Abnormal collagen assembly, though normal phenotype, in alginate bead cultures of chick embryo chondrocytes. Exp Cell Res 246 (1999) 98-107.
[230] M. Baccarani-Contri, D. Vincenzi, D. Quaglino, Jr., G. Mori, and I. Pasquali-Ronchetti, Localization of human placenta lysyl oxidase on human placenta, skin and aorta by immunoelectronmicroscopy. Matrix 9 (1989) 428-36.
[231] H.M. Kagan, M.A. Williams, S.D. Calaman, and E.M. Berkowitz, Histone H1 is a substrate for lysyl oxidase and contains endogenous sodium borotritide-reducible residues. Biochem Biophys Res Commun 115 (1983) 186-92.
[232] M. Giampuzzi, G. Botti, M. Di Duca, L. Arata, G. Ghiggeri, R. Gusmano, R. Ravazzolo, and A. Di Donato, Lysyl oxidase activates the transcription activity of human collagene III promoter. Possible involvement of Ku antigen. J Biol Chem 275 (2000) 36341-9.
[233] P. Laurent, A. Janoff, and H.M. Kagan, Cigarette smoke blocks cross-linking of elastin in vitro. Am Rev Respir Dis 127 (1983) 189-92.
[234] A.H. Palamakumbura, and P.C. Trackman, A fluorometric assay for detection of lysyl oxidase enzyme activity in biological samples. Anal Biochem 300 (2002) 245-51.
[235] W. Li, M.A. Nugent, Y. Zhao, A.N. Chau, S.J. Li, I.N. Chou, G. Liu, and H.M. Kagan, Lysyl oxidase oxidizes basic fibroblast growth factor and inactivates its mitogenic potential. J Cell Biochem 88 (2003) 152-64.
[236] P. Atsawasuwan, Y. Mochida, M. Katafuchi, M. Kaku, K.S. Fong, K. Csiszar, and M. Yamauchi, Lysyl oxidase binds transforming growth factor-beta and

regulates its signaling via amine oxidase activity. J Biol Chem 283 (2008) 34229-40.
[237] C. Jourdan-Le Saux, O. Le Saux, T. Donlon, C.D. Boyd, and K. Csiszar, The human lysyl oxidase-related gene (LOXL2) maps between markers D8S280 and D8S278 on chromosome 8p21.2-p21.3. Genomics 51 (1998) 305-7.
[238] C. Jourdan-Le Saux, H. Tronecker, L. Bogic, G.D. Bryant-Greenwood, C.D. Boyd, and K. Csiszar, The LOXL2 gene encodes a new lysyl oxidase-like protein and is expressed at high levels in reproductive tissues. J Biol Chem 274 (1999) 12939-44.
[239] H. Saito, J. Papaconstantinou, H. Sato, and S. Goldstein, Regulation of a novel gene encoding a lysyl oxidase-related protein in cellular adhesion and senescence. J Biol Chem 272 (1997) 8157-60.
[240] Z. Vadasz, O. Kessler, G. Akiri, S. Gengrinovitch, H.M. Kagan, Y. Baruch, O.B. Izhak, and G. Neufeld, Abnormal deposition of collagen around hepatocytes in Wilson's disease is associated with hepatocyte specific expression of lysyl oxidase and lysyl oxidase like protein-2. J Hepatol 43 (2005) 499-507.
[241] T. Pascal, F. Debacq-Chainiaux, A. Chretien, C. Bastin, A.F. Dabee, V. Bertholet, J. Remacle, and O. Toussaint, Comparison of replicative senescence and stress-induced premature senescence combining differential display and low-density DNA arrays. FEBS Lett 579 (2005) 3651-9.
[242] K.C. Muller, L. Welker, K. Paasch, B. Feindt, V.J. Erpenbeck, J.M. Hohlfeld, N. Krug, M. Nakashima, D. Branscheid, H. Magnussen, R.A. Jorres, and O. Holz, Lung fibroblasts from patients with emphysema show markers of senescence in vitro. Respir Res 7 (2006) 32.
[243] O. Holz, I. Zuhlke, E. Jaksztat, K.C. Muller, L. Welker, M. Nakashima, K.D. Diemel, D. Branscheid, H. Magnussen, and R.A. Jorres, Lung fibroblasts from patients with emphysema show a reduced proliferation rate in culture. Eur Respir J 24 (2004) 575-9.
[244] M. Monticone, Y. Liu, L. Tonachini, M. Mastrogiacomo, S. Parodi, R. Quarto, R. Cancedda, and P. Castagnola, Gene expression profile of human bone marrow stromal cells determined by restriction fragment differential display analysis. J Cell Biochem 92 (2004) 733-44.
[245] A.K. Kiemer, K. Takeuchi, and M.P. Quinlan, Identification of genes involved in epithelial-mesenchymal transition and tumor progression. Oncogene 20 (2001) 6679-88.
[246] H. Peinado, M. Del Carmen Iglesias-de la Cruz, D. Olmeda, K. Csiszar, K.S. Fong, S. Vega, M.A. Nieto, A. Cano, and F. Portillo, A molecular role for lysyl oxidase-like 2 enzyme in snail regulation and tumor progression. Embo J 24 (2005) 3446-58.
[247] H. Akagawa, A. Narita, H. Yamada, A. Tajima, B. Krischek, H. Kasuya, T. Hori, M. Kubota, N. Saeki, A. Hata, T. Mizutani, and I. Inoue, Systematic screening of lysyl oxidase-like (LOXL) family genes demonstrates that LOXL2 is a susceptibility gene to intracranial aneurysms. Hum Genet 121 (2007) 377-87.
[248] S. Contente, K. Kenyon, D. Rimoldi, and R.M. Friedman, Expression of gene rrg is associated with reversion of NIH 3T3 transformed by LTR-c-H-ras. Science 249 (1990) 796-8.

[249] A. Hajnal, R. Klemenz, and R. Schafer, Up-regulation of lysyl oxidase in spontaneous revertants of H-ras-transformed rat fibroblasts. Cancer Res 53 (1993) 4670-5.
[250] H. Oberhuber, B. Seliger, and R. Schafer, Partial restoration of pre-transformation levels of lysyl oxidase and transin mRNAs in phenotypic ras revertants. Mol Carcinog 12 (1995) 198-204.
[251] S. Jeay, S. Pianetti, H.M. Kagan, and G.E. Sonenshein, Lysyl oxidase inhibits ras-mediated transformation by preventing activation of NF-kappa B. Mol Cell Biol 23 (2003) 2251-63.
[252] A.H. Palamakumbura, S. Jeay, Y. Guo, N. Pischon, P. Sommer, G.E. Sonenshein, and P.C. Trackman, The propeptide domain of lysyl oxidase induces phenotypic reversion of ras-transformed cells. J Biol Chem 279 (2004) 40593-600.
[253] R.S. Tan, T. Taniguchi, and H. Harada, Identification of the lysyl oxidase gene as target of the antioncogenic transcription factor, IRF-1, and its possible role in tumor suppression. Cancer Res 56 (1996) 2417-21.
[254] E.R. Hamalainen, R. Kemppainen, H. Kuivaniemi, G. Tromp, A. Vaheri, T. Pihlajaniemi, and K.I. Kivirikko, Quantitative polymerase chain reaction of lysyl oxidase mRNA in malignantly transformed human cell lines demonstrates that their low lysyl oxidase activity is due to low quantities of its mRNA and low levels of transcription of the respective gene. J Biol Chem 270 (1995) 21590-3.
[255] H. Kuivaniemi, R.M. Korhonen, A. Vaheri, and K.I. Kivirikko, Deficient production of lysyl oxidase in cultures of malignantly transformed human cells. FEBS Lett 195 (1986) 261-4.
[256] C. Ren, G. Yang, T.L. Timme, T.M. Wheeler, and T.C. Thompson, Reduced lysyl oxidase messenger RNA levels in experimental and human prostate cancer. Cancer Res 58 (1998) 1285-90.
[257] T. Rost, V. Pyritz, I.O. Rathcke, T. Gorogh, A.A. Dunne, and J.A. Werner, Reduction of LOX- and LOXL2-mRNA expression in head and neck squamous cell carcinomas. Anticancer Res 23 (2003) 1565-73.
[258] R. Nishimura, T. Hasebe, Y. Tsubono, M. Ono, M. Sugitoh, T. Arai, and K. Mukai, The fibrotic focus in advanced colorectal carcinoma: a hitherto unrecognized histological predictor for liver metastasis. Virchows Arch 433 (1998) 517-22.
[259] T. Hasebe, K. Mukai, H. Tsuda, and A. Ochiai, New prognostic histological parameter of invasive ductal carcinoma of the breast: clinicopathological significance of fibrotic focus. Pathol Int 50 (2000) 263-72.
[260] C. Colpaert, P. Vermeulen, E. Van Marck, and L. Dirix, The presence of a fibrotic focus is an independent predictor of early metastasis in lymph node-negative breast cancer patients. Am J Surg Pathol 25 (2001) 1557-8.
[261] R.C. Siegel, K.H. Chen, J.S. Greenspan, and J.M. Aguiar, Biochemical and immunochemical study of lysyl oxidase in experimental hepatic fibrosis in the rat. Proc Natl Acad Sci U S A 75 (1978) 2945-9.
[262] Y. Murawaki, Y. Kusakabe, and C. Hirayama, Serum lysyl oxidase activity in chronic liver disease in comparison with serum levels of prolyl hydroxylase and laminin. Hepatology 14 (1991) 1167-73.
[263] G. Akiri, E. Sabo, H. Dafni, Z. Vadasz, Y. Kartvelishvily, N. Gan, O. Kessler, T. Cohen, M. Resnick, M. Neeman, and G. Neufeld, Lysyl oxidase-related protein-

1 promotes tumor fibrosis and tumor progression in vivo. Cancer Res 63 (2003) 1657-66.
[264] C. Jourdan-Le Saux, C. Gleyzal, J.M. Garnier, M. Peraldi, P. Sommer, and J.A. Grimaud, Lysyl oxidase cDNA of myofibroblast from mouse fibrotic liver. Biochem Biophys Res Commun 199 (1994) 587-92.
[265] H.M. Kagan, Lysyl oxidase: mechanism, regulation and relationship to liver fibrosis. Pathol Res Pract 190 (1994) 910-9.
[266] M. Decitre, C. Gleyzal, M. Raccurt, S. Peyrol, E. Aubert-Foucher, K. Csiszar, and P. Sommer, Lysyl oxidase-like protein localizes to sites of de novo fibrinogenesis in fibrosis and in the early stromal reaction of ductal breast carcinomas. Lab Invest 78 (1998) 143-51.
[267] Y. Kim, S. Peyrol, C.K. So, C.D. Boyd, and K. Csiszar, Coexpression of the lysyl oxidase-like gene (LOXL) and the gene encoding type III procollagen in induced liver fibrosis. J Cell Biochem 72 (1999) 181-8.
[268] J.T. Erler, K.L. Bennewith, M. Nicolau, N. Dornhofer, C. Kong, Q.T. Le, J.T. Chi, S.S. Jeffrey, and A.J. Giaccia, Lysyl oxidase is essential for hypoxia-induced metastasis. Nature 440 (2006) 1222-6.
[269] D.A. Kirschmann, E.A. Seftor, S.F. Fong, D.R. Nieva, C.M. Sullivan, E.M. Edwards, P. Sommer, K. Csiszar, and M.J. Hendrix, A molecular role for lysyl oxidase in breast cancer invasion. Cancer Res 62 (2002) 4478-83.
[270] H. Peinado, F. Portillo, and A. Cano, Switching on-off Snail: LOXL2 versus GSK3beta. Cell Cycle 4 (2005) 1749-52.
[271] J.P. Thiery, Epithelial-mesenchymal transitions in development and pathologies. Curr Opin Cell Biol 15 (2003) 740-6.
[272] H. Sellak, E. Franzini, J. Hakim, and C. Pasquier, Reactive oxygen species rapidly increase endothelial ICAM-1 ability to bind neutrophils without detectable upregulation. Blood 83 (1994) 2669-77.
[273] K. Csiszar, S.F. Fong, A. Ujfalusi, S.A. Krawetz, E.P. Salvati, J.W. Mackenzie, and C.D. Boyd, Somatic mutations of the lysyl oxidase gene on chromosome 5q23.1 in colorectal tumors. Int J Cancer 97 (2002) 636-42.
[274] N.A. Kolchanov, E.V. Ignatieva, E.A. Ananko, O.A. Podkolodnaya, I.L. Stepanenko, T.I. Merkulova, M.A. Pozdnyakov, N.L. Podkolodny, A.N. Naumochkin, and A.G. Romashchenko, Transcription Regulatory Regions Database (TRRD): its status in 2002. Nucleic Acids Res 30 (2002) 312-7.
[275] K.J. Livak, and T.D. Schmittgen, Analysis of relative gene expression data using real-time quantitative PCR and the 2(-Delta Delta C(T)) Method. Methods 25 (2001) 402-8.
[276] M.O. De Nichilo, and K.M. Yamada, Integrin alpha v beta 5-dependent serine phosphorylation of paxillin in cultured human macrophages adherent to vitronectin. J Biol Chem 271 (1996) 11016-22.
[277] M.J. Hendrix, E.A. Seftor, R.E. Seftor, and I.J. Fidler, A simple quantitative assay for studying the invasive potential of high and low human metastatic variants. Cancer Lett 38 (1987) 137-47.
[278] L. Madisen, D.I. Hoar, C.D. Holroyd, M. Crisp, and M.E. Hodes, DNA banking: the effects of storage of blood and isolated DNA on the integrity of DNA. Am J Med Genet 27 (1987) 379-90.

[279] J. Sambrook, E.F. Fritsch, T. Maniatis, N. Irwin, and T. Maniatis, Molecular cloning : a laboratory manual, Cold Spring Harbor Laboratory Press, Cold Spring Harbor, N.Y., 1989.
[280] A. Peraud, S. Mondal, C. Hawkins, M. Mastronardi, K. Bailey, and J.T. Rutka, Expression of fascin, an actin-bundling protein, in astrocytomas of varying grades. Brain Tumor Pathol 20 (2003) 53-8.
[281] R. Sharma, J.A. Kramer, and S.A. Krawetz, Lysyl oxidase, cellular senescence and tumor suppression. Biosci Rep 17 (1997) 409-14.
[282] L. Garrigue-Antar, N. Hartigan, and K.E. Kadler, Post-translational modification of bone morphogenetic protein-1 is required for secretion and stability of the protein. J Biol Chem 277 (2002) 43327-34.
[283] H.M. Lazarus, W.W. Cruikshank, N. Narasimhan, H.M. Kagan, and D.M. Center, Induction of human monocyte motility by lysyl oxidase. Matrix Biol 14 (1995) 727-31.
[284] W. Li, G. Liu, I.N. Chou, and H.M. Kagan, Hydrogen peroxide-mediated, lysyl oxidase-dependent chemotaxis of vascular smooth muscle cells. J Cell Biochem 78 (2000) 550-7.
[285] S.L. Payne, B. Fogelgren, A.R. Hess, E.A. Seftor, E.L. Wiley, S.F. Fong, K. Csiszar, M.J. Hendrix, and D.A. Kirschmann, Lysyl oxidase regulates breast cancer cell migration and adhesion through a hydrogen peroxide-mediated mechanism. Cancer Res 65 (2005) 11429-36.
[286] D.D. Schlaepfer, S.K. Mitra, and D. Ilic, Control of motile and invasive cell phenotypes by focal adhesion kinase. Biochim Biophys Acta 1692 (2004) 77-102.
[287] M.D. Schaller, Paxillin: a focal adhesion-associated adaptor protein. Oncogene 20 (2001) 6459-72.
[288] S. Yang, R. Yip, S. Polena, M. Sharma, S. Rao, P. Griciene, J. Gintautas, and H. Jerome, Reactive oxygen species increased focal adhesion kinase production in pulmonary microvascular endothelial cells. Proc West Pharmacol Soc 47 (2004) 54-6.
[289] A. Borel, D. Eichenberger, J. Farjanel, E. Kessler, C. Gleyzal, D.J. Hulmes, P. Sommer, and B. Font, Lysyl oxidase-like protein from bovine aorta. Isolation and maturation to an active form by bone morphogenetic protein-1. J Biol Chem 276 (2001) 48944-9.
[290] K.S. Fong, B. Fogelgren, S.F. Fong, and K. Csiszar, Lysyl oxidase, UCSD-Nature Molecule Pages, doi:10.1038/mp.a002989.01, 2006.
[291] A.L. Kierszenbaum, Histology and cell biology : an introduction to pathology, Mosby, St. Louis, Mo., 2002.
[292] J.M. Lay, G. Bane, C.S. Brunkan, J. Davis, L. Lopez-Diaz, and L.C. Samuelson, Enteroendocrine cell expression of a cholecystokinin gene construct in transgenic mice and cultured cells. Am J Physiol Gastrointest Liver Physiol 288 (2005) G354-61.
[293] R. Shaoul, D. Hong, Y. Okada, E. Cutz, and M.A. Marcon, Lineage development in a patient without goblet, paneth, and enteroendocrine cells: a clue for intestinal epithelial differentiation. Pediatr Res 58 (2005) 492-8.
[294] J.P. Lynch, and T.C. Hoops, The genetic pathogenesis of colorectal cancer. Hematol Oncol Clin North Am 16 (2002) 775-810.

[295] R. Montesano, M. Hollstein, and P. Hainaut, Genetic alterations in esophageal cancer and their relevance to etiology and pathogenesis: a review. Int J Cancer 69 (1996) 225-35.
[296] T. Arai, Y. Akiyama, A. Yamamura, T. Hosoi, T. Shibata, K. Saitoh, S. Okabe, and Y. Yuasa, Allelotype analysis of early colorectal cancers with lymph node metastasis. Int J Cancer 79 (1998) 418-23.
[297] L. Du Plessis, E. Dietzsch, M. Van Gele, N. Van Roy, P. Van Helden, M.I. Parker, D.K. Mugwanya, M. De Groot, M.P. Marx, M.J. Kotze, and F. Speleman, Mapping of novel regions of DNA gain and loss by comparative genomic hybridization in esophageal carcinoma in the Black and Colored populations of South Africa. Cancer Res 59 (1999) 1877-83.
[298] F. Lerebours, S. Olschwang, B. Thuille, A. Schmitz, P. Fouchet, P. Laurent-Puig, F. Boman, J.F. Flejou, G. Monges, F. Paraf, P. Bedossa, J.C. Sabourin, R.J. Salmon, R. Parc, and G. Thomas, Deletion mapping of the tumor suppressor locus involved in colorectal cancer on chromosome band 8p21. Genes Chromosomes Cancer 25 (1999) 147-53.
[299] I. Tomlinson, M. Ilyas, V. Johnson, A. Davies, G. Clark, I. Talbot, and W. Bodmer, A comparison of the genetic pathways involved in the pathogenesis of three types of colorectal cancer. J Pathol 184 (1998) 148-52.
[300] S. Kapitanovic, T. Cacev, S. Radosevic, S. Spaventi, R. Spaventi, and K. Pavelic, APC gene loss of heterozygosity, mutations, E1317Q, and I1307K germ-line variants in sporadic colon cancer in Croatia. Exp Mol Pathol 77 (2004) 193-200.
[301] T. Arai, Y. Akiyama, H. Nagasaki, N. Murase, S. Okabe, T. Ikeuchi, K. Saito, T. Iwai, and Y. Yuasa, EXTL3/EXTR1 alterations in colorectal cancer cell lines. Int J Oncol 15 (1999) 915-9.
[302] B.Z. Yuan, X. Zhou, M.E. Durkin, D.B. Zimonjic, K. Gumundsdottir, J.E. Eyfjord, S.S. Thorgeirsson, and N.C. Popescu, DLC-1 gene inhibits human breast cancer cell growth and in vivo tumorigenicity. Oncogene 22 (2003) 445-50.
[303] J.M. Flanagan, S. Healey, J. Young, V. Whitehall, D.A. Trott, R.F. Newbold, and G. Chenevix-Trench, Mapping of a candidate colorectal cancer tumor-suppressor gene to a 900-kilobase region on the short arm of chromosome 8. Genes Chromosomes Cancer 40 (2004) 247-60.
[304] A. Kaneda, M. Kaminishi, K. Yanagihara, T. Sugimura, and T. Ushijima, Identification of silencing of nine genes in human gastric cancers. Cancer Res 62 (2002) 6645-50.
[305] A. Kaneda, K. Wakazono, T. Tsukamoto, N. Watanabe, Y. Yagi, M. Tatematsu, M. Kaminishi, T. Sugimura, and T. Ushijima, Lysyl oxidase is a tumor suppressor gene inactivated by methylation and loss of heterozygosity in human gastric cancers. Cancer Res 64 (2004) 6410-5.
[306] V.N. Babenko, P.S. Kosarev, O.V. Vishnevsky, V.G. Levitsky, V.V. Basin, and A.S. Frolov, Investigating extended regulatory regions of genomic DNA sequences. Bioinformatics 15 (1999) 644-53.
[307] S.J. Vermeulen, T.R. Chen, F. Speleman, F. Nollet, F.M. Van Roy, and M.M. Mareel, Did the four human cancer cell lines DLD-1, HCT-15, HCT-8, and HRT-18 originate from one and the same patient? Cancer Genet Cytogenet 107 (1998) 76-9.

[308] S.L. Payne, M.J. Hendrix, and D.A. Kirschmann, Paradoxical roles for lysyl oxidases in cancer--a prospect. J Cell Biochem 101 (2007) 1338-54.
[309] H. Peinado, G. Moreno-Bueno, D. Hardisson, E. Perez-Gomez, V. Santos, M. Mendiola, J.I. de Diego, M. Nistal, M. Quintanilla, F. Portillo, and A. Cano, Lysyl oxidase-like 2 as a new poor prognosis marker of squamous cell carcinomas. Cancer Res 68 (2008) 4541-50.
[310] C.M. Nelson, and M.J. Bissell, Of extracellular matrix, scaffolds, and signaling: tissue architecture regulates development, homeostasis, and cancer. Annu Rev Cell Dev Biol 22 (2006) 287-309.
[311] R. Pankov, and K.M. Yamada, Fibronectin at a glance. J Cell Sci 115 (2002) 3861-3.
[312] L. Christensen, The distribution of fibronectin, laminin and tetranectin in human breast cancer with special attention to the extracellular matrix. APMIS Suppl 26 (1992) 1-39.
[313] S.L. Schor, and A.M. Schor, Phenotypic and genetic alterations in mammary stroma: implications for tumour progression. Breast Cancer Res 3 (2001) 373-9.
[314] A. Toninello, P. Pietrangeli, U. De Marchi, M. Salvi, and B. Mondovi, Amine oxidases in apoptosis and cancer. Biochim Biophys Acta 1765 (2006) 1-13.
[315] J. Fang, T. Seki, and H. Maeda, Therapeutic strategies by modulating oxygen stress in cancer and inflammation. Adv Drug Deliv Rev (2009).
[316] S.L. Payne, M.J. Hendrix, and D.A. Kirschmann, Lysyl oxidase regulates actin filament formation through the p130(Cas)/Crk/DOCK180 signaling complex. J Cell Biochem 98 (2006) 827-37.
[317] H. Bouterfa, A.R. Darlapp, E. Klein, T. Pietsch, K. Roosen, and J.C. Tonn, Expression of different extracellular matrix components in human brain tumor and melanoma cells in respect to variant culture conditions. J Neurooncol 44 (1999) 23-33.
[318] M. Caffo, A. Germano, G. Caruso, F. Meli, S. Galatioto, M.P. Sciacca, and F. Tomasello, An immunohistochemical study of extracellular matrix proteins laminin, fibronectin and type IV collagen in paediatric glioblastoma multiforme. Acta Neurochir (Wien) 146 (2004) 1113-8; discussion 1118.
[319] S. Jung, A. Hinek, A. Tsugu, S.L. Hubbard, C. Ackerley, L.E. Becker, and J.T. Rutka, Astrocytoma cell interaction with elastin substrates: implications for astrocytoma invasive potential. Glia 25 (1999) 179-89.
[320] S. Jung, J.T. Rutka, and A. Hinek, Tropoelastin and elastin degradation products promote proliferation of human astrocytoma cell lines. J Neuropathol Exp Neurol 57 (1998) 439-48.
[321] J. Silver, Inhibitory molecules in development and regeneration. J Neurol 242 (1994) S22-4.
[322] L. Olson, Regeneration in the adult central nervous system: experimental repair strategies. Nat Med 3 (1997) 1329-35.
[323] Y. Li, and G. Raisman, Sprouts from cut corticospinal axons persist in the presence of astrocytic scarring in long-term lesions of the adult rat spinal cord. Exp Neurol 134 (1995) 102-11.
[324] L.L. Rankin, M. Chvapil, R. Misiorowski, P. Johnson, and P.R. Weinstein, Diffusion characteristics of beta-aminopropionitrile in peripheral nerve. Exp Neurol 79 (1983) 97-105.

[325] G.M. Gilad, and V.H. Gilad, Beta-aminopropionitrile treatment can accelerate recovery of mice after spinal cord injury. Eur J Pharmacol 430 (2001) 69-72.
[326] J.S. Hardwick, and B.M. Sefton, Activation of the Lck tyrosine protein kinase by hydrogen peroxide requires the phosphorylation of Tyr-394. Proc Natl Acad Sci U S A 92 (1995) 4527-31.
[327] J.P. Secrist, L.A. Burns, L. Karnitz, G.A. Koretzky, and R.T. Abraham, Stimulatory effects of the protein tyrosine phosphatase inhibitor, pervanadate, on T-cell activation events. J Biol Chem 268 (1993) 5886-93.
[328] M. Gonzalez-Rubio, S. Voit, D. Rodriguez-Puyol, M. Weber, and M. Marx, Oxidative stress induces tyrosine phosphorylation of PDGF alpha-and beta-receptors and pp60c-src in mesangial cells. Kidney Int 50 (1996) 164-73.
[329] H. Tang, Q. Hao, S.A. Rutherford, B. Low, and Z.J. Zhao, Inactivation of SRC family tyrosine kinases by reactive oxygen species in vivo. J Biol Chem 280 (2005) 23918-25.
[330] G.G. Chiang, and B.M. Sefton, Phosphorylation of a Src kinase at the autophosphorylation site in the absence of Src kinase activity. J Biol Chem 275 (2000) 6055-8.
[331] S.G. Rhee, Y.S. Bae, S.R. Lee, and J. Kwon, Hydrogen peroxide: a key messenger that modulates protein phosphorylation through cysteine oxidation. Sci STKE 2000 (2000) PE1.
[332] T. Kanazawa, T. Watanabe, S. Kazama, T. Tada, S. Koketsu, and H. Nagawa, Poorly differentiated adenocarcinoma and mucinous carcinoma of the colon and rectum show higher rates of loss of heterozygosity and loss of E-cadherin expression due to methylation of promoter region. Int J Cancer 102 (2002) 225-9.
[333] C.D. Hough, C.A. Sherman-Baust, E.S. Pizer, F.J. Montz, D.D. Im, N.B. Rosenshein, K.R. Cho, G.J. Riggins, and P.J. Morin, Large-scale serial analysis of gene expression reveals genes differentially expressed in ovarian cancer. Cancer Res 60 (2000) 6281-7.
[334] K. Ono, T. Tanaka, T. Tsunoda, O. Kitahara, C. Kihara, A. Okamoto, K. Ochiai, T. Takagi, and Y. Nakamura, Identification by cDNA microarray of genes involved in ovarian carcinogenesis. Cancer Res 60 (2000) 5007-11.
[335] A. Gohla, K. Eckert, and H.R. Maurer, A rapid and sensitive fluorometric screening assay using YO-PRO-1 to quantify tumour cell invasion through Matrigel. Clin Exp Metastasis 14 (1996) 451-8.
[336] S.J. Vermeulen, E.A. Bruyneel, M.E. Bracke, G.K. De Bruyne, K.M. Vennekens, K.L. Vleminckx, G.J. Berx, F.M. van Roy, and M.M. Mareel, Transition from the noninvasive to the invasive phenotype and loss of alpha-catenin in human colon cancer cells. Cancer Res 55 (1995) 4722-8.
[337] H.A. Lucero, and H.M. Kagan, Lysyl oxidase: an oxidative enzyme and effector of cell function. Cell Mol Life Sci 63 (2006) 2304-16.
[338] G.E. Lind, L. Thorstensen, T. Lovig, G.I. Meling, R. Hamelin, T.O. Rognum, M. Esteller, and R.A. Lothe, A CpG island hypermethylation profile of primary colorectal carcinomas and colon cancer cell lines. Mol Cancer 3 (2004) 28.
[339] J.M. Perez-Pomares, A. Phelps, M. Sedmerova, R. Carmona, M. Gonzalez-Iriarte, R. Munoz-Chapuli, and A. Wessels, Experimental studies on the spatiotemporal expression of WT1 and RALDH2 in the embryonic avian heart: a model for the

regulation of myocardial and valvuloseptal development by epicardially derived cells (EPDCs). Dev Biol 247 (2002) 307-26.
[340] R. Eferl, and E.F. Wagner, AP-1: a double-edged sword in tumorigenesis. Nat Rev Cancer 3 (2003) 859-68.
[341] M.A. Huber, N. Azoitei, B. Baumann, S. Grunert, A. Sommer, H. Pehamberger, N. Kraut, H. Beug, and T. Wirth, NF-kappaB is essential for epithelial-mesenchymal transition and metastasis in a model of breast cancer progression. J Clin Invest 114 (2004) 569-81.
[342] N. Polgar, B. Fogelgren, J.M. Shipley, and K. Csiszar, Lysyl oxidase interacts with hormone placental lactogen and synergistically promotes breast epithelial cell proliferation and migration. J Biol Chem 282 (2007) 3262-72.
[343] K.K. Kaulsay, H.C. Mertani, J. Tornell, G. Morel, K.O. Lee, and P.E. Lobie, Autocrine stimulation of human mammary carcinoma cell proliferation by human growth hormone. Exp Cell Res 250 (1999) 35-50.
[344] S. Mukhina, H.C. Mertani, K. Guo, K.O. Lee, P.D. Gluckman, and P.E. Lobie, Phenotypic conversion of human mammary carcinoma cells by autocrine human growth hormone. Proc Natl Acad Sci U S A 101 (2004) 15166-71.
[345] P. Chakravarti, M.K. Henry, and F.W. Quelle, Prolactin and heregulin override DNA damage-induced growth arrest and promote phosphatidylinositol-3 kinase-dependent proliferation in breast cancer cells. Int J Oncol 26 (2005) 509-14.
[346] M.R. Sarrias, J. Gronlund, O. Padilla, J. Madsen, U. Holmskov, and F. Lozano, The Scavenger Receptor Cysteine-Rich (SRCR) domain: an ancient and highly conserved protein module of the innate immune system. Crit Rev Immunol 24 (2004) 1-37.
[347] J.E. Skonier, M.A. Bowen, A. Aruffo, and J. Bajorath, CD6 recognizes the neural adhesion molecule BEN. Protein Sci 6 (1997) 1768-70.
[348] T. Sasaki, C. Brakebusch, J. Engel, and R. Timpl, Mac-2 binding protein is a cell-adhesive protein of the extracellular matrix which self-assembles into ring-like structures and binds beta1 integrins, collagens and fibronectin. Embo J 17 (1998) 1606-13.
[349] J. Takito, L. Yan, J. Ma, C. Hikita, S. Vijayakumar, D. Warburton, and Q. Al-Awqati, Hensin, the polarity reversal protein, is encoded by DMBT1, a gene frequently deleted in malignant gliomas. Am J Physiol 277 (1999) F277-89.
[350] M.A. Chrenek, P. Wong, and V.M. Weaver, Tumour-stromal interactions. Integrins and cell adhesions as modulators of mammary cell survival and transformation. Breast Cancer Res 3 (2001) 224-9.
[351] B. Ozdamar, R. Bose, M. Barrios-Rodiles, H.R. Wang, Y. Zhang, and J.L. Wrana, Regulation of the polarity protein Par6 by TGFbeta receptors controls epithelial cell plasticity. Science 307 (2005) 1603-9.

Publications

Articles discussed in the thesis:

Hollosi P, Yakushiji J, Fong KS, Csiszar K, Fong SFT
Lysyl oxidase-like 2 promotes migration in non-invasive breast cancer cells but not in normal breast epithelial cells
International Journal of Cancer 2009; accepted, in press

Laczko R, Szauter KM, Jansen MK, Hollosi P, Molnar J, Muranyi M, Fong KS, Hinek A, Csiszar K
Lysyl oxidase (LOX) promotes FAK/paxillin activation and migration in invasive astrocytes
Neuropathol Appl Neurobiol. 2007 Dec;33(6):631-43.

Fong SF, Dietzsch E, Fong KS, Hollosi P, Asuncion L, He Q,
Parker MI, Csiszar K
Lysyl oxidase-like 2 expression is increased in colon and esophageal
tumors and associated with less differentiated colon tumors
Genes Chromosomes Cancer 2007 Jul;46(7):644-55

Articles not discussed in the thesis:

Peterfia B, Hollosi P, Szilak L, Timar F, Paku S, Jeney A, Kovalszky I.
Role of syndecan-1 proteoglycan in the invasiveness of HT-1080 fibrosarcoma
Magy Onkol. 2006;50(2):115-20. Hungarian.

Kovalszky I, Dudas J, Gallai M, Hollosi P, Tatrai P, Tatrai E, Schaff Z
Proteoglycans in the liver
Magy Onkol. 2004; 48(3):207-13. Hungarian.

Kiss AL, Botos E, Turi A, Mullner N, Hollosi P, Kovalszky I
Ocadaic acid treatment alters the intracellular localization of caveolin-1 and caveolin-2 in HepG2 cells human isolated coronary arteries
Acta Biol Szeged 2003; 47:11-17

Acknowledgements

I would like to express my sincere thanks to my supervisor Ilona Kovalszky for her continuous support in my scientific career. She created a professional and supportive working environment that allowed me to finish my doctoral studies at the maximum level of comfort.

I would like to express my deepest gratitude to my supervisors Katalin Csiszár and Sheri Fong, for guiding me through the three years of active research in the field of matrix biology, teaching me professional attitude towards designing, conducting, and evaluating laboratory experiments.

I also thank all my coworkers at the Semmelweis University and at the University of Hawai'i at Manoa for sharing great scientific and personal discussions, helping me grow both professionally and both as a human being.

I thank the directors and staff members at the Semmelweis University Pathological Sciences Doctoral School for being so supportive of me, especially to László Kopper, András Jeney, Matolcsy András, and Cecília Laczik.

And last, but definitely not least, I thank to my family and friends for being what they are and always providing me with the best they could give.

Study I was supported by National Institutes of Health grants AR47713 and G12RR003096.

Study II was supported by National Center for Research Resources grant: G12-RR-003061; National Cancer Institute grant CA 76580; National Institutes of Health; and South African Medical Research Council, University of Cape Town.

Study III was sponsored by National Cancer Institute through Cancer Research Center of Hawaii grant CA71789; National Center for Research Resources grant G12-RR-003061; Ingeborg V.F. McKee Fund of the Hawaii Community Foundation.